This dissertation has been
microfilmed exactly as received

70-7675

BERTRAND, Richard David, 1942-

NMR STUDIES OF PHOSPHORUS COMPOUNDS.

Iowa State University, Ph.D., 1969
Chemistry, organic

University Microfilms, Inc., Ann Arbor, Michigan

NMR STUDIES OF PHOSPHORUS COMPOUNDS

by

Richard David Bertrand

A Dissertation Submitted to the
Graduate Faculty in Partial Fulfillment of
The Requirements for the Degree of
DOCTOR OF PHILOSOPHY

Major Subject: Inorganic Chemistry

Approved:

Signature was redacted for privacy.

In Charge of Major Work

Signature was redacted for privacy.

Head of Major Department

Signature was redacted for privacy.

Dean of Graduate College

Iowa State University
Ames, Iowa

1969

TABLE OF CONTENTS

	Page
INTRODUCTION	1
EXPERIMENTAL	18
RESULTS	26
DISCUSSION	89
SUGGESTIONS FOR FURTHER WORK	139
LITERATURE CITED	142
ACKNOWLEDGMENTS	147

INTRODUCTION

General

The application of high resolution nuclear magnetic resonance spectroscopy to problems of chemical interest results from the dependence of the nmr parameters, the chemical shift and spin-spin coupling constants, upon the nature of the electronic environments of the magnetic nuclei which are studied. The theory of high resolution nmr is developed in several standard text books (1, 2, 3) and will not be discussed here.

The purpose of the studies reported upon in this dissertation was to obtain data which might aid in our understanding of the nature of the bonding of phosphorus to other elements, such as transition metals, carbon, nitrogen, oxygen, fluorine and sulfur. These studies included the determination of the magnitude and sign of geminal ^{31}P-^{31}P spin-spin coupling constants in a number of transition metal complexes which contain two molecules of a trivalent phosphorus-containing ligand bound to the metal through phosphorus. Observations were made as to changes in the values and signs of $^{2}J_{PP}$ with changes in the nature of the groups attached to phosphorus as well as changes in the stereochemistry of the complexes. The complexes studied include complexes of group VI carbonyls, iron carbonyl and palladium halides of the phosphorus ligands $P[N(CH_3)_2]_3$, $P(OCH_3)_3$ and $P(CH_3)_3$. These results will be discussed in terms of the theory of spin-spin coupling developed by Pople and

Santry (4).

The results of the first systematic study of vicinal ^{31}P-^{31}P coupling will also be reported. The systems employed were the bicyclic di-phosphorus compound $P(OCH_2)_3P$ and several of its derivatives. Changes in ^{31}P chemical shifts, the magnitudes and signs of ^{31}P-^{31}P spin-spin coupling constants as well as $^2J_{PH}$ and $^3J_{PH}$ values as a function of the groups attached to the lone pair electrons on the phosphorus atoms were determined. These groups include oxygen, sulfur, CH_3^+ and transition metal carbonyl moieties such as $Cr(CO)_5$.

Finally, the results of studies on the effects of aromatic solvents upon the chemical shifts of protons in bicyclic molecules will be discussed. These results are interpreted in terms of a collision-complex, solute-solvent interaction model.

Spin-spin Coupling

The mechanisms by which isotropic nuclear spin-spin coupling is transmitted through the electrons of a molecule were first postulated by Ramsey (5). He indicated that there were three mechanisms by which coupling information could be transmitted. Coupling due to the interactions of the nuclear magnetic moment with the magnetic field produced by the orbital motion of the electrons induces orbital electronic currents which in turn induces non-vanishing magnetic fields at the site of the second nucleus. This contribution was termed spin-orbit coupling. A second interaction was postulated which

results from the interaction of the magnetic moment of the electron and the magnetic moment of the nucleus which again establishes non-vanishing magnetic fields at a second nucleus. Thirdly, the interaction between the nuclear magnetic moments of the coupling nuclei with electrons which have density at the coupled nuclei is felt to dominate the other two. Since only s electrons have electron density at the nucleus, this coupling is transmitted via electrons in s orbitals and is termed the contact interaction. Ramsey showed that each of these coupling mechanisms are independent of each other, that is, cross terms between the Hamiltonians which express the form of each type of coupling vanish. He also developed analytical expressions for each of these mechanisms using second-order perturbation theory.

A theorem of second-order perturbation theory (6) states that the contribution to the total energy of a system due to the presence of a second order perturbation is given by Equation 1.

$$E^{(2)} = - \sum_{n \neq k} \frac{|(\psi_n|H_1|\psi_k)|^2}{E_n^{(0)} - E_k^{(0)}} \qquad 1$$

where $E^{(2)}$ is the second order energy contribution, the ψ_n and ψ_k are the eigenfunctions of the unperturbed Hamiltonian, H_1 is the first order perturbation Hamiltonian and $E_n^{(0)}$ and $E_k^{(0)}$ are the eigenvalues for the unperturbed states ψ_n and ψ_k.

Nuclear spin-spin coupling is strictly a second order phenomenon, since the first order perturbation contribution to the total energy is zero (3), that is, there is no contribution to spin-spin coupling due to the ground state. The second order contribution to the energy due to the contact interaction takes the form of Equation 1, where k = 0 and the sum is over all states but the ground state, that is, over all excited states. Moreover, E_n is the energy of the unperturbed excited state. The Hamiltonian for the contact interaction is expressed by Equation 2, where

$$H_1 = \frac{16\beta h}{6} \sum_n \sum_i \gamma_i \delta(\hat{r}_{n,i}) \hat{S}_n \cdot \hat{I}_i \qquad 2$$

$\beta = eh/4\pi mc$ is the Bohr magneton, $\hat{S}_n$ the spin vector for the n^{th} electron, $\hat{I}$ is the nuclear spin vector of the i^{th} nucleus and $\delta(\hat{r}_{ni})$ is the Dirac delta function which picks out only electrons (n) at the nucleus (i), i.e., is zero when $\hat{r}_{ni} \neq 0$. It has been shown (5) that for two nuclei i and i' the energy of this interaction is

$$E_{ii'} = -2\left(\frac{16\beta h}{6}\right)^2 \gamma_i \gamma_{i'} \sum_{m \neq 0} \sum_{nn'} (E_m - E_0)^{-1} (\psi_0 | \delta(\hat{r}_{ni}) \hat{S}_n \cdot \hat{I}_i | \psi_m) \qquad 3$$

$$(\psi_m | \delta(\hat{r}_{n'i'}) \hat{S}_{n'} \cdot I_i | \psi_0)$$

since the integration is to be carried out over the electrons, $\hat{I}_i$ and $\hat{I}_{i'}$ may be removed leaving

$$\hat{E}_{ii'} = \hat{I}_i \cdot \hat{J}_{ii'} \cdot \hat{I}_{i'} \qquad 4$$

and

$$\hat{J}_{ii'} = -2\left(\frac{16\beta h}{6}\right)^2 \gamma_i \gamma_{i'} \sum_{m\neq 0} \sum_{n} \sum_{n'} (E_m - E_0)^{-1} (\psi_0 | \delta(\hat{r}_{ni}) \hat{S}_n | \psi_m) \qquad 5$$

$$(\psi_m | \delta(\hat{r}_{n'i'}) \hat{S}_{n'} | \psi_0)$$

where $\hat{J}_{ii'}$ is a second rank tensor. It can be shown that $\hat{J}_{ii'}$ may be replaced by one-third the sum of its diagonal elements (3), that is $1/3\mathrm{Tr}(\hat{J}_{ii'})$, which is scalar. Therefore,

$$E_{ii'} = 1/3\mathrm{Tr}(\hat{J}_{ii'}) \hat{I}_i \hat{I}_{i'} \qquad 6$$

and

$$J_{ii'} = -\frac{2}{3h}\left(\frac{16\beta h}{6}\right)^2 \gamma_i \gamma_{i'} \sum_{m\neq 0} \sum_{n} \sum_{n'} (E_n - E_0)^{-1} (\psi_0 | \delta(\hat{r}_{ni}) \hat{S}_n | \psi_m) \cdot \qquad 7$$

$$(\psi_m | \delta(\hat{r}_{ni'}) \hat{S}_{n'} | \psi_0)$$

where $\mathrm{Tr}(\hat{J}_{ii'})$ has been written as the dot product of the two vectors involved in its definition and expressed in Hz by dividing by h.

McConnell (7) employed the use of LCAO-MO wave functions in the calculations of spin-spin couplings, $J_{ii'}$. These functions take the form

$$\psi_J = \Sigma C_{Ji} \phi_j \qquad 8$$

where the ϕ_j are the atomic orbitals of the atoms forming the molecule. It is possible to show the proportionality

$$J_{ii',\alpha-}(S_i|\delta(\hat{r}_i)|S_i)(S_{i'}|\delta(\hat{r}_{i'})|S_{i'})\ x \qquad 9$$

$$\sum_{k}^{occ}\ \sum_{l}^{unocc}\ (E_k-E_l)^{-1}C_{ki}C_{li}C_{ki'}C_{li'}$$

where S_i represents the valence s atomic orbitals, thus $(S_i|\delta(\hat{r}_i)|S_i)$ represents the square of the valence s electron density at the nucleus i. McConnell replaced the value of (E_k-E_l) by an average excitation energy $(^3\Delta E)$ which results in the expression of this proportionality by

$$J_{ii',\alpha-}(^3\Delta E)^{-1}(S_i|\delta(\hat{r}_i)\ S_i)(S_{i'}|\delta(\hat{r}_{i'})|S_{i'})P^2_{ii'} \qquad 10$$

where $P_{ii'}$, the bond order, is

$$P_{ii'} = 2\sum_{J} C_{Ji}C_{Ji'} = 2\sum_{K} C_{Ki}C_{Ki'}. \qquad 11$$

Proportionality 10 does not admit the possibility of negative contact interactions, which are indeed found experimentally, where as Equation 9 does allow this possibility. Indeed, according to the symmetry of the molecular orbitals involved in the k→l transitions which have some "s character" (i.e., have a value for C_{is} and $C_{i's}$) the signs of the C's will be positive or negative, and can give rise to either a positive or negative product for the C's.

The theory represented by Equation 9 has been applied to many systems of coupling nuclei. The refinement of the theory (8-15) has been based primarily upon refinements in the molecular orbital treatment which has been used and correspondingly better values for the energies of the various transitions involved. This theory has been applied especially by Pople and coworkers (8, 9) and Cowley and coworkers (10-12) in describing a wide variety of couplings between magnetic nuclei, including ^{1}H, ^{11}B, ^{13}C, ^{14}N, ^{17}O, ^{19}F, ^{29}Si and ^{31}P. However, no quantitative application of this theory to ^{31}P-^{31}P couplings over more than one bond has been made. This has been hampered somewhat by a lack of experimental results. There have been a large number of geminal ^{31}P-^{31}P coupling values reported (16) wherein the central atom is carbon, nitrogen, oxygen or a metal atom, but very few sign determinations have been reported for this type of coupling. There are only two values reported for vicinal ^{31}P-^{31}P coupling. These are for <u>trans</u> $(CH_3O)_2P(O)CH = CH(O)P(OCH_3)_2$ ($^{3}J_{PP}$ = 37.2 Hz(17)) and for $P(OCH_2)_3P$ (J = -38.1 Hz(18)) which was determined while this work was in progress. The sign of the former coupling was not reported. Numerous compounds have been synthesized (16) which give rise to vicinal ^{31}P-^{31}P coupling, but these values have not been reported.

It can be seen from the brief description which has been given of the theory of spin-spin coupling that the determination of the magnitudes and signs of these parameters offers a

potential source of information about chemical bonding. Thus, a correct picture of the eigenfunctions and eigenvalues of a given molecular system must correctly predict the magnitude and signs of the isotropic coupling constants between magnetic nuclei therein. Likewise, it should be possible to make a statement as to the changes in the bonding of such a collection of atoms resulting from changes in the nature of the groups which are attached to the coupling atoms or intervening bridging atoms. Such trends require knowledge of the trends in coupling constants as substitution changes. The determination of the signs of these parameters is very important, since a change in coupling constants can involve a change in sign. The importance of this possibility will be discussed later for cases where this occurs in the compounds which were investigated for this dissertation.

The methods by which the relative signs of spin-spin coupling constants are obtained from double resonance experiments have been discussed by several authors (19-23). An example of the application of secondary weak perturbing radio-frequency fields (24) to the determinations of the relative signs of spin-spin coupling constants in an AMX three spin system is described in the results section of this dissertation. The application of double resonance experiments employing the ^{13}C satellite resonances in the determination of the relative signs of the coupling constants, including $^{2}J_{PP}$ in a compound

such as cis $Mo[P(OCH_3)_3]_2(CO)_4$ has been discussed by Finer and Harris (21), and the results of such experiments on the latter compound are discussed in detail in the results section.

Aromatic Solvent Effects

It is known that proton chemical shifts are dependent upon the solvent used to dissolve the compound under investigation. The factors (25) which may influence proton chemical shift are (a) the solvent bulk susceptibility, (b) solvent magnetic anisotropy (c) Van der Waals interactions and (d) the reaction field of the solvent in the case of a polar solute. An analysis and discussion of the factors is contained in a recent review by Laszlo (26). In order to isolate the effect of one of these factors, the changes due to the other three must be minimized. In determining the effect of aromatic solvents upon chemical shifts, the effects due to bulk susceptibility changes can be overcome by the use of an internal reference standard, and using as a reference solvent one which has nearly the same bulk susceptibility as the aromatic solvent under investigation. Van der Waals interactions have a negligible contribution to the chemical shift when changing from an inert to an aromatic solvent (25). The reaction field of the solvent is not as easily ignored for polar solutes. The reaction field (27) is a secondary electric field which arises in a polar or polarizable solvent under the influence of the permanent dipole moment of the solute. The reaction field thus modifies the

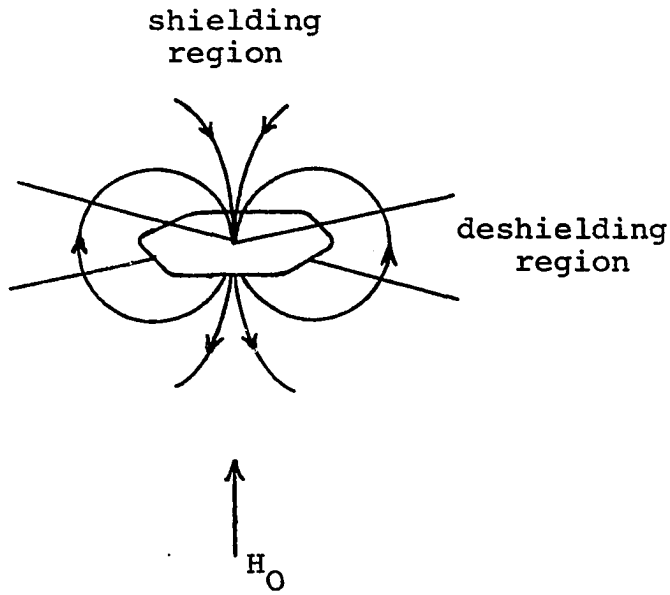
electronic distribution of the solute molecule. The extent of this perturbation depends upon the polarizability of the solvent and the dipole moment of the solute. This factor can be eliminated by using a reference solvent system which has the same polarizability or dielectric constant.

There are two very similar models which have been proposed to explain the shift change for protons in polar molecules when the solvent is changed from an inert solvent (e.g., carbon tetrachloride or n-hexane) to an aromatic solvent (e.g., benzene or toluene). Laszlo terms this effect the aromatic solvent induced shift (ASIS). One model involves a dipole-induced dipole collision complex between the solute and solvent that results in a specific orientation of the solvent molecule with respect to the dipolar functional group in the solute. Because of the anistoropy of the aromatic solvent molecule, the protons of the solute will be shielded or deshielded depending upon their position with respect to the complexed solvent molecule. The other model contains the proposal that charge transfer complexes are formed between the solvent and solute, thus ordering the solvent about the solute and allowing the magnetic anisotropy of the solute to affect proton chemical shifts.

The second model which has been proposed as the origin of ASIS involves the possibility of the formation of charge transfer complexes. It is similar to the induced-dipole-dipole model in that the configuration of the complex will be such

that the solute molecule will avoid the nodal plane of the aromatic solvent molecules which has no electrons for donation. Rather, the aromatic molecule will tend to bind the solute along its axis perpendicular to the plane. The resulting overlap which occurs between the donor and acceptor molecular orbitals concentrates electron density between the aromatic solvent molecule and the site of coordination. This process reduces the possibility of donation of electrons from the opposite face of the aromatic solvent molecule to another molecule of solute. Thus a 1:1 solvent:solute complex is postulated, and shielding or deshielding of the protons in the substrate molecule will occur depending upon their disposition with respect to the shielding and deshielding regions of the aromatic molecule in the complex.

The origin of the anisotropy of aromatic molecules has been the subject of a recent controversy. The original picture proposed by Pauling (28) states that π electrons of such molecules are free and that under the influence of a magnetic field, an interatomic current will be established. This current will generate a magnetic field opposed to the applied magnetic field at the center of the ring. Lines of magnetic flux are then established as shown below,



The field at the edge of the ring is then in the same direction as the applied field. Thus, aromatic protons resonate at lower fields than protons in saturated hydrocarbons. Protons which are above the center of the ring would then be expected to be highly shielded, as is observed for p-polymethylene benzenes (29). Using this concept, Johnson and Bovey (30) calculated values which are expected for the shielding contributions from such ring currents as a function of position relative to the center of benzene. Musher has challenged the mathematical ideas underlying the concept of ring currents (31, 32). His challenge rests upon his conclusion that the physical picture of the circulation of delocalized electrons giving rise to large susceptibilities is invalid since this model is based

upon the incorrect non-gauge-invariant Langevin-Pauli formula of diamagnetism. Furthermore, he points out errors in mathematical manipulation in the original treatment which if corrected, do not lead to the concept of ring currents. Replacement of the Langevin-Pauli formula with the presently accepted Van Vleck formula for diamagnetism is not consistent with the ring current theory. Gaidis and West (33) attempted to support the concept of ring currents but were rebutted by Musher (34). Musher concludes that the anisotropy of aromatics results from the sum of the anisotropies of the C-C and CH bonds formed in planar arrangement and he is able to correctly calculate the anisotropies of numerous aromatics on this basis. Whatever the origin of the anisotropy of aromatic molecules, this property is undoubtedly responsible for the effects which were discussed above.

There are four characteristics which describe these models. First of all, the solvent must interact with the solute in a specific geometry as was discussed previously. Secondly, these models require the existence of a solute:solvent interaction which can be formally described as an effective 1:1 complex. The determination of the actual stoichiometry of these complexes is difficult to prove. The equilibrium considerations which follow are based on an effective 1:1 complex. Thus the equilibrium

$$A + S \rightleftharpoons AS \qquad 12$$

can be expressed as a formation constant

$$K = \frac{(AS)}{(A)(S)} \qquad 13$$

where (A), (S) and (AS) are the concentrations of the solute, solvent and complex, respectively. If the usual assumption is made that the observed chemical shift is the weighted average of the chemical shifts of the free solute, δ_0^A, and the pure complex, δ_{AS}^A, it can be shown (35) that

$$\Delta = \delta_{obs}^A - \delta_0^A = \frac{(S)}{1+(S)K}(\delta_{AS}^A - \delta_0^A) = \frac{(S)}{1+(S)K}\Delta_0 \qquad 14$$

where Δ is the observed shift resulting from the association and Δ_0 is the chemical shift of the pure complex. Further, the equations

$$\frac{1}{\Delta} = \frac{1}{K\Delta_0}\frac{1}{(S)} + \frac{1}{\Delta_0} \qquad 15$$

and

$$\frac{\Delta}{(S)} + \Delta K = \Delta_0 K \qquad 16$$

can be derived. It can be seen from Equation 16 that if the 1:1 complex exists, a plot of $\Delta/(S)$ versus Δ should yield a straight line of slope -K. Fort (36) has indicated that the converse is not necessarily true.

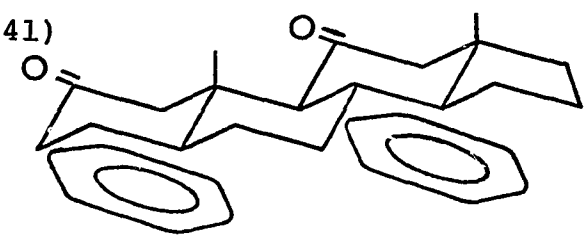
Thirdly, the 1:1 solute:solvent interaction models proposed allow the calculation of the entropy and enthalpy of formation of the complexes from shift versus temperature data. (See the results section.)

The fourth characteristic of these models involves the lifetimes of the complexes. In the liquid phase, the time a molecule spends in a given orientation between collisions is 10^{-10} to 10^{-11} sec. (26) which represents the minimum duration of any complex. However, the nmr time scale is much slower. In order to observe resonances due to a free molecule and a complexed molecule, the lifetime of the complex must be longer than the reciprocal of the frequency difference between the resonances. The shifts involved for the ASIS phenomenon are in the range 0-60 Hz which fixes the lifetime limit at $\sim 10^{-2}$ sec. In other words, the aromatic solvent molecules are exchanging faster than the individual shifts of either the uncomplexed or complexed solute molecules can be detected by nmr spectroscopy. Thus, an averaged spectrum which is weighted by the population of the two individual components is observed.

It might be mentioned that Kuntz and Johnston (37) have proposed a collision complex model in which the reaction field effect is not considered in explaining the effect of nonaromatic solvents upon the chemical shift of protons in polar molecules. They derived equations expressing the expected dependence of the chemical shift of solute protons upon concentration of active solvent in an inert solvent for 1:1 complexes, as well

as complexes with other stoichiometries. These authors point out that equilibria involving 1:1 or 1:1 and 1:2 solute:solvent complexes are sufficient to empirically describe the observed effects. However, they do not consider the mechanism by which the solvents studied bring about the observed shifts.

Numerous studies have been reported concerning the effect of aromatic solvents on the chemical shifts of protons in molecules containing polar substituents. Proton shifts in aromatic solvents have been observed for molecules containing carbonyl, nitro, and nitrile substituents (26, 38, 39) and from the bulk of the literature on this subject (26), significant proton chemical shift differences in such molecules are generally found. Important applications of the ASIS phenomenon to configurational and conformational analysis has been made (26), particularly in the field of steroid molecules. A broad study of this area by Williams and coworkers was recently reviewed by Williams (40). These investigators have proposed a model in which a 1:1 collision complex is formed between the solute and solvent molecules wherein the aromatic solvent is oriented in a particular fashion by the polar substituent, as shown below, (41)



The interaction between the ketone and the aromatic solvent is believed to be a dipole-induced-dipole interaction. The dipole moment of the carbonyl function is parallel to the plane of the steroid, and in the complex, the plane of the solute and solvent are parallel. Protons which are nearby experience the effect of the diamagnetic anisotropy of the benzene ring, and are either shielded or deshielded to an extent determined by their location with respect to the complexed solvent.

The system which was studied for this dissertation involves polar bicyclooctane type molecules, such as $HC(OCH_2)_3CCH_3$ or $P(OCH_2)_3CCH_3$ in benzene and toluene. The results of the study are interpreted in terms of a collision complex model similar to the first of those just described. Temperature studies were also carried out to determine the enthalpy and entropy of formation of these complexes. Results of studies using the aromatic solvent hexafluorobenzene are also included which are also explained in terms of a collision complex, but with a different geometry than that postulated to occur with the hydrocarbon aromatics.

EXPERIMENTAL

Materials

The transition metal complexes of ligands other than $P(OCH_2)_3P$ were a generous gift of Mr. Frederic B. Ogilvie while those of $P(OCH_2)_3P$ were generously supplied by Mr. David Allison as were $SP(OCH_2)_3P$, the phosphonium salts of this ligand and $OP(CH_2O)_3CCH_3$. The compounds $P(OCH_2)_3CH_3$ (42), $HC(OCH_2)_3CCH_3$ (43), $OP(OCH_2)_3PO$ (44), $SP(OCH_2)_3PO$ (44) and $P(CH_2O)_3CCH_3$ (45) were prepared by methods previously reported in the literature. The bicyclic phosphite $P(OCH)_3(CH_2)_3$ and the orthoacetate $CH_3C(OCH_2)_3CCH_3$ were a gift of Dr. Ross Compton. Deuterochloroform was obtained from Columbia Organic Chemicals Co., Inc. Deuteroacetonitrile and hexadeuterobenzene were obtained from Merk Sharp & Dohme of Canada Limited. Hexadeuterodimethylsulfoxide was obtained from Mallinckrodt Chemical Works. Trifluoroacetic acid (white label) was obtained from Eastman Organic Chemicals, as was the trimethyl phosphite (yellow label), triethyl orthoformate (white label) and trimethyl orthoacetate (white label). The trimethyl phosphite was purified by distillation from sodium whereas the white label compounds were used without further purification. Non-deuterated nmr solvents were reagent grade. Acetonitrile was dried by storing over Linde 3A molecular sieves. Benzene, toluene and n-hexane were purified by refluxing over sodium with a small quantity of benzophenone. When the solutions

became blue because of the formation of the water sensitive $Na^{+}[(C_6H_5)_2C\text{-}O]^{-}$, distillation was carried out through an 8" vigeroux column. Hexafluorobenzene was obtained from Aldrich Chemical Co., Inc., and used without further purification. Tris-dimethylamino phosphine (white label) was obtained from Eastman Organic Chemicals and purified by distillation on a platinum spinning band column (55°/10 mm). Hexamethylphosphoramide was obtained from Aldrich Chemical Co., Inc., and used without further purification.

Preparations

2,6,7 trioxa-1,4-diphosphabicyclo[2.2.2.]octane

This compound was prepared by the method of Coskran and Verkade (44) utilizing the modifications developed by Guyer, Rathke and Verkade (46).

1,4-dimethyl-2,6,7-trioxa-1-phosphabicyclo[2.2.2]octane tetrafluoroborate

To a suspension of 3.0 g (20 mmoles) of trimethyloxonium tetrafluoroborate (prepared according to the procedure of Meerwein (47)) in 10 ml of methylene chloride was added slowly 3.0 g (20 mmoles) of $P(OCH_2)_3CCH_3$ dissolved in 10 ml of methylene chloride. The reaction mixture immediately began to effervesce, indicating the loss of dimethyl ether. Crystals formed upon cooling to -20° which were collected by suction filtration and dried in vacuo. The compound was characterized

by its proton nmr spectrum in CD_3CN which indicated a singlet due to the 4-methyl protons at δ = 1.00 ppm, a doublet due to the 1-methyl protons at δ = 2.32 ppm ($^2J_{PH}$ = 19 Hz) and a doublet due to the methylene protons 4.87 ppm ($^3J_{PH}$ = 5 Hz) relative to TMS as an internal standard. The yield was ∿75%.

Trimethoxymethylphosphonium tetrafluoroborate

This compound was prepared as above using trimethyl phosphite. The solid was obtained as above in ∿50% yield. The proton nmr spectrum in CD_3CN indicates a doublet due to the methyl protons at δ = 2.14 ppm ($^2J_{PH}$ = 18 Hz) and a doublet due to the methoxy protons, δ = 4.10 ppm ($^3J_{PH}$ = 11 Hz) relative to TMS as an internal standard.

Instrumentation

The solvent-dependent nmr chemical shifts were measured on a Varian A-60 nmr spectrometer equipped with a variable temperature probe. Frequency calibration was provided by the use of standard sideband techniques (1) employing a Hewlett-Packard model 200 CD audio frequency oscillator as well as a Hewlett-Packard model 521 CR frequency counter. Chemical shifts are believed accurate to ±.1 Hz. Temperature calibration was accomplished by measuring the chemical shift of the hydroxyl proton with respect to either the methyl or methylene resonances for methanol or ethylene glycol, respectively, at each temperature, and obtaining the value of the temperature from the plot of chemical shift versus temperature supplied by Varian in the

A-60 operating manual. The temperature stability of this system is reported to be ±1°. Internal tetramethyl silane (~5% V/V) was used as the standard.

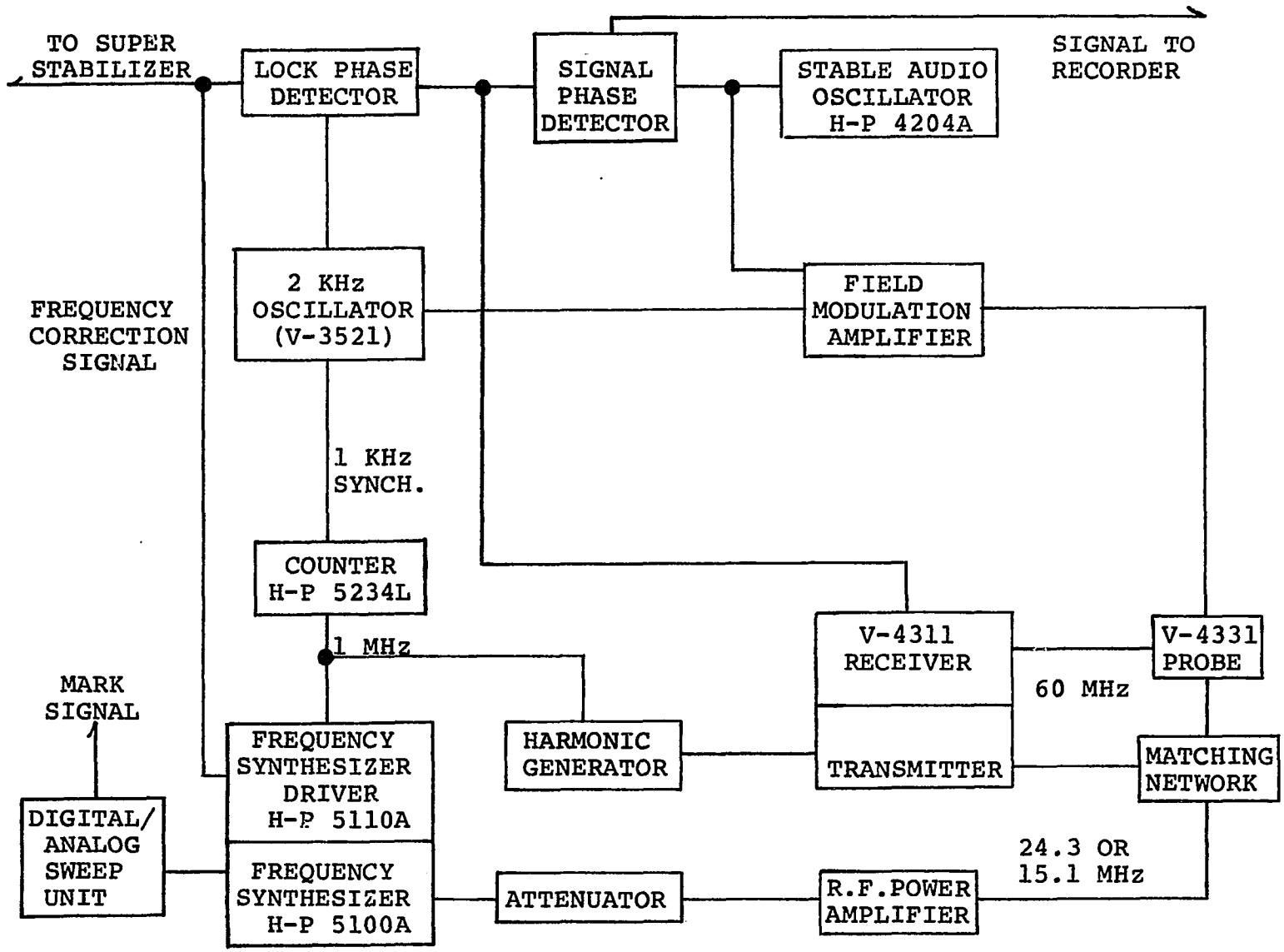
The double resonance experiments necessary for determining the relative signs of the spin-spin coupling constants were performed on a Varian HR-60 nmr spectrometer operating at 14,100 gauss modified for field-frequency lock. The instrument is provided with a Hewlett-Packard model 5100A frequency synthesizer and model 5110A frequency synthesizer driver as well as a Hewlett-Packard model 5243L frequency counter. The V-4331 probe is double tuned to accept either the 15.09 MHz or 24.29 MHz perturbing frequency for ^{13}C or ^{31}P, respectively, from the frequency synthesizer simultaneously with the 60.00 MHz frequency from the V-4311 radio frequency source. The field-frequency locking circuits are activated by phase detection (in dispersion mode) of a sharp resonance signal of an internal standard. The signal detected is the first upper-field 2KHz sideband produced by field modulation of the main resonance signal. Any drift in the field produces a change from zero of the voltage of this signal. This voltage is returned to zero by means of the application of a small current to the galvanometer of the flux stabilizer in such a way that the field is changed in a sense opposite to the drift. The lock phase detector is tied in with the synthesizer driver. Frequency stabilization is provided by tying the 2KHz field modulation

oscillator circuits, the V-4311 transmitter circuits, the frequency counter clock and the signal phase detector to either the frequency synthesizer or the synthesizer driver. The spectrometer can be operated in frequency sweep mode by application of an additional field modulation frequency. This spectrometer is also equipped with a digital/analog sweep circuit which allows sweeping one decade of the frequency synthesizer, or a Wavetech model 111 voltage controlled oscillator, either of which may be used as the secondary frequency source. The time base for the digital/analog sweep circuit is derived from the frequency synthesizer. By the application of a fixed frequency from a very stable oscillator (Hewlett-Packard model 4204A), it is possible to set the field modulation to a frequency which corresponds to the maximum amplitude of a resonance absorption signal to be investigated. Using the digital/analog sweep unit and synthesizer, frequencies corresponding to those necessary for the resonance condition of other nuclei (^{31}P or ^{13}C) at ∿14,100 gauss can be scanned producing INDOR spectra of the other nuclei (48). The stability of the spectrometer is on the order of one part in 10^8 for several weeks. A block diagram indicating the configuration of the components comprising the spectrometer is shown in Figure 1.[1]

---

[1]King, R. W., Ames, Iowa. Block diagram of modified Varian HR-60 N.M.R. spectrometer. Private communication. 1969.

Figure 1. A block diagram of the Varian HR-60 nmr spectrometer modified for field-frequency lock


TO SUPER STABILIZER
LOCK PHASE DETECTOR
SIGNAL PHASE DETECTOR
STABLE AUDIO OSCILLATOR H-P 4204A
SIGNAL TO RECORDER
FREQUENCY CORRECTION SIGNAL
2 KHz OSCILLATOR (V-3521)
FIELD MODULATION AMPLIFIER
1 KHz SYNCH.
COUNTER H-P 5234L
1 MHz
V-4311 RECEIVER
V-4331 PROBE
60 MHz
MARK SIGNAL
FREQUENCY SYNTHESIZER DRIVER H-P 5110A
HARMONIC GENERATOR
TRANSMITTER
MATCHING NETWORK
DIGITAL/ ANALOG SWEEP UNIT
FREQUENCY SYNTHESIZER H-P 5100A
ATTENUATOR
R.F.POWER AMPLIFIER
24.3 OR 15.1 MHz

Calibration of the spectra was performed in the following way. The digital/analog sweep unit which drove the frequency synthesizer was capable of triggering a marking pen attached to the Varian G-10 chart recorder at a fixed time interval that could be varied by the operator. The marks made by this pen could then be assigned frequencies to $\pm$.1 Hz by stopping the sweep unit at a point corresponding to the various marks on the chart. The radio frequency output of the synthesizer could then be read from the frequency counter. Spectra were recorded by sweeping in both frequency directions and the centers of the various resonance peaks were determined by linear interpolation. The results for the two scans were then averaged. A typical sweep rate for the ^{31}P INDOR frequency was 0.15 Hz/sec while it was 0.03 Hz/sec for ^{13}C INDOR spectroscopy.

The spectra were obtained on saturated solutions of the compounds studied in the solvents indicated in the results section. The HR-60 probe temperature was determined to be 27.5°C.

RESULTS

Theoretical Considerations

There are two general methods which may be employed in determining the signs of coupling constants when direct analysis of the spectrum does not afford such information. One of these is to determine directly the signs of coupling constants by methods described by Buckingham (49). The experiment involves the determination of the high resolution nmr spectrum of the molecule which contains the coupling nuclei under conditions such that the molecule is partially oriented with respect to the magnetic field. In such a situation the molecules under investigation have translational motion but only limited rotational freedom. Thus, the anisotropic dipole-dipole couplings between magnetic nuclei within the same molecule do not average to zero and give rise to large splittings in the magnetic resonance spectrum. By analysis of the perturbation of the isotropic spin-spin coupling upon this spectrum, the signs of the isotropic spin-spin coupling constants as well as other molecular parameters are obtained. The orientation which is required can be forced by imposing large electric fields on the sample containing the polar molecules of interest, or obtaining the nmr spectrum in a solvent which is in a nematic phase.

The experiments are difficult to perform, however, and the alternate method of obtaining the signs of spin-spin

coupling constants employs the double resonance experiment. This type of internuclear double resonance (INDOR) experiment relates the energy levels involved in the nuclear spin transitions of one nucleus with those of another with which coupling occurs. The relationship between the ordering of the transition energies of one nucleus with respect to the order of the transition energies of a second nucleus which is coupled to the first nucleus can be determined when both nuclei are coupled to a third nucleus. This information yields the relative signs of the couplings of the first two nuclei to the third. A proof of the relationship by which the relative signs of coupling constants can be related from double resonance experiments is given by Friedman and Gutowsky (22) and is further discussed by Whiffen (23) for the case in which the magnetogyric ratios of the coupling nuclei have different signs. The nuclei which were studied for this dissertation all have nuclear spin $I = \frac{1}{2}$ and have the same sign for their magnetogyric ratios. Thus the determination of the relative signs of coupling constants from double resonance experiments is relatively straightforward.

If one of the coupling constants has a sign which is known from other experiments and is known not to change sign under differing chemical conditions, and if the other two signs can be related to this sign, the absolute signs of the other two couplings are determined. For example, the sign of $^{1}J_{CH}$ is known to be positive (49) in numerous cases. Since the values observed for this coupling fall in the range of 110 to 220 Hz

(49) with no values close to zero it is postulated that the coupling is always positive. Relating the signs of other couplings to this positive coupling constant in a given molecule then determines the absolute sign of the other coupling constants.

As an example of how the signs of the couplings in a three and four spin system are determined, a description of the experiments which were performed on $OP(OCH_2)_3PO$ will be given. First, the three spin system consisting of the protons and the two phosphorus atoms in molecules of $OP(OCH_2)_3PO$ that contain only ^{12}C atoms will be considered. In order to determine the relative signs of the coupling constants, the manner in which the various transitions for the coupling nuclei are related must be determined, and this can be done by double resonance experiments. This author has employed the internuclear double resonance technique (to INDOR) which is now described.

The procedure for obtaining INDOR spectra and deducing the connectedness of the various transitions involves setting the spectrometer so as to continuously monitor one of the proton resonances. That is, the observing frequency is set to correspond to the maximum amplitude of one of the resonances without perturbing it, i.e., without saturation. The spectrometer described in the experimental section only allows this to be done with the proton region. Then, radiofrequency power is applied to the probe which corresponds in frequency to that necessary to cause transitions of the nuclei under investigation,

i.e., ∿24.29 MHz for ^{31}P or 15.08 MHz for ^{13}C. It is possible to sweep these radiofrequency regions and by using small amplitudes of such a secondary irradiating frequency, the frequencies which perturb the transition under observation can be detected. Only frequencies which correspond to transitions of the irradiated nucleus having an energy level in common with the resonance under observation will perturb the line under observation.

Transitions of a particular state can be represented by a change in the product spin eigenfunction of a particular nucleus representing the eigenvalues of the system. For spin-$\frac{1}{2}$ nuclei, there are two spin states that this nucleus can possess (i.e., α and β) and transitions involving absorption of energy of a particular nucleus correspond to an $\alpha \rightarrow \beta$ change. A particular state of a collection of such nuclei can be represented by a product of these functions for each nucleus.

For the case at hand there are actually six protons and two phosphorus atoms, thus, the product function describing any single state of the system is composed of eight α's and/or β's. However, a change of only one of the six protons from α to β will give rise to an absorption in the proton region. Thus for any particular combination of the two spin functions of the two phosphorus nuclei, a change in spin state for any one of the protons gives rise to a transition and so the resonance lines observed in the proton spectrum are multiply degenerate. It

should be noted that the energy of the transition of any of these equivalent protons is the same as for any other, no matter what the spin states of the other protons are. Since there are four distinct product functions of the two phosphorus spins ($\alpha\alpha$, $\alpha\beta$, $\beta\alpha$, $\beta\beta$), each of these states gives rise to a degenerate transition in the proton spectrum.

The observed nmr spectrum for the proton region as well as the ^{31}P region is represented schematically in Figure 2. The actual INDOR spectra that were obtained are reproduced in Figure 3. Table 1 gives a representation of the origins and and connectednesses of the transitions in terms of the product spin functions involved in the various transitions. This representation was deduced from the results of the experiments indicated by Figure 2 and its essential features depend upon the sign relation between the coupling constants.

As indicated, transitions in the proton spectrum result from one of the six protons changing spin, $\alpha \rightarrow \beta$. Instead of indicating the possible transitions which are degenerate for the protons, the general case is indicated by placing the proton spin function in parentheses. Transitions in the ^{31}P spectrum occurs because one of the phosphorus nuclei changes spin. As a result of the various product functions possible for the six equivalent proton spins, the phosphorus resonances occur as septets. Rather than writing out all these combinations of spin functions for each phosphorus transition, the composite of product functions is indicated by (^{1}H) for each band.

Figure 2. A schematic representation of the ^{1}H and ^{31}P spectra of $OP(OCH_2)_3PO$

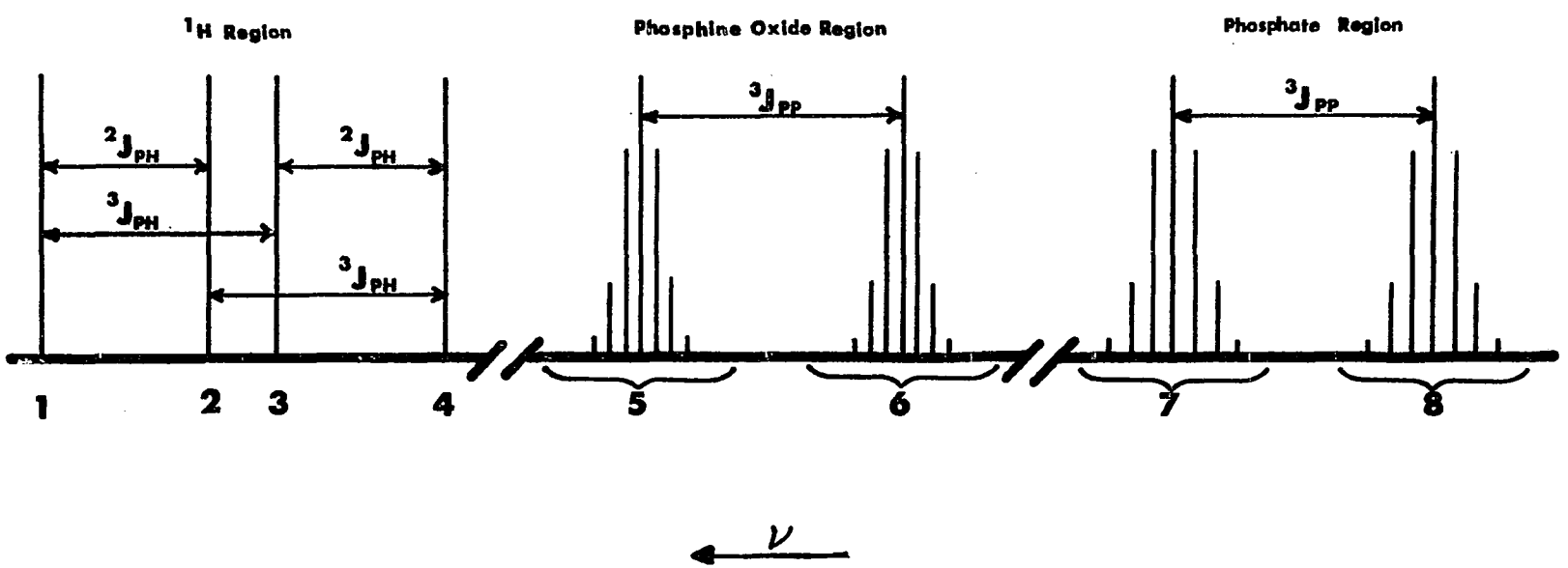

^{1}H Region
Phosphine Oxide Region
Phosphate Region
$^2J_{PH}$
$^3J_{PH}$
$^2J_{PH}$
$^3J_{PH}$
$^3J_{PP}$
$^3J_{PP}$
1
2
3
4
5
6
7
8
ν

Figure 3. The INDOR spectra of $OP(O^{12}CH_2)_3PO$ in d_6-DMSO

The numbers in parentheses represent the modulation frequency used to observe a particular proton resonance when the spectrometer was locked on benzene at exactly 60.002 MHz. The nine-digit numbers represent the frequency of the perturbing radio frequency at the center of each of the four septets. The splittings due to $^2J_{PH}$, $^3J_{PH}$ and $^3J_{PP}$ are indicated and have average observed values of -8.2, +8.3 and +139.1 Hz, respectively. Only the center three numbers of each septet are shown.

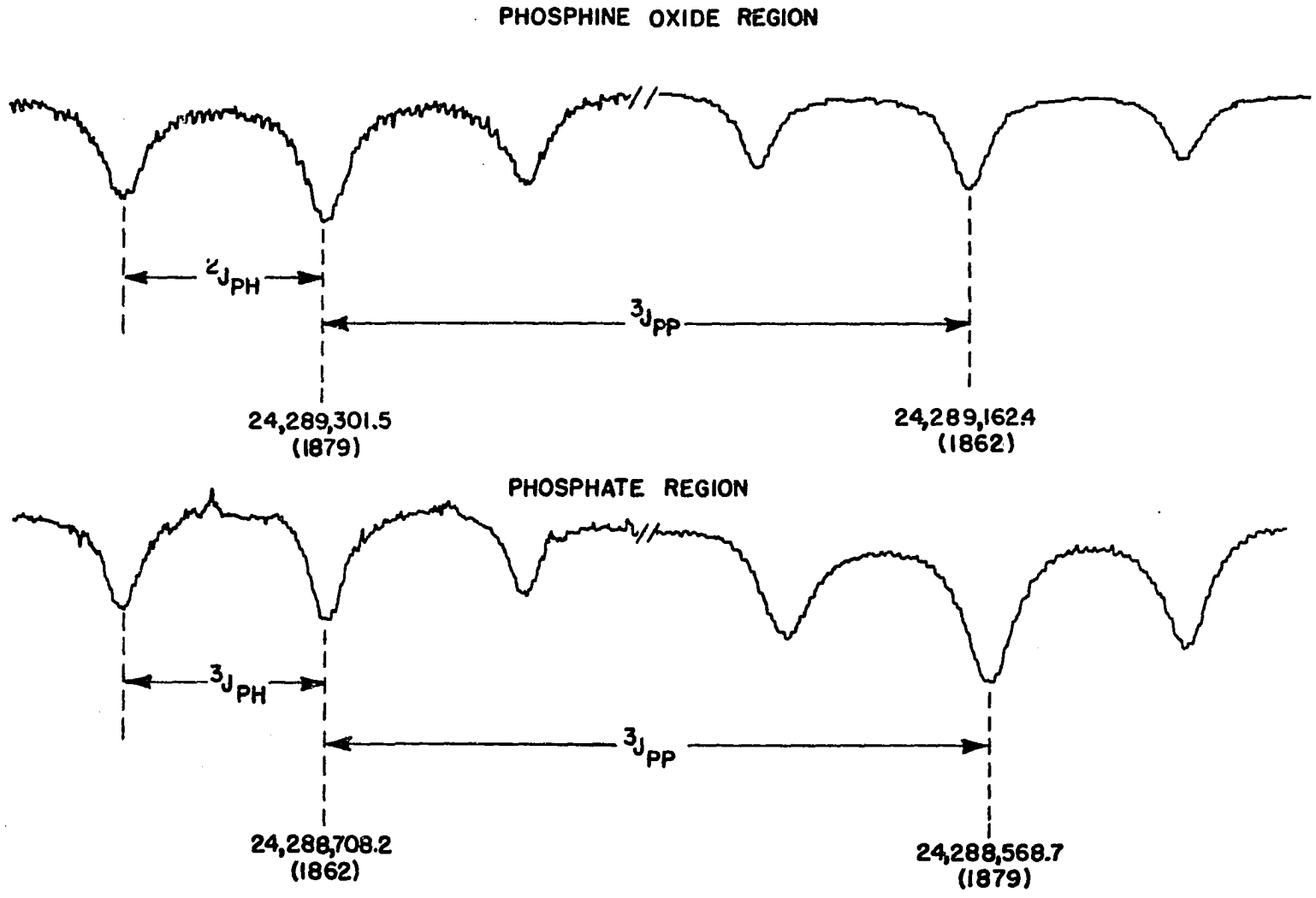

PHOSPHINE OXIDE REGION
$^2J_{PH}$
$^3J_{PP}$
24,289,301.5
(1879)
24,289,162.4
(1862)
PHOSPHATE REGION
$^3J_{PH}$
$^3J_{PP}$
24,288,708.2
(1862)
24,288,568.7
(1879)

Table 1. A representation of the origin and connectedness of the ^{1}H and ^{31}P nmr lines of $OP(OCH_2)_3PO$ given in Figure 2. These results were obtained from INDOR experiments on the ^{1}H spectrum

Line(s)	Origin[a]	Connectedness[b]
1	$(\alpha)^{c}\alpha\alpha\rightarrow(\beta)\alpha\alpha$	5,8
2	$(\alpha)\beta\alpha\rightarrow(\beta)\beta\alpha$	5,7
3	$(\alpha)\alpha\beta\rightarrow(\beta)\alpha\beta$	6,8
4	$(\alpha)\beta\beta\rightarrow(\beta)\beta\beta$	6,7
5	$(^{1}H)^{c}\alpha\alpha\rightarrow(^{1}H)\beta\alpha$	1,2
6	$(^{1}H)\alpha\beta\rightarrow(^{1}H)\beta\beta$	3,4
7	$(^{1}H)\alpha\beta\rightarrow(^{1}H)\beta\beta$	2,4
8	$(^{1}H)\alpha\alpha\rightarrow(^{1}H)\alpha\beta$	1,3

[a]The spin functions are ordered ^{1}H, $^{31}P(CH_2)_3$ and $^{31}P(O)_3$.

[b]The first four sets of numbers in this column represent the lines which when irradiated are found to perturb lines (1-4) in the ^{1}H spectrum. The remaining sets are found by deduction from the connectedness of first four.

[c]See text.

The data represented in Figure 2 were taken by employing lines 1 and 4, the highest and lowest frequency lines in the proton spectrum. The connectedness of lines 2 and 3 to the lines in the ^{31}P spectrum can be deduced from these experiments by considering how the indicated couplings split this portion of the spectrum. It can be seen that the difference between

line 1 and 2 involves a change in the spin state of the phosphine oxide phosphorus, but that line 2 has the same spin function as line 1 for the phosphate phosphorus. Therefore, since it was shown experimentally that line 1 connects line 5 in the phosphine oxide region, line 2 must also connect here. The difference between band 5 and 6 involves a change in the spin state of the phosphate phosphorus. Likewise, the difference between band 7 and 8 is a change in the spin state of the phosphine oxide phosphorus. Hence line 2 must be connected to band 7 if line 1 was connected to band 8. By similar arguments, the connectedness of line 3 to band 6 and 8 can be deduced.

It may be inferred from the proof of Freidman and Gutowsky that by observing the effect of irradiating the resonances in the phosphine oxide region upon the transitions in the proton spectrum, that the sign relationships between the coupling of the phosphorus nuclei and the coupling between the phosphate phosphorus and the protons is determined. This is so because as stated earlier the difference between bands 5 and 6 is a difference in the spin state of the phosphate phosphorus, and by the irradiation of these bands, a determination has been made of the relative ordering of the spin functions of the phosphate phosphorus as revealed by $^{3}J_{PP}$ to the ordering of the proton spin functions as revealed by $^{3}J_{PH}$. An analogous result obtains for $^{3}J_{PP}$ and $^{2}J_{PH}$ from irradiation in the phosphate

phosphorus region. Since the relative signs of these coupling constants determines the ordering of the transitions, a determination of the origins of the transitions allows the determination of the relative signs of the couplings.

The lowest frequency ^{1}H line is perturbed by irradiation of the high-frequency member of the ^{31}P doublet. This means that $^{2}J_{PH}$ is opposite in sign to $^{3}J_{PP}$. Tickling in the phosphine oxide ^{31}P region reveals that the highest-frequency member of the ^{1}H spectrum is perturbed by irradiating the high-frequency member of the phosphine oxide ^{31}P doublet. Consequently, $^{3}J_{PH}$ is opposite in sign to $^{3}J_{PP}$. The values of the couplings $^{3}J_{PH}$ and $^{2}J_{PH}$ are obtained from the splittings in the ^{1}H spectrum as well as from the splittings in the INDOR spectra. $^{3}J_{PP}$ is the spacing between the centers of the two septets of the phosphate or phosphine oxide ^{31}P region.

The natural abundance of ^{13}C is 1.1% and so 3.3% of the molecules of $OP(OCH_2)_3PO$ will have one ^{13}C atom. Since ^{13}C has a spin I of 1/2, the observable feature of the proton nmr spectrum of these molecules in natural abundance is a pair of satellite resonances nearly equidistant from the resonances due to the molecules not containing ^{13}C atoms. The separation of these two satellites from each other is $^{1}J_{CH}$. The intensity of each satellite resonance is about 0.5% of that due to molecules not containing ^{13}C. These resonances are difficult to observe unless the spectra are obtained on neat liquids or the solubility in a suitable solvent is at least 25% wt./vol. Also

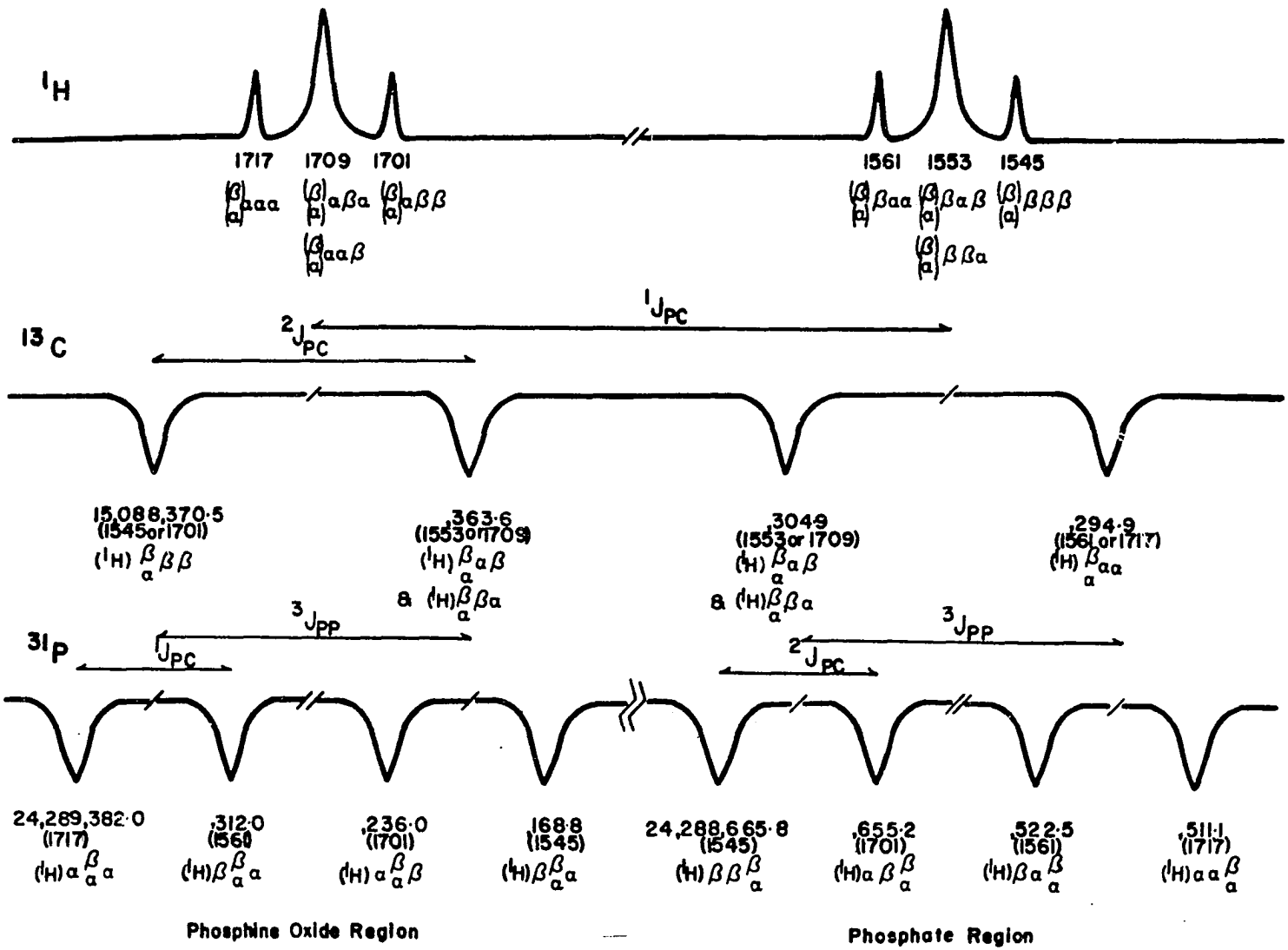
present are molecules of $OP(OCH_2)_3PO$ having two ^{13}C atoms. Their abundance is so low, however, that they are undetectable in natural abundance by single scan nmr spectroscopy.

By observing the resonances due to those molecules of $OP(OCH_2)_3PO$ that have one ^{13}C atom, it is possible to relate $^3J_{PH}$ to $^1J_{CH}$ via $^2J_{PC}$, and $^2J_{PH}$ to $^1J_{CH}$ via $^1J_{PC}$ by the same sort of experiment described above. Since $^3J_{PP}$ can be related to both $^3J_{PH}$ and $^2J_{PH}$ by these methods, the sign of $^3J_{PP}$ relative to these couplings is determined by two apparently independent routes. Moreover, since $^1J_{CH}$ is assumed to be positive, the signs of the other couplings can be determined absolutely.

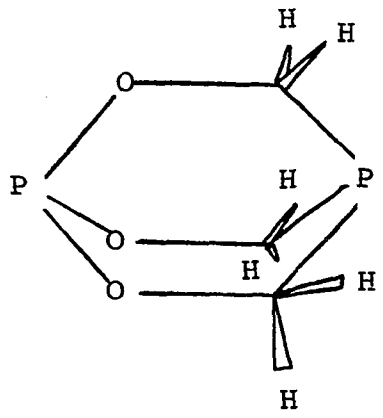
The results obtained for the double resonance experiments employing the ^{13}C satellite resonances of the ^1H spectrum of $OP(OCH_2)_3PO$ are represented schematically in Figure 4. Associated with each resonance is a set of product spin functions which is consistent with the observed connectedness. At the top of the figure is represented the ^{13}C proton satellites, each of which was composed of three broad lines having width at half-height of 6 Hz. This broadness is undoubtedly due to long-range coupling from protons in the molecule not located on the ^{13}C atoms. Molecular models show quite clearly that each ^{13}C methylene proton in a molecule containing a ^{13}C methylene carbon is in a planar "W" configuration with a chemically and magnetically different proton on each of the ^{12}C methylene carbon

Figure 4. A schematic representation of the ^{1}H spectrum of $OP(OCH_2)_3PO$ containing one atom of ^{13}C per molecule and the results of INDOR experiments in the ^{13}C and ^{31}P region

The numbers in parentheses represent the modulation frequency used to observe a particular proton resonance when the spectrometer was locked on the OH resonance of the solvent, trifluoroacetic acid at exactly 60.002 MHz. The nine-digit numbers represent the frequencies of the perturbing radio frequency at the center of each line shown. Only the last four digits of the nine-digit numbers are given for all but one of the lines for any of the resonances due to a particular nucleus, since the first five are the same. The splittings in the INDOR spectra due to $^{1}J_{PC}$, $^{2}J_{PC}$ and $^{3}J_{PP}$ are indicated.


^1H
1717 1709 1701
$\binom{\beta}{\alpha}\alpha\alpha\alpha$ $\binom{\beta}{\alpha}\alpha\beta\alpha$ $\binom{\beta}{\alpha}\alpha\beta\beta$
$\binom{\beta}{\alpha}\alpha\alpha\beta$
1561 1553 1545
$\binom{\beta}{\alpha}\beta\alpha\alpha$ $\binom{\beta}{\alpha}\beta\alpha\beta$ $\binom{\beta}{\alpha}\beta\beta\beta$
$\binom{\beta}{\alpha}\beta\beta\alpha$
$^1J_{PC}$
$^2J_{PC}$
^{13}C
15,088,370·5
(1545 or 1701)
$(^1H)\ \beta_\alpha\beta\beta$
,363·6
(1553 or 1709)
$(^1H)\ \beta_\alpha\beta$
& $(^1H)\beta_\alpha\beta\alpha$
3049
(1553 or 1709)
$(^1H)\ \beta_\alpha\beta$
& $(^1H)\beta_\alpha\beta\alpha$
,294·9
(1561 or 1717)
$(^1H)\ \beta_{\alpha\alpha}$
$^3J_{PP}$
$^1J_{PC}$
^{31}P
$^3J_{PP}$
$^2J_{PC}$
24,289,382·0
(1717)
$(^1H)\alpha\beta_\alpha\alpha$
,312·0
(1561)
$(^1H)\beta\beta_\alpha\alpha$
,236·0
(1701)
$(^1H)\alpha\beta_\alpha\beta$
168·8
(1545)
$(^1H)\beta\beta_\alpha\alpha$
24,288,665·8
(1545)
$(^1H)\beta\beta\beta_\alpha$
,655·2
(1701)
$(^1H)\alpha\beta\beta_\alpha$
,522·5
(1561)
$(^1H)\beta\alpha\beta_\alpha$
,511·1
(1717)
$(^1H)\alpha\alpha\beta_\alpha$
Phosphine Oxide Region
Phosphate Region

atoms, as shown. This configuration is known to be conducive



to four-bond couplings and gives rise to a coupling of about 2 Hz (50). It should also be mentioned that the proton spectrum due to molecules containing only ^{12}C was a simple triplet in trifluoroacetic acid and not a doublet of doublets as observed in d_6-DMSO. Some of the poorer resolution then must have arisen from the small but detectable solvent dependences of $^{2}J_{PH}$ and $^{3}J_{PH}$. Because of the apparent slow decomposition of $OP(OCH_2)_3PO$ in d_6-DMSO, trifluoroacetic acid was used as the solvent for the lengthy INDOR work on the ^{13}C satellites. The consequence of the overlap of the central peaks of the doublet of doublets will be discussed shortly.

The ^{13}C INDOR spectrum shown in Figure 4 is the central doublet of doublets of the triplet of doublet of doublets expected. This spectrum arises as a result of splitting due to the coupling by the two directly bound protons ($^{1}J_{CH}$ = 156.7 Hz) and the two unlike phosphorus nuclei ($^{1}J_{PC} \cong 68$ Hz, $^{2}J_{PC} \cong 9$ Hz).

The ^{13}C INDOR lines were quite broad, possibly due to coupling between the ^{13}C atom and protons on the ^{12}C methylene carbons.

The ^{31}P INDOR spectrum resulting from those molecules that have one ^{13}C is as expected (Figure 4). Each of the different phosphorus nuclei are split into a doublet of doublets by spin-spin coupling with the other phosphorus and coupling to ^{13}C. The spectrum is broadened by unresolved coupling to the protons.

The analysis of a four spin system has been performed by Baker (51) using a complete energy level diagram, but this method is arduous. The present author has analyzed this system using a subspectral approach. Although the method has not been explicitly set out, it is implicit in the work of others (19, 20, 52). Groups of three nuclei are considered in which one member of the group is always the protons. The composite of two protons on a single ^{13}C is assumed to behave effectively as one spin since they are equivalent.

Consider the three spin system composed of the protons and the two phosphorus nuclei employing the ^{13}C satellites in the ^{1}H spectrum. It is observed from irradiation experiments in the ^{31}P region that the higher-frequency transition of the phosphine oxide phosphorus for a given spin state of the phosphate phosphorus is connected with the highest-frequency resonance of one of the ^{13}C proton satellites and that the opposite is true for the connectedness of the phosphate phosphorus transitions. Therefore, the sign of $^{2}J_{PH}$ is opposite to $^{3}J_{PH}$ and $^{3}J_{PP}$. Thus

the results presented previously using the resonances resulting from molecules not containing ^{13}C are implicit in the results employing either of the ^{13}C satellites due to the two spin states of this nucleus.

The three-spin system of the ^{1}H and ^{13}C nuclei and the phosphine oxide nucleus is considered next. This can be done by considering the results for one of the two spin states of the phosphate phosphorus, since either state of this nucleus yields the same conclusions. Consider the proton resonances due to one or the other of the spin states of the phosphate phosphorus in one of the ^{13}C satellites. It can be seen that the higher-frequency absorption of both pairs of resonances due to the different spin states of the phosphate phosphorus in the ^{1}H spectrum is connected to the lower-frequency member of one of the pairs of resonances in the ^{13}C spectrum due to the two spin states of the phosphate phosphorus. The same conclusions apply to the other ^{13}C satellite in the proton spectrum. Furthermore, the higher-frequency resonance of each of the two pairs of resonances phosphine oxide ^{31}P spectrum due to the two spin states of the phosphate phosphorus is connected to the higher-frequency ^{13}C satellite in the ^{1}H spectrum. This means that $^{1}J_{CH}$ and $^{1}J_{PC}$ have the same sign which is opposite to that of $^{2}J_{PH}$. Since $^{3}J_{PP}$ and $^{3}J_{PH}$ were determined to be opposite in sign to $^{2}J_{PH}$, it follows that they have the same signs as $^{1}J_{CH}$. Therefore, since $^{1}J_{CH}$ is positive, $^{3}J_{PP}$, $^{3}J_{PH}$ and $^{1}J_{PC}$ are also positive, where as $^{2}J_{PH}$ is negative.

The same logic may be applied to the three spin system consisting of the phosphate phosphorus, the ^{13}C carbon and its attached protons. It is seen in Figure 4 that for a given ^{13}C satellite a given pair of resonances due to the same spin state of the phosphine oxide phosphorus is connected to one of the pairs of absorptions in the ^{13}C spectrum arising from the same phosphine oxide spin state. In each case, the lower-frequency member of one pair is connected to the higher-frequency member of the other. The same results are observed for the other ^{13}C satellite in the ^{1}H spectrum. It was also observed that the lower-frequency member of the pair of absorptions arising from a given spin state of the phosphine oxide phosphorus in the phosphate ^{31}P spectrum is connected to the higher-frequency ^{13}C satellite in the ^{1}H spectrum. The same was true of the lower-frequency absorption in the ^{31}P spectrum for the other spin state of the phosphine oxide phosphorus. Therefore, $^{3}J_{PH}$ and $^{1}J_{CH}$ have the same sign which is opposite to $^{2}J_{PC}$. As before, since $^{3}J_{PP}$ and $^{3}J_{PH}$ were determined to be opposite in sign to $^{2}J_{PH}$, it follows that $^{3}J_{PP}$ has the same sign as $^{1}J_{CH}$ and so $^{2}J_{PH}$ has a sign which is opposite to $^{1}J_{CH}$. Since $^{1}J_{CH}$ is positive, $^{3}J_{PH}$ and $^{3}J_{PP}$ have positive signs, whereas $^{2}J_{PH}$ and $^{2}J_{PC}$ are negative.

The experimental work was somewhat simplified by the observation that the ^{13}C satellites were actually triplets due to overlap of the center two members of the expected doublet of doublets. This means that the central band of this triplet

stems from two combinations of spin states of each phosphorus whereas the outer members arise from only one such combination. Hence the centers of the triplets are observed to be perturbed when the frequencies corresponding to the energies of the ^{13}C transitions connected to both these combinations of phosphorus spin states are irradiated as is indicated in Figure 4.

This completes the analysis of the double resonance results for the determination of the relative signs of the six coupling constants in this system. The results which have been obtained for the determination of the signs and magnitudes of the coupling constants and the chemical shifts of the phosphorus atoms for the derivatives of $P(OCH_2)_3P$ are given in Table 2 and Table 3. Table 4 presents the values of the nmr parameters for some compounds analogous to those for which data is presented in Tables 2 and 3.

For the parent compound, $P(OCH_2)_3P$, long range coupling caused the ^{13}C proton satellite resonances of the ^{1}H spectrum to appear as a broadened triplet instead of the expected doublet of doublets. Because the small POCH coupling was obscured, it was not possible to observe proton resonances due to the two spin states of the phosphite phosphorus and consequently it was not possible to determine $^{2}J_{PC}$. All the other couplings could be evaluated and the signs determined by the methods previously described. For the other compounds listed, limited quantities or limited solubilities prevented the observation of the ^{13}C

Table 2. NMR parameters for $P(OCH_2)_3P$ and its derivatives

Compound	$^2J_{PH}$ [a]	$^3J_{PH}$ [a]	$^3J_{PP}$ [b]	$\delta^{31}_{P(O)_3}$ [c]	$\delta^{31}_{P(C)_3}$ [c]	Solvent
$P(OCH_2)_3P$	+8.9	+2.5	-37.2	- 89.78	+66.99	$(CD_3)_2SO$
$(OC)_5MoP(OCH_2)_3P$	+8.8	+5.0	- 4.6	-130.82	+68.60	CH_3CN
$(OC)_5CrP(OCH_2)_3P$	+8.5	+5.3	- 3.0	-154.47	+68.57	CH_3CN
cis-$[(OC)_4Cr][P(OCH_2)_3P]_2$	(+) (8.4)	(+) (5.3)	- 2.4	-157.21	+68.52	CH_3CN
$(OC)_5WP(OCH_2)_3P$	+8.5	+5.3	- 0.4	-109.09	+68.75	CH_3CN
eq-$(OC)_4FeP(OCH_2)_3P$	+8.2	(+) (6.1)	+ 7.6	-159.76	+68.10	CH_3CN
ax-$(OC)_4FeP(OCH_2)_3P$	+8.5	+6.1	+ 8.6	-157.44	+71.38	CH_3CN
$[CH_3P(OCH_2)_3P]BF_4$	+8.5	+6.6	+46.2	- 51.03	+59.80	CH_3CN

[a] All these J values in Hz refer to couplings between nuclei in the bicyclic system, and are precise to $\pm$0.4 Hz. Most of these values were determined from splittings in the INDOR spectra. For those cases in which the splitting was not resolved in the INDOR spectra, the sign is given in parentheses, and the value as determined from the ^1H spectrum is given below the sign indication; these latter values are from reference 53.

[b] These J values are precise to $\pm$ 0.4 Hz, except where indicated.

[c] ^{31}P chemical shifts in ppm are relative to external 85% H_3PO_4, and are precise to $\pm$ 0.02 ppm.

Table 2 (Continued)

Compound	$^{2}J_{PH}$ [a]	$^{3}J_{PH}$ [a]	$^{3}J_{PP}$ [b]	$\delta^{31}P(O)_3$ [c]	$\delta^{31}P(C)_3$	Solvent
ax-$(OC)_4FeP(CH_2O)_3P$	(+) (0.4)	(+) (2.8)	+47.1 ± 2.5	- 87.37	-22.42	CH_3CN
$SP(OCH_2)_3P$	+7.6	+7.5	+ 48.1	- 52.06	+70.89	$(CD_3)_2SO$
$(OC)_5MoP(OCH_2)_3PMo(CO)_5$	+2.1	+5.2	+ 63.7	-130.97	+18.94	CH_3CN
$(OC)_5CrP(OCH_2)_3PCr(CO)_5$	(+) (2.0)	(+) (5.6)	+66.1 ± 0.8	-155.52	- 8.21	CH_3CN
$(OC)_5WP(OCH_2)_3PW(CO)_5$	(+) (1.5)	+5.5	+ 73.8	-108.37	+36.34	CH_3CN
$(OC)_4FeP(OCH_2)_3PFe(CO)_4$	(+) (0.4)	+6.2	+ 95.3	-160.40	-22.06	CH_3CN
$[P(OCH_2)_3P-CH_3]BF_4$	-5.4	+3.1	+114.6	- 89.58	- 2.56	CH_3CN
$OP(OCH_2)_3PO$	+8.2	8.3	+139.1	+ 18.17	- 5.48	$(CD_3)_3SO$
from ^{13}C satellites	(-)	(+)	+144.2	--	--	CF_3COOH
$[(OC)_5WP(OCH_2)_3PCH_3]BF_4$	-5.6	+6.1	+143.2	-113.00	- 2.98	$(CD_3)_2CO$
$SP(OCH_2)_3PO$	-9.0	+8.2	+151.3	- 49.20	- 5.50	$(CD_3)_2SO$

Table 3. Miscellaneous nmr parameters for $P(OCH_2)P$ and its derivatives

Compound	Parameter	Value[a]
$P(OCH_2)_3P$	$^1J_{CH}$	+153.1 ± 0.2
	$^1J_{PC}$	-15 ± 1
	$\delta_{^{13}C}$	- 37.88 ± 0.1
$OP(OCH_2)_3PO$	$^1J_{CH}$	+156.7 ± 0.2
	$^1J_{PC}$	+ 67.8 ± 0.7
	$^2J_{PC}$	- 8.5 ± 0.7
	$\delta_{^{13}C}$	- 37.28 ± 0.02
$[(OC)_5W(P(OCH_2)_3PCH_3]BF_4$	$\lvert^2J_{PCH_3}\rvert$	17.5 ± 0.5
$[P(OCH_2)_3PCH_3]BF_4$	$\lvert^2J_{PCH_3}\rvert$	17.0 ± 0.5
$[CH_3P(OCH_2)_3P]BF_4$	$\lvert^2J_{PCH_3}\rvert$	18.7 ± 0.2

[a]Coupling constants are in Hz. ^{13}C chemical shifts are with respect to the methyl carbon of external glacial acetic acid.

Table 4. NMR parameters for some compounds analogous to those for which nmr data are reported in Table 2

Compound	$^2J_{PH}$ [a]	$^3J_{PH}$ [a]	$\delta_{^{31}P}$ [b]	Solvent
$P(OCH_2)_3CCH_3$ [c]	--	2	-91.5	CH_3CN
$P(CH_2O)_3CCH_3$	8.0	-	+80.5	C_6H_6
$[CH_3P(OCH_2)_3CCH_3]BF_4$	19.0 ± 0.5	5.1	-60.15	CH_3CN
$OP(OCH_2)_3CCH_3$ [c]	--	7	+ 7.97	$(CH_3)_2SO$
$OP(CH_2O)_3CCH_3$	7.5	-	-16.00	CD_3CN
$SP(OCH_2)_3CCH_3$ [c]	--	6	-57.4	$(CH_3)_2SO$
$(OC)_5CrP(OCH_2)_3CC_2H_5$ [d]	--	4.3	-162	$CDCl_3$
$(OC)_5MoP(OCH_2)_3CC_2H_5$ [d]	--	4.2	-136	$CDCl_3$
$(OC)_5WP(OCH_2)_3CC_2H_5$ [d]	--	4.4	-114	$CDCl_3$

[a] Coupling constants are in Hz.

[b] ^{31}P chemical shifts are in ppm relative to external 85% H_3PO_4. Values not referenced to other workers were determined by this author using the INDOR technique.

[c] Values of the parameters for this compound were taken from reference 54.

[d] Values of the parameters for this compound were taken from reference 55.

satellites in the ^{1}H region. For these cases, the reasonable assumption was made that $^{3}J_{PH}$ remains positive, no matter what the groups attached to phosphorus are and the sign assignments were made on this basis. This assumption will be examined later.

The ^{31}P chemical shifts obtained in this work by the INDOR technique were calculated in the following manner. It was observed that the center of the trimethylphosphite ^{31}P resonance occurred at 24,292,490.3 Hz when the field was such that the protons in the internal standard benzene resonate at 60,002,000.0 Hz. Since the former compound has a ^{31}P resonance of 140.0 ppm (assumed 140.00 ppm)(16) downfield from external 85% phosphoric acid, the frequency of H_3PO_4 at this polarizing field can be calculated using the usual convention (1),

$$\frac{\Xi - 24,292,490.3}{\Xi} = -140.00 \times 10^{-6}$$

whence $\Xi_{H_3PO_4}$ (C_6H_6) = 24,289,089.8 Hz. In practice, acetonitrile and tetramethylsilane (TMS) were also employed in some cases as locking standards. It was determined that acetonitrile and TMS resonate at 330.3 Hz and 436.8 Hz to lower frequency, respectively, than benzene at 60,002,000.0 Hz and constant field. Therefore the frequency of the ^{31}P resonance of 85% H_3PO_4 when the spectrometer is locked at 60,002,000.0 Hz on these two compounds is given by

$$\equiv_{H_3PO_4}(CH_3CN) = 24,289,089.8 \times \frac{60,002,000.0}{60,001,669.7} = 24,289,223.5 \text{ Hz}$$

and

$$\equiv_{H_3PO_4}(TMS) = 24,289,089.8 \times \frac{60,002,000.0}{60,001,563.2} = 24,289,266.6 \text{ Hz}$$

It should be noted that since a higher field was required to polarize the protons of these latter two compounds than for benzene at the same frequency, the frequency at which 85% H_3PO_4 is expected to resonate is increased by a factor which is the fraction that the field was increased in observing the protons of CH_3CN or TMS at 60,002,000.0 Hz, in accordance with the Larmor equation (1). In order to determine an unknown ^{31}P chemical shift by the INDOR technique, the difference between the $\equiv_{H_3PO_4}$ for the standard which was used and the $\equiv$ determined for the compound under investigation is determined, and this divided by the $\equiv_{H_3PO_4}$ of the proton standard used, following the usual convention (1). This means that the $\equiv$ values for the ^{31}P resonances which are deshielded with respect to 85% phosphoric acid at constant field are larger and those that are more shielded than 85% phosphoric acid are smaller than $\equiv_{H_3PO_4}$. The chemical shifts reported in Tables 2 and 3 are in ppm. Since line positions were determined to at least $\pm$ 0.4 Hz, these chemical shifts are precise to $\pm$ 0.02 ppm. Most ^{31}P chemical shifts determined by direct observation are reported to only $\pm$ 0.1 ppm and so the INDOR method allows ^{31}P chemical

shifts to be determined five times more precisely than by direct observation. The other advantage of this method is that, except for ^{3}H, perturbations are being observed on the nucleus which is most sensitive to the nmr technique. This means an optimum signal to noise ratio may be achieved. Indeed, for sparingly soluble compounds this is a most convenient method of obtaining information about nuclei other than ^{1}H. In this regard, it might be pointed out that although ^{31}P is 100% abundant in phosphorus, it is only about 6% as sensitive to detection by nmr spectroscopy. The ^{13}C isotope is only 1.1% abundant in carbon and has a sensitivity only 1.58% that of protons at the same field strength (1), hence the actual sensitivity to detection by direct observation of natural abundance ^{13}C is about one-sixthousandths that of protons. For natural abundance ^{13}C, the sensitivity to observation of the ^{13}C satellites in the proton spectrum is about sixty-three times that for the observation of the ^{13}C resonance itself.

For $OP(OCH_2)_3PO$, the chemical shift difference in Hz between the two phosphorus nuclei is only about 2.5 times the coupling between them. This means that only the coupling constant and not the chemical shifts may be determined directly from the spectrum. The spectrum was analyzed as an AB subspectrum (2) giving the values for the chemical shifts reported in Table 2. The actual chemical shift difference is 527.4 Hz compared to the frequency difference between the centers of the

two doublets of septets of 545.5 Hz. For the other compounds reported, the ratio of δ_{PP} to $^{3}J_{PP}$ is greater than 10, and so the centers of the doublet of septets for each ^{31}P resonance represents their chemical shifts.

The ^{13}C chemical shifts in this dissertation are given with respect to the ^{13}C isotope of the methyl group of acetic acid as an external standard and were determined in the same manner as were the ^{31}P chemical shifts discussed earlier. Incidental to this study, the nmr parameters for the compound $[CH_3P(OCH_3)_3]^+BF_4^-$ were also determined and these results are presented in Table 5.

Geminal ^{31}P-^{31}P Coupling

The systems for which the values and signs of geminal ^{31}P-^{31}P couplings were determined were of the type $L_2M(CO)_4$ where M = Cr, Mo, and W, $Fe(CO)_3L_2$ or L_2PdX_2 where L was the ligand $P(OCH_3)_3$, $P(CH_3)_3$ or $P[N(CH_3)_2]_3$ and X = Cl or I. These spin systems may be classified as $X_nAA'X'_n$ spin systems after the nomenclature of Corio (56), where n is the number of protons in the X part of the spectrum (e.g., 9 in $P(OCH_3)_3$ or 18 in $P[N(CH_3)_2]_3$) and A is phosphorus. For some of these compounds, the values and signs of the other parameters which determine the appearance of the spectrum were also determined. Incidental to this study, the values and signs of the couplings in $P[N(CH_3)_2]_3$ and $OP[N(CH_3)_2]_3$ were also determined for comparison with the complexed $P[N(CH_3)_2]_3$.

Table 5. NMR parameters for $[CH_3P(OCH_3)_3]BF_4$

Parameter	Value[a]
$^1J_{CH}$[b]	+140.9 ± 0.1
$^1J_{CH}$[c]	+153.0 ± 0.1
$^1J_{PC}$	+132.4 ± 0.4
$^2J_{PC}$	- 6.8 ± 0.4
$^2J_{PH}$	- 17.8 ± 0.1
$^3J_{PH}$	+ 11.4
$\delta_{^{31}P}$	- 53.95 ± 0.02
$\delta_{^{13}C}$[b]	+ 14.59 ± 0.02
$\delta_{^{13}C}$[c]	- 48.47 ± 0.02

[a]Coupling constants are in Hz. ^{31}P chemical shifts are relative to external 85% H_3PO_4. ^{13}C chemical shifts are relative to the methyl carbon of external glacial acetic acid.

[b]The carbon referred to in this parameter is the phosphine carbon.

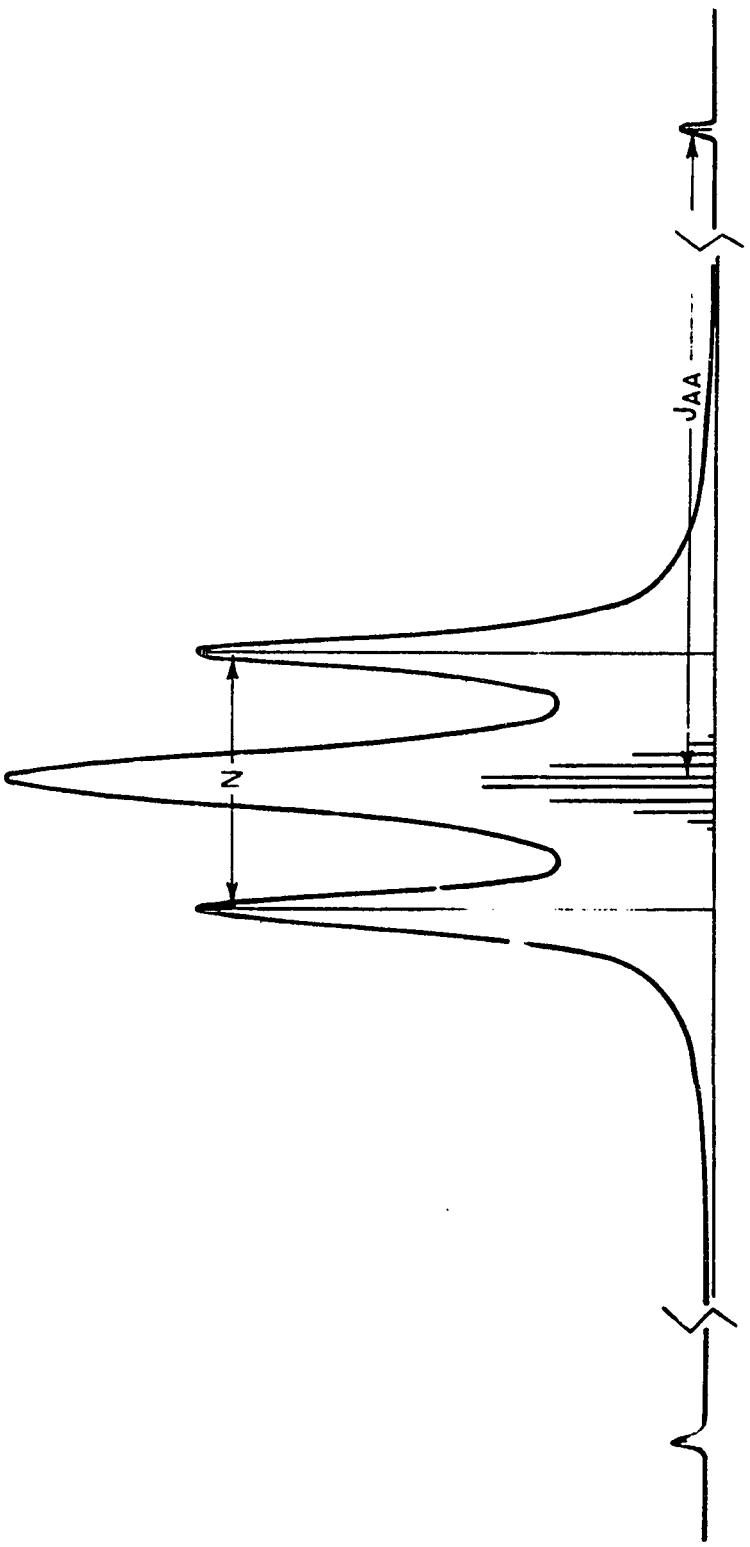
[c]The carbon referred to in this parameter is the methoxy carbon.

The parameters which determine the appearance of the X part of the $X_nAA'X'_n$ spectrum are $N = J_{AX} + J_{AX'}$, $L = J_{AX} - J_{AX'}$, and $J_{AA'}$. Harris (57) has derived equations which define the energies and the relative intensities of the X part of the spectrum in terms of these parameters, assuming $J_{XX'} = 0$. The general features of the X spectrum which appear in Figure 5 include a sharp doublet of separation N centered ν_X as well as 2n pairs of lines symmetrically placed about ν_X. The intensity of this portion of the spectrum is evenly divided between the N doublet and the 2n pairs of lines. These 2n pairs of lines may be divided into two sets, the so-called "inner" lines and the "outer" lines. For the typical case in which values of $L/J_{AA} < 1$, these designations refer to the lines which occur between and outside the members of the N doublet, respectively. Only the first outer line pair is represented in Figure 5. Harris also showed that the intensity of the outer lines is quite small compared to that of the inner lines. However, in the event that the first pair of outer lines in the spectrum can be found, it is possible to determine the value of $J_{AA'}$ ($^2J_{PP}$ in our application), since the separation between it and the most intense inner line is $J_{AA'}$.

As the value of $J_{AA'}$ increases for a particular value of N and L, the frequency distribution of the inner and outer lines changes. The separation between the first inner line and the first outer line remains $J_{AA'}$, but the intensity of the outer

Figure 5. Apparent triplet for the X part of an $X_6AA'X'_6$; system arising from overlapping of the inner lines when $J_{AA'} >> L$

The intensity of the first outer pair of lines has been exaggerated.

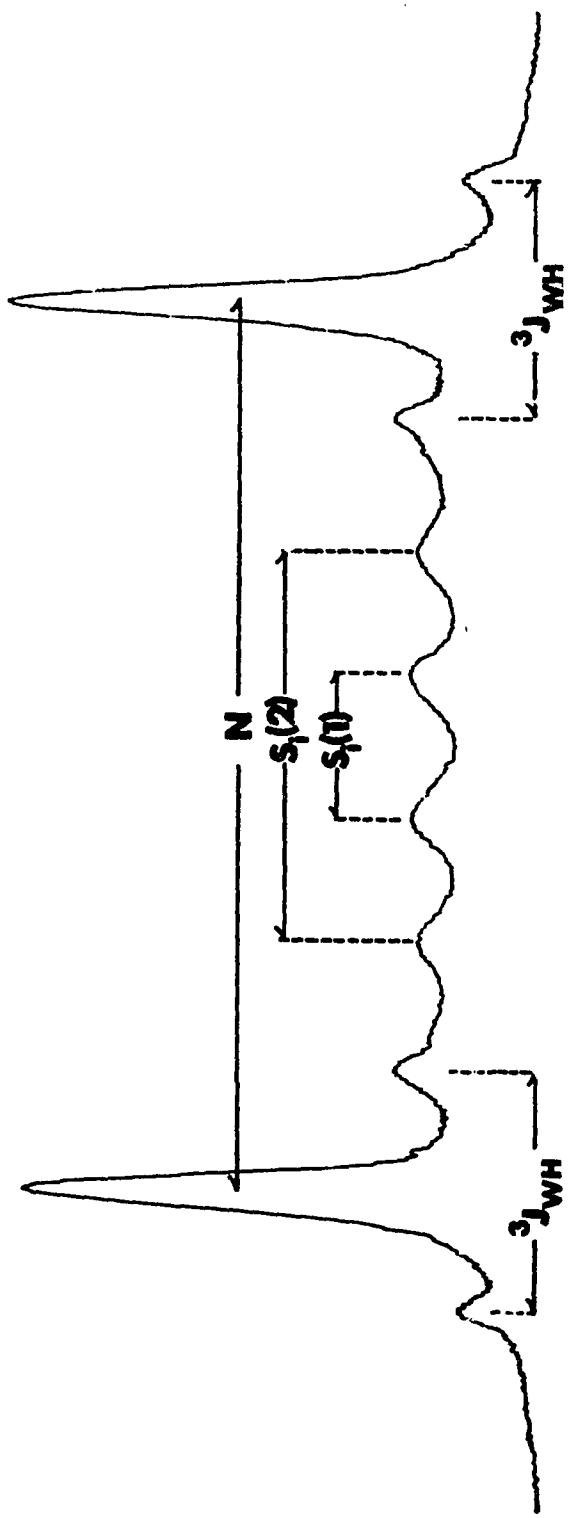

N
JAA

line decreases as $J_{AA'}$ increases. Hence it becomes experimentally quite difficult to find this line for $J_{AA'}$ > 100 Hz at realizable concentrations of the compounds studied. The separations of the inner lines becomes smaller as $J_{AA'}$ increases. For $|J_{AA'}| >> L$, the spectrum has the appearance of an apparent triplet. The distribution of the frequencies and intensities of these inner lines determines the band shape of the portion of the spectrum between the N doublet. Only in rare cases can the fine structure due to the inner lines be resolved, and so only the envelope of these resonances is observed. From line shape considerations, Ogilvie (58) has been able to calculate values of $J_{AA'}$, ($^2J_{PP}$) in coordination complexes by fitting spectra calculated from the Harris equations to the observed band shapes. For the limitations of this method, see his dissertation (58).

In addition to the determination of $J_{AA'}$ from the observation of the first outer pair of lines or from the band shape of the central resonance, $J_{AA'}$ as well as L may be determined from the separations of the first two inner pairs of lines. This calculation is demonstrated for <u>cis</u>-$W[P(CH_3)_3]_2(CO)_4$, the proton spectrum of which is shown in Figure 6. This is the only compound among those studied for which this calculation could be performed, since the proton spectra of the other compounds did not show the fine structure revealed in the spectrum shown in Figure 6. Harris has shown that

Figure 6. H' nmr spectrum of the central bands of <u>cis</u>-$(OC)_4W[P(CH_3)_3]_2$

The meanings and values of the splitting parameters indicated is given in the text.


$^3J_{WH}$
N
$S_i(2)$
$S_i(1)$
$^3J_{WH}$

$$|J_{AA'}| = [3S_i(1) + S_i(2)][S_i(1) - S_i(2)/2[3S_i(1) - S_i(2)] \quad 17$$

$$L^2 = S_i(1) \cdot S_i(2) \cdot [S_i(1) + S_i(2)]/[3S_i(1) - S_i(2)]. \quad 18$$

Since $S_i(1)$ = 1.15 Hz and $S_i(2)$ = 3.16 Hz, $|^2J_{PP}|$ = 22.9 Hz and L = 7.35 Hz. N is observed directly from the spectrum to be 7.09 Hz. The value of J_{PP} reported is in good agreement with that obtained from the separation of the first inner and outer lines, where J_{PP} was observed to be 25.0 Hz. It should be pointed out that the calculations of $J_{AA'}$ and L^2 using Equations 17 and 18 are quite subject to errors resulting from imprecision in the determination of the line positions. Using a value for $S_i(1)$ of 1.16 Hz, an increase in this parameter of 0.01 Hz from that observed gives a $^2J_{PP}$ of 20.8 Hz and L = 7.11 Hz if $S_i(2)$ is held at 3.16 Hz. From the definitions of L and N, the values of $^2J_{PH}$ is -7.22 Hz and $^4J_{PH}$ is + 0.13 Hz. This compares with a value of -7.34 $\pm$ 0.05 Hz for $^2J_{PH}$ and +0.25 $\pm$ 0.05 Hz for $^4J_{PH}$ from the curve fitting procedures employing a value of 25.0 Hz for $^2J_{PP}$ (58).

In addition to the resonance lines already discussed, there are four additional satellite lines due to coupling of the 14% abundant ^{183}W isotope (I = 1/2) with the protons. The value of $^3J_{WH}$ is determined from the splitting to be 1.93 $\pm$ 0.02 Hz. INDOR experiments employing these satellites indicate that $^1J_{WP}$ is 209.8 $\pm$ 1 Hz, and of the same sign as $^3J_{WH}$. Because it was

not possible to irradiate ^{183}W, it was not possible to relate these signs to the sign of N, which is known to be negative.

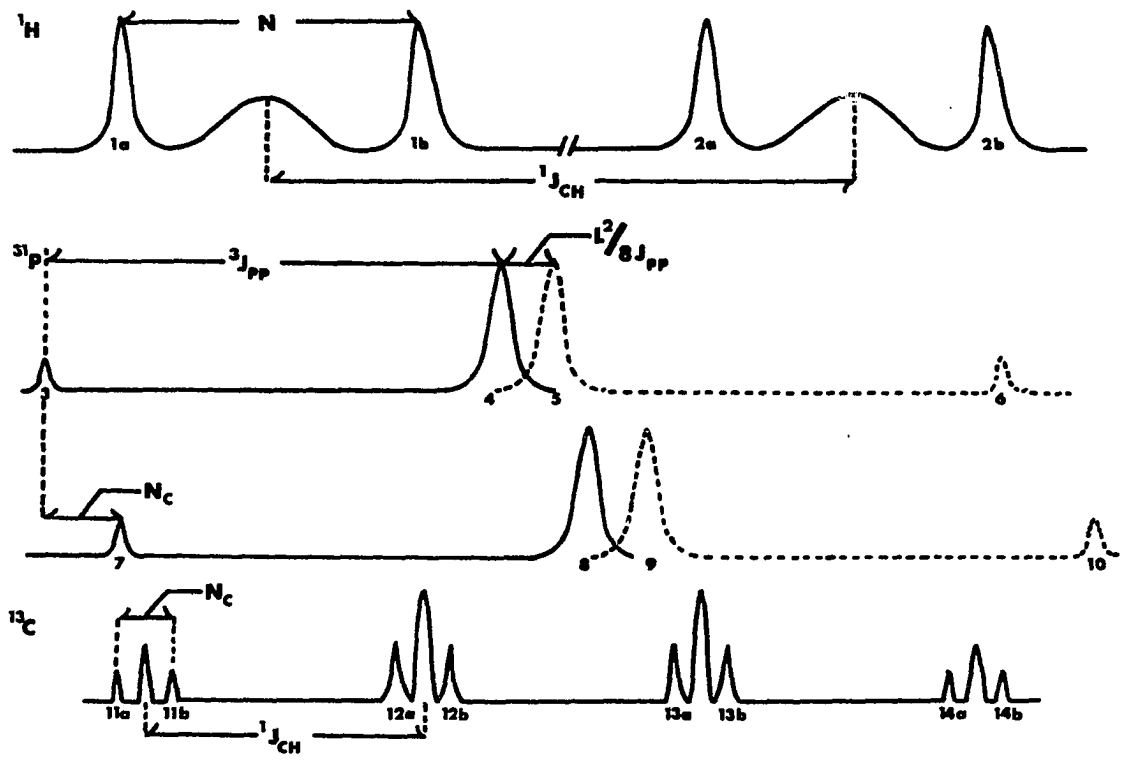
The method by which the value and sign of $^2J_{PP}$ may be determined relative to N in $X_nAA'X'_n$ systems involves double resonance experiments while observing the ^{13}C satellite resonances in the proton spectrum. The experiment necessary for these determinations has been described by Finer and Harris (21). A schematic representation of the ^1H, ^{31}P and ^{13}C spectra which are expected for molecules of this type is presented in Figure 7. Couplings of the protons to the ^{13}C and ^{31}P nuclei have been ignored except for $^1J_{CH}$.

As an example, consider molecules of <u>trans</u>-$(OC)_4Mo[P(OCH_3)_3][P(OCH_3)_2(O^{13}CH_3)]$. The proton spectrum of the protons attached to the ^{13}C consists of two systems of bands separated by $^1J_{CH}$ which are quite similar in shape to the single system of bands observed for those molecules not containing ^{13}C atoms. Coupling between the protons of this molecule not on the ^{13}C atom and the protons on the ^{13}C atom is apparently too small to result in an additional splitting or broadening of the ^{13}C satellite peaks in the compounds studied.

The ^{31}P resonance for the molecules containing one ^{13}C nucleus appears as two AB patterns because of the two spin states of ^{13}C. Because of the presence of the ^{13}C nucleus in one of the phosphorus-containing moieties, the two phosphorus nuclei are no longer chemically equivalent. The AB coupling

Figure 7. Schematic representation of the ^{1}H, ^{13}C and the ^{31}P nmr spectra of a disubstituted complex such as cis-$(OC)_4Mo[P(OCH_3)_3][P(OCH_3)_2(O^{13}CH_3)]$

The ^{1}H resonance due to those protons not on ^{13}C atoms has been eliminated. ^{13}C-^{1}H coupling other than $^{1}J_{CH}$ has been ignored for the sake of clarity. Different scales have been used for the spectra due to different nuclei. The band numbers are those referred to in the text. The two a b subspectra of the ^{31}P spectrum are drawn separately; for clarity dashed lines are used for half of each subspectrum.


^1H
N
1a
1b
2a
2b
$^1J_{CH}$
^{31}P
$^3J_{PP}$
$L^2/8J_{PP}$
3
4
5
6
N_C
7
8
9
10
^{13}C
N_C
11a
11b
$^1J_{CH}$
12a
12b
13a
13b
14a
14b

($^2J_{PP}$ in this case) may be determined from an AB spectrum as indicated in Figure 7. Although the intensity of the bands 3, 6, 7 and 10 is very small, a perturbation of either the a or b lines of bands 1 and 2 is observed if sufficient radio frequency power is applied at the position of any of the weak ^{31}P bands. If for either of the spin states of ^{13}C, the higher-frequency bands 3 or 7 are shown to be connected to the higher-frequency lines of the appropriate ^{13}C satellite, then $^2J_{PP}$ has the same sign as N, otherwise their signs are opposite. It is theoretically possible to show which AB ^{31}P spectrum is connected to which ^{13}C proton satellite, and so determine the relative signs of $^1J_{CH}$ and $N_C(=J_{PC} + J_{P'C})$.

The ^{13}C spectrum of such a compound as shown in Figure 7 consists of a 1:3:3:1 quartet of bands. The quartet splitting arises because of $^1J_{CH}$. The origin of the lines comprising each of these bands is analogous to the origins of the lines in the bands of the ^1H spectrum. There is a doublet with splitting N_C, and between the doublet lines is a band composed of 2 lines arising from transitions of the ^{13}C nucleus between states for which there is mixing between the two spin states of the two phosphorus nuclei. By determining the relative connectedness of the a or b lines of the ^1H spectrum with the a and b lines in the ^{13}C spectrum, the relative sign of N to N_C is determined. If the highest-frequency line of band 1 or 2 (i.e., 1a or 2a) is connected with the highest-frequency line of bands 11, 12,

13 and 14, then the signs of N and N_C are the same. If the lowest-frequency lines of band 1 or 2 is connected to the highest-frequency line of bands 11, 12, 13 and 14, then the signs of N and N_C are opposite.

The double resonance experiments necessary to establish the connectedness of the various resonances of the three nuclei involved are very similar to those described in detail for $OP(OCH_2)_3PO$. For the bis-trimethyl phosphite complex of molybdenum under consideration, it was observed that the highest-frequency line of band 1 (i.e., line 1a in Figure 7) is connected to the lowest-frequency line of the bands in the ^{13}C spectrum (i.e., the b lines). The separation of the a and b lines in the ^{13}C spectrum was determined to be 2.9 Hz. Therefore, N is opposite in sign to N_C, where N_C = 2.9 Hz. It was not possible in the case of the trimethyl phosphite complexes to resolve the difference in the frequency of the bands in the phosphorus spectrum due to the two spin states of ^{13}C, since N_C is very small compared to the width of ^{31}P bands arising from the unresolved splitting due to proton coupling. Therefore, it was not possible to directly relate the sign of N to the sign of $^1J_{CH}$. However, a complete determination of the signs and magnitudes of the couplings in the liquid complex $(OC)_5Mo[P(OCH_3)_3]$ was performed, and the sign of $^3J_{PH}$ (= 11.6 Hz) was determined to be positive. It was expected that the sign of N would be positive, since $^3J_{PH}$ is positive in the free

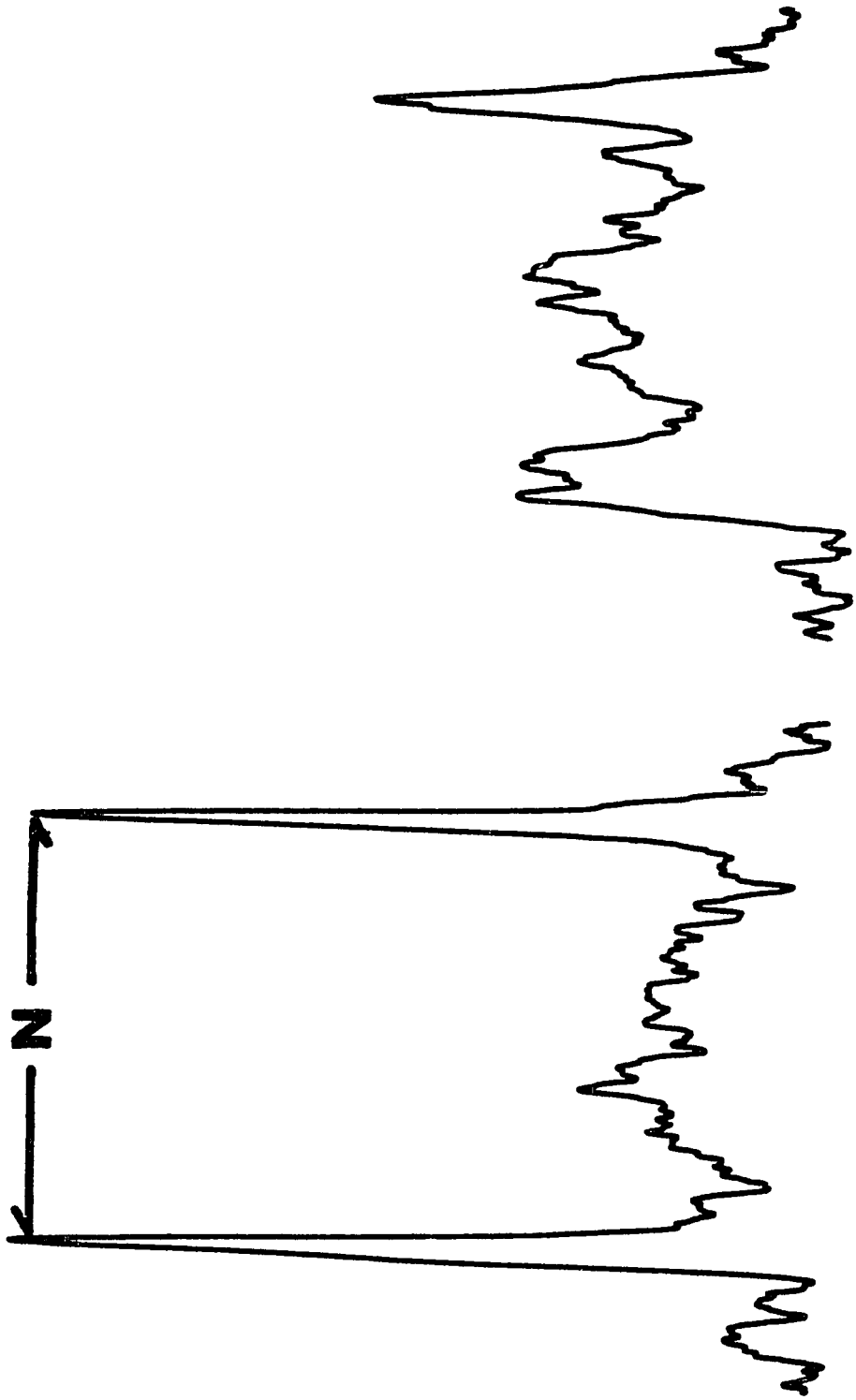
ligand (+10.0 Hz) (19) and trimethyl phosphate (+10.5 Hz) (19) and the observed values are close to the value of 11.6 Hz observed for the trimethyl phosphite complexes. Therefore it is assumed that the signs of $^{3}J_{PH}$ in the bis-trimethyl phosphite complex is positive.

Furthermore, it is expected that the contribution to N of the five-bond PH coupling in the bis-trimethyl phosphite complexes is negligible, since it has been observed that for mixed complexes of the type cis and trans-$[(OC)_4MoP(OCH_3)_3P(OCH_2)_3CCH_3]$ that no splitting of the main $^{3}J_{PH}$ doublet due to $^{5}J_{PH}$ is observed (59).

Figure 8 shows a comparison of a scan of one of the ^{13}C satellite bands of cis-bis-(trimethyl phosphite)molybdenum tetracarbonyl under ordinary circumstances with a scan of this same band when either band 6 or 7 of Figure 7 is irradiated. Irradiating at a frequency of ∿40.5 Hz less than the frequency of the centers of bands 4, 5, 8 and 9 causes the high frequency line to be broadened compared to the low frequency line. The low frequency line is also somewhat decreased in intensity, undoubtedly due to the fact that the center bands 4 and 5 or 8 and 9 have some intensity at bands 6 or 10, and high radio frequency power is required to cause the observed effect. This result indicates that $^{3}J_{PP}$ is of opposite sign to N and hence $^{3}J_{PP}$ is negative. For the complexes of the other ligands that were studied, it was possible to relate N to $^{1}J_{CH}$, and so $^{3}J_{PP}$

Figure 8. Two scans of one of the ^{13}C satellite resonances of <u>cis</u>-$(OC)_4Mo[P(OCH_3)_3]_2$ which demonstrate the determination of the relative signs of N and $^2J_{PP}$

Frequency increases left to right in both scans. The scan on the left was obtained while irradiating at a frequency 40 Hz greater than the frequency of the center of the central bands of the ^{31}P ab subspectrum (bands 4, 5, 8 and 9 in Figure 7). Since the lower frequency member of the N doublet is perturbed, N and $^2J_{PP}$ have opposite sign.


N

could be related to $^{1}J_{CH}$. In some cases, for a particular ligand, the sign of N was assumed not to change from one complex to another in order for the determination of the relative sign of $^{3}J_{PP}$ to N to give the absolute sign of $^{3}J_{PP}$.

The results of the nmr studies of the disubstituted transition metal carbonyl complexes in which the sign of $^{3}J_{PP}$ were determined are given in Table 6. The results of the nmr study of the compounds $P[N(CH_3)_2]_3$, $OP[N(CH_3)]_2$ and $(OC)_5Mo[P(OCH_3)_3]$ are given in Table 7. The ^{13}C and ^{31}P chemical shifts were calculated as previously described.

Aromatic Solvent Induced Shifts

It was observed for the bicyclic compounds $P(OCH_2)_3CCH_3$, $HC(OCH_2)_3CCH_3$, $CH_3C(OCH_2)_3CCH_3$ and $HC(OCH)_3(CH_2)_3$ that the ^{1}H chemical shifts with respect to internal TMS are greatly affected in aromatic solvents compared to their values in non-aromatic solvents. The results of a study of these effects are presented in Table 8. The chemical shift values are those for the indicated protons at solute concentrations for which no change was observed in the chemical shift with further dilution. Data are also presented for these compounds dissolved in hexafluorobenzene. Similar data are presented in Table 9 for $P(OCH_3)_3$ and $HC(OCH_3)_3$.

Table 6. NMR parameters for disubstituted metal complexes. The spectra were obtained in d_6-benzene, except where indicated. L = $P(OCH_3)_3$, L' = $P[N(CH_3)_2]_3$, L" = $P(CH_3)_3$

Compound	N	N_c [a]	$^1J_{CH}$	$^2J_{PP}$	$\delta_{^{31}P}$ [b]	$\delta_{^{31}C}$ [c]
cis-$(OC)_4MoL_2$	+11.6±0.1 [d]	-3.1±0.4	+144.9±0.4	-40.5±0.1 [e]	-164.77	-31.29
trans-$(OC)_4MoL_2$	+11.6±0.1 [d]	-1.7±0.4	+144.4±0.4	+162 ±5 [f]	-174.2±.1	-31.44
cis-PdL_2Cl_2 [g]	+12.9±0.2 [d]	-3.7±0.2	+148.5±0.2	+79.9±0.2 [e]	-96.29	-35.05

[a] These values obtained from ^{13}C INDOR spectra.

[b] ^{31}P chemical shifts are in ppm with respect to 85% phosphoric acid and are precise to ±0.02 ppm except where noted.

[c] ^{13}C chemical shifts are in ppm with respect to the methyl group of neat glacial acetic acid and are precise to ±0.02 ppm.

[d] The sign of this value assumed the same as $^3J_{PH}$ in $(OC)_5MoP(OCH_3)_3$, since for this compound the separation of the resonances due to the 2 spin states of ^{13}C in the ^{31}P INDOR spectrum could not be distinguished. See the text.

[e] Determined from the separation of the first outer pair of lines from the first inner pair of lines in the ^1H spectrum. See the text.

[f] Determined from the difference in the frequency of the central band and the outer band of the AB spectrum in the ^{31}P region which was determined by the INDOR technique.

[g] Determined on a saturated solution in $CDCl_3$.

Table 6 (Continued)

Compound	N	N_c [a]	$^1J_{CH}$	$^2J_{PP}$	$\delta_{^{31}P}$ [b]	$\delta_{^{13}C}$ [c]
trans-$(OC)_4CrL'_2$ [hi]	+9.84±0.02	---	---	-17±5 [f]	-178.19	---
trans-$(OC)_4MoL'_2$	+10.2±0.1	+10.6±0.4	+136.1±0.1	+101±1 [e]	-154.39	---
trans-$(OC)_4WL'_2$ [i]	+10.4±0.1	---	---	+81±5 [f]	-134.17	---
trans-$(OC)_4FeL'_2$	+9.6±0.1	+5.6±0.4	+135.5±0.1	+65±10 [f]	-170.18	---
cis-$(OC)_4CrL''_2$ [i]	-6.9±0.1	---	+128.7±0.2	-36±1 [e]	-6.34	---
trans-$(OC)_4CrL''_2$ [i]	-7.4±0.1	---	---	-28.5±1 [e]	-21.00	---
cis-$(OC)_4MoL''_2$	-6.3±0.1	+28.5±0.4	+129 ±1	-29.7±0.1 [e]	+17.75	-5.58
cis-$(OC)_4WL''_2$ [i]	-7.09±0.2	---	---	-25.0±0.1	+40.53	---
trans-PdL''_2I_2 [g]	-7.0±0.1	+37.4±0.4	+130.4±0.1	+572±5 [f]	+27.71	-0.25

[h] Determined on a saturated solution in CS_2.

[i] The sign of $^2J_{PP}$ for this compound was related to N by the double resonance techniques described in the text. The sign of N was assumed from the results of the experiments on the other distributed complexes of the same ligand.

Table 7. NMR parameters for $P[N(CH_3)_2]_3$, $OP[N(CH_3)_2]_3$ and $(OC)_5Mo[P(OCH_3)_3]$

Parameter	$P[N(CH_3)_2]_3$	$OP[N(CH_3)_2]_3$	$(OC)_5Mo[P(OCH_3)]_3$
$^1J_{CH}$	+133.5±.1[a]	+136.2±.4[b]	+146.8±1[a]
	+133.6±.4[b]		+146.2±.4[b]
$^2J_{PC}$	+19.4±.4	+2.2±.4	-2.3±.4
$^3J_{PH}$	+8.8±.1	+9.30±0.03	+11.6±.2
$\lvert^3J_{CH}\rvert$	4.1±0.5	4.1±.4	---
$\delta_{^{31}P}$[c]	-121.85	-23.01	-161.22
$\delta_{^{13}C}$[d]	-26.94	-16.82	-31.24

[a]Determined from the ^1H spectrum.

[b]Determined from the ^{13}C INDOR spectrum.

[c]^{31}P chemical shifts in ppm are relative to 85% phosphoric acid and are precise to ± 0.02 ppm.

[d]^{13}C chemical shifts in ppm are relative to the methyl carbon of glacial acetic acid and are precise to ± 0.02 ppm.

Table 8. Chemical shifts of the protons of some symmetrical bicyclic molecules in various solvents at infinite dilutions. Chemical shifts are in Hz with respect to internal TMS. The negative value indicates that the proton is more shielded than TMS.

Solvent	$P(OCH_2)_3CCH_3$		$HC(OCH_2)_3CCH_3$			$HC(OCH)(CH_2)_3$		$CH_3(OCH_2)_3CCH_3$		
	$\delta C\underline{H}_2$	$\delta C\underline{H}_3$	$\delta \underline{H}$-C	$\delta C\underline{H}_2$	$\delta C\underline{H}_3$	$\delta \underline{H}$-C	$\delta C\underline{H}_{ax}$	$\delta C\underline{H}_3$-C(O)$_3$	$\delta C\underline{H}_2$	δC-$C\underline{H}_3$
CCl_4	226.0	43.2	319.0	228.0	47.0	322.0	99.0	77.0	211.0	46.0
$\underline{n}$-C_6H_{14}	227.0	36.8	318.3	224.6	45.4	324.0	--	--	--	--
C_6H_{12}	227.0	36.0	--	--	--	324.0	95.5[a]	--	--	--
C_6H_6	204.0	-12.0	343.0	210.0	0	352.2	60.6	93.0	212.0	6.0
$C_6H_5CH_3$	--	--	336.0	208.0	4.0	--	--	--	--	--
C_6F_6	--	--	282.0	226.2	57.0	288.0	111.6	52.2	225.0	55.8

[a]This value determined in C_6D_{12}.

An indication of the manner in which the ^1H chemical shift changes with the concentration of benzene in an inert solvent is given by the plot in Figure 9. Herein are plotted the chemical shift of the methyl and methylene protons versus the mole fraction of benzene in carbon tetrachloride where the solute concentration was less than 3% weight per unit volume. It can be seen that the chemical shifts are a continuous function of mole fraction of benzene.

If it is assumed that the interaction of the aromatic solvent with the solute involves a 1:1 complex, the equilibrium constant for the formation of the complex can be measured as a function of temperature, giving the thermodynamic entropy (ΔS) and enthalpy (ΔH) of formation for the complex. Assuming an

Table 9. Chemical shifts of the protons of trimethyl phosphite and trimethyl orthoformate at infinite dilution in benzene and carbon tetrachloride

Solvent	$P(OCH_3)_3$	$HC(OCH_3)_3$	
	δCH_3	$\delta H\text{-}C$	δCH_3
CCl_4	206.4	78.6	190.2
C_6H_6	200.4	78.6	187.8

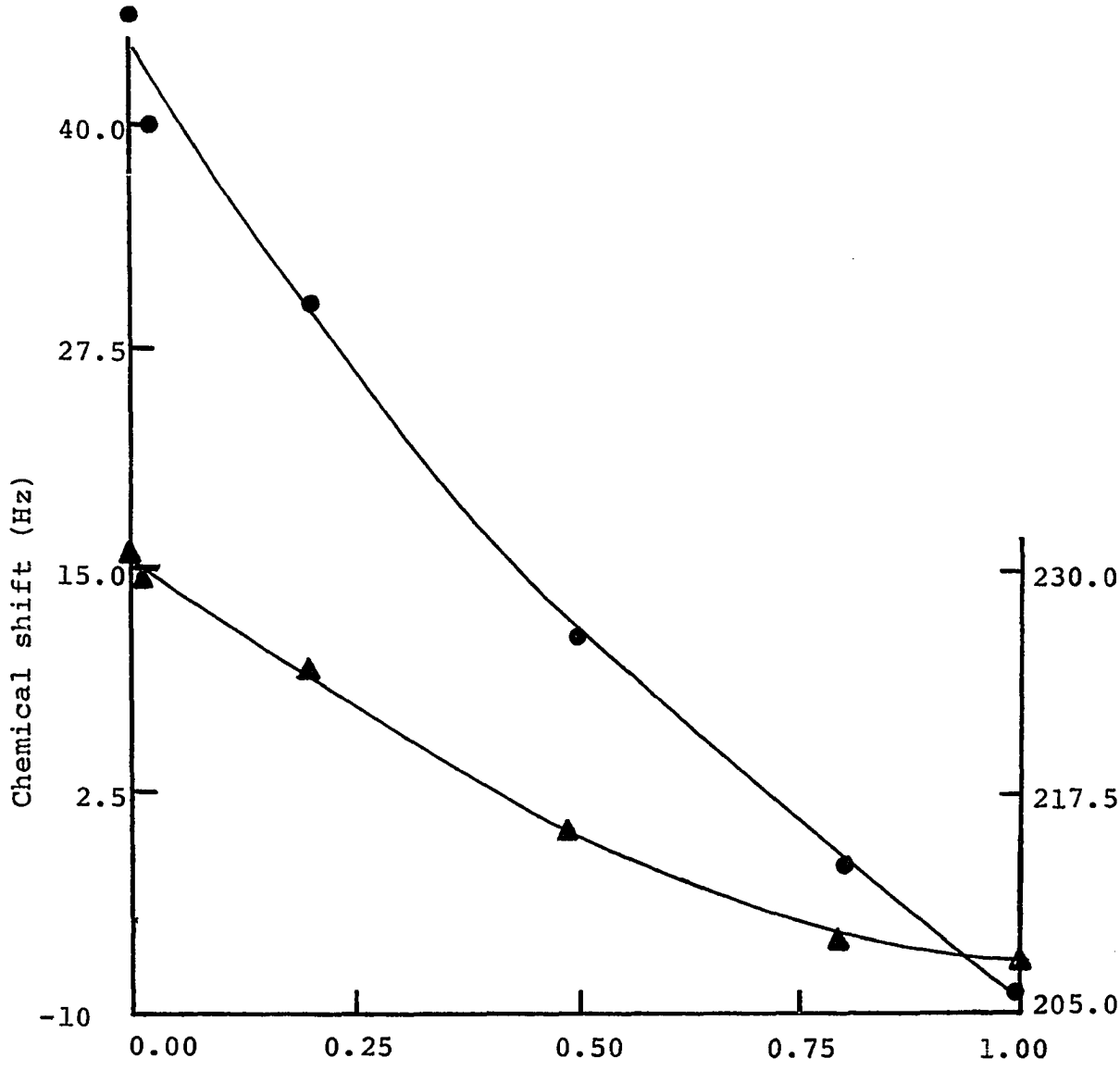


Figure 9. The ^{1}H chemical shift for the methyl (O) and methylene (Δ) protons of $P(OCH_2)_3CCH_3$ as a function of the mole fraction of benzene in carbon tetrachloride

The left ordinate is that for the chemical shift of the methyl protons. The right ordinate is that for the chemical shift of the methylene protons. The concentration of $P(OCH_2)_3CCH_3$ in these solutions was less than 3% wt/vol. Chemical shifts are in Hz on the δ scale.

equilibrium of the form

$$\text{solute} + \text{solvent} = \text{solute} \cdot \text{solvent} \qquad 19$$

$$K = \frac{[\text{solute} \cdot \text{solvent}]}{[\text{solute}]} = \frac{f}{1-f} \qquad 20$$

where f is the fraction of solute tied up in the complex. The measured chemical shift of the solute protons (δ) will be a weighted mean of the chemical shift of the unassociated solute (δ_a) and that in the complex (δ_c), that is

$$\delta = f\delta_c + (1-f)\delta_a \qquad 21$$

therefore,

$$K = \frac{\delta - \delta_a}{\delta_c - \delta} . \qquad 22$$

Since

$$\Delta F^o = -RT\ln K = \Delta H - T\Delta S, \qquad 23$$

$$K = \frac{\delta - \delta_a}{\delta_c - \delta} = e^{\frac{\Delta S}{R}} e^{-\frac{\Delta H}{RT}} . \qquad 24$$

Therefore

$$\delta = \frac{\delta_c \exp(-\Delta H/RT)\exp(\Delta S/R)}{1 + \exp(-\Delta H/RT)\exp(\Delta S/R)} - \frac{\delta a}{1 + \exp(-\Delta H/RT)\exp(\Delta S/R)} \qquad 25$$

In this equation δ has been expressed as a function of four parameters, δ_c, ΔH, ΔS and δ_a and an independent variable T.

It is possible to simplify Equation 25 by the following considerations. When the temperature is high, $kT >> \Delta H$ and the equilibrium will lie to the left. At high temperature the solute proton chemical shifts, measured with respect to internal standard TMS, will be due only to the different chemical nature of the solute compared to the TMS standard and the reaction field of the solvent. The aromatic solvent that was used in the temperature studies in this dissertation was toluene, since it allows the study of these effects over a wider temperature range than is possible with benzene. In order to isolate the ASIS phenomenon from the reaction field, the use of a non-complexing solvent with the same polarizability as toluene must be used, ignoring the effects of other forces such as Van der Waals interactions.

On lowering the temperature, the random distribution of the aromatic solvent molecules breaks down, as one position is more favored than the rest. At low temperatures where $kT << \Delta H$, the solute molecules will be completely tied up in the complex. The chemical shift of the protons in question will be the shift at high temperatures plus that due to the formation of the complex.

The two solvents n-hexane and toluene have similar polarizabilities (25) and hence the effect of the reaction field can be eliminated by the use of n-hexane as reference solvent.

Thus, the high temperature chemical shift δ_a can be considered to be the chemical shift of the protons in question when the solvent is n-hexane. If chemical shifts are measured relative to $\delta_a = 0$, then $\delta = f\delta_c$ and Equation 25 becomes

$$\delta = \frac{\delta_c \exp(-\Delta H/RT)\exp(\Delta S/R)}{1 + \exp(-\Delta H/RT)\exp(\Delta S/R)} \qquad 26$$

which on rearranging takes the form

$$\frac{1}{\delta} = \frac{1}{\delta_c}\left[e^{\Delta H/RT}\, e^{-\Delta S/R} + 1\right] \qquad 27$$

It is possible to fit the dependent variable $1/\delta$ to the independent variable T and the parameters ΔH, ΔS and $1/\delta_c$ by non-linear least squares curve fitting techniques (60). From Equation 23, it is possible to calculate a value for K at any temperature.

The results of the temperature studies that were carried out are presented in Table 10. Plots of temperature versus chemical shift for the formyl and the methyl protons of $HC(OCH_2)_3CCH_3$; the methyl and methylene protons of $P(OCH_2)_3CCH_3$; the formyl and the axial protons of $HC(OCH)_3(CH_2)_3$ are presented in Figures 10, 11, 12, 13, 14, and 15, respectively. As can be seen from the data, the chemical shifts of the quatorial and methine protons of $HC(OCH)_3(CH_2)_3$ are little affected by temperature changes. The results of the fit using the iterative non-linear least squares program of Moore and Zeigler (60) is

Table 10. Data for the chemical shifts in Hz from internal TMS of the protons in some bicyclic molecules as a function of temperature in toluene. The concentration of solute was in all cases less than 3% wt/V

Temp.[a]	$P(OCH_2)_3CH_3$		$HC(OCH_2)_3CCH_3$			$H\text{-}C(OCH_2)_3(CH_2)_3$		
	CH_2	CH_3	H-C	CH_2	CH_3	$H\text{-}C(O)_3$	CH_{ax}	CH_{eq}
-70.0	198.3	-22.2	344.3	206.6	-10.0	356.5	48.5	150.0
-50.0	199.2	-18.3	343.0	206.6	-7.1	353.0	53.5	148.8
-31.0		-15.2	341.8	207.3	-4.6	350.6	56.5	150.5
-17.2	200.8	-13.0	340.1	207.0	-1.6	348.3	59.0	151.0
+2.5	202.2	-9.6	338.2	205.3	+1.7	346.3	61.5	151.0
+14.0	203.1	-7.8	337.5	207.3	+3.2	345.4	62.5	150.5
+27.5	203.9	-5.8	336.4	210.1	+5.0	343.9	64.0	150.5
+37.0	204.6	-4.6		208.2	+6.4	343.4	66.0	152.0
+48.0	205.2	-3.1	334.6	210.6	+7.8	342.1	67.0	152.5
+61.0	206.0	-1.3	333.6	211.2	+9.1	341.2	68.0	153.0
+75.0	206.4	∿0.9	332.5	211.8	+11.1	340.5	69.0	152.5
+89.0	206.2	+2.6	331.7	211.4	+12.4	339.0	70.5	152.5
+103.0	207.7	+4.0	330.6	211.5	+13.5	338.6	72.0	153.0

[a]Temperatures are in °C and are accurate ± 1°.

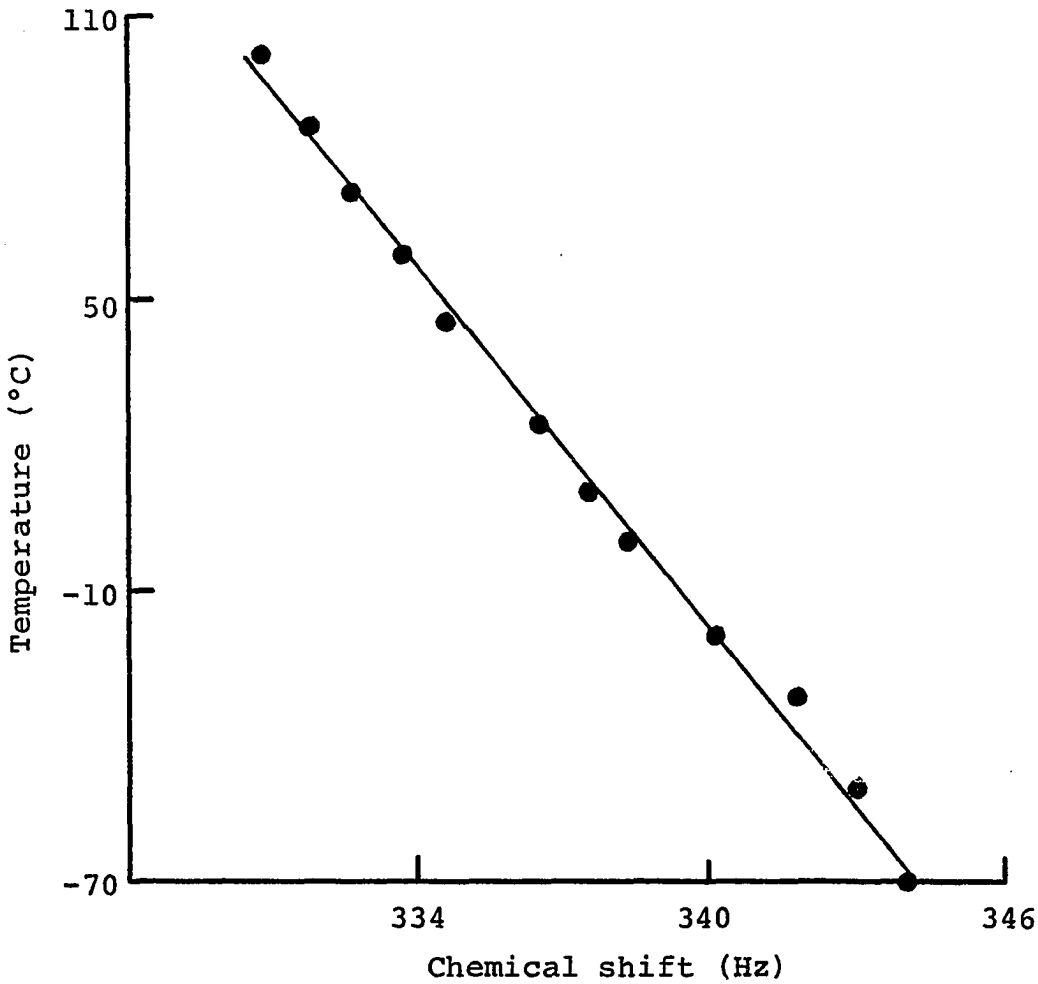


Figure 10. Plot of temperature versus chemical shift for the formyl proton of $HC(\overline{OCH_2})_3CCH_3$ in toluene

The chemical shift is in Hz from internal TMS on the δ scale and the concentration of the solute was less than 3% wt/v

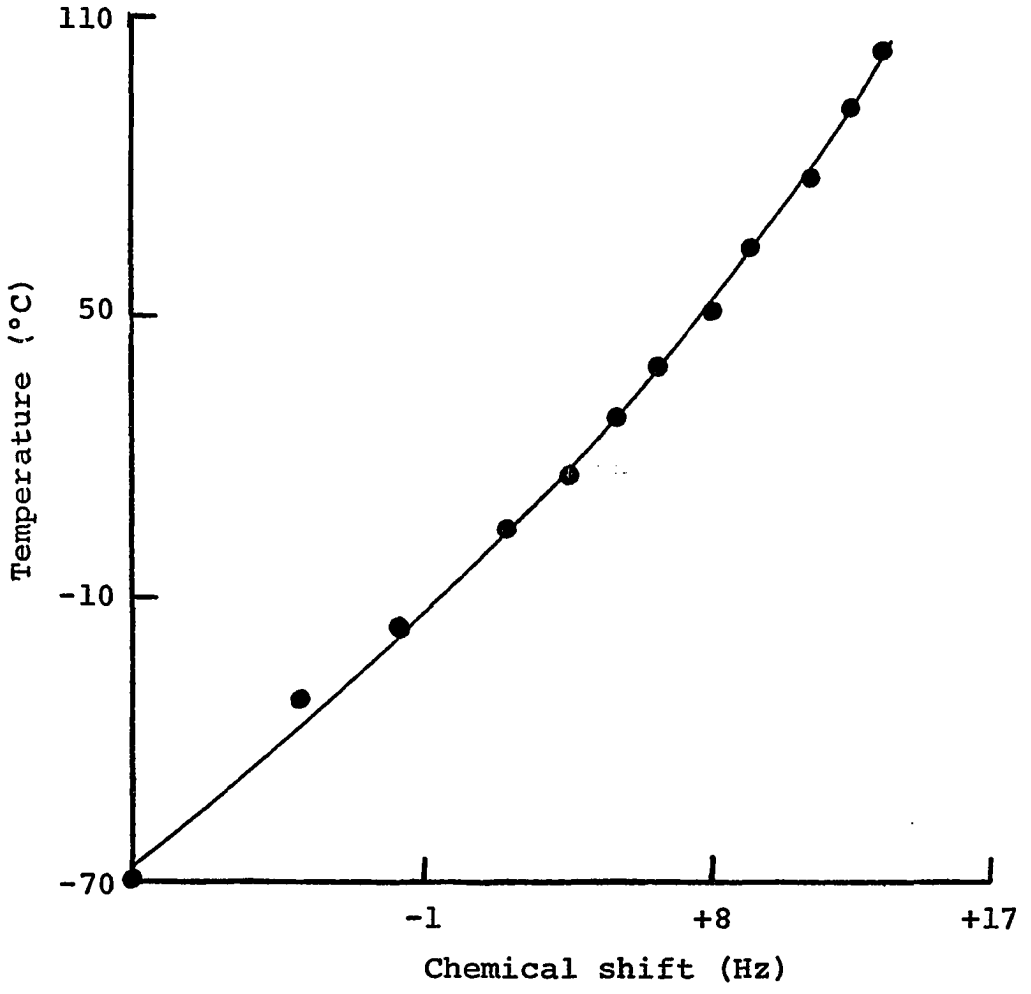


Figure 11. Plot of temperature versus chemical shift for the methyl protons of $HC(OCH_2)_3CCH_3$ in toluene

The chemical shift is in Hz from internal TMS on the δ scale and the concentration of the solute was less than 3% wt/v

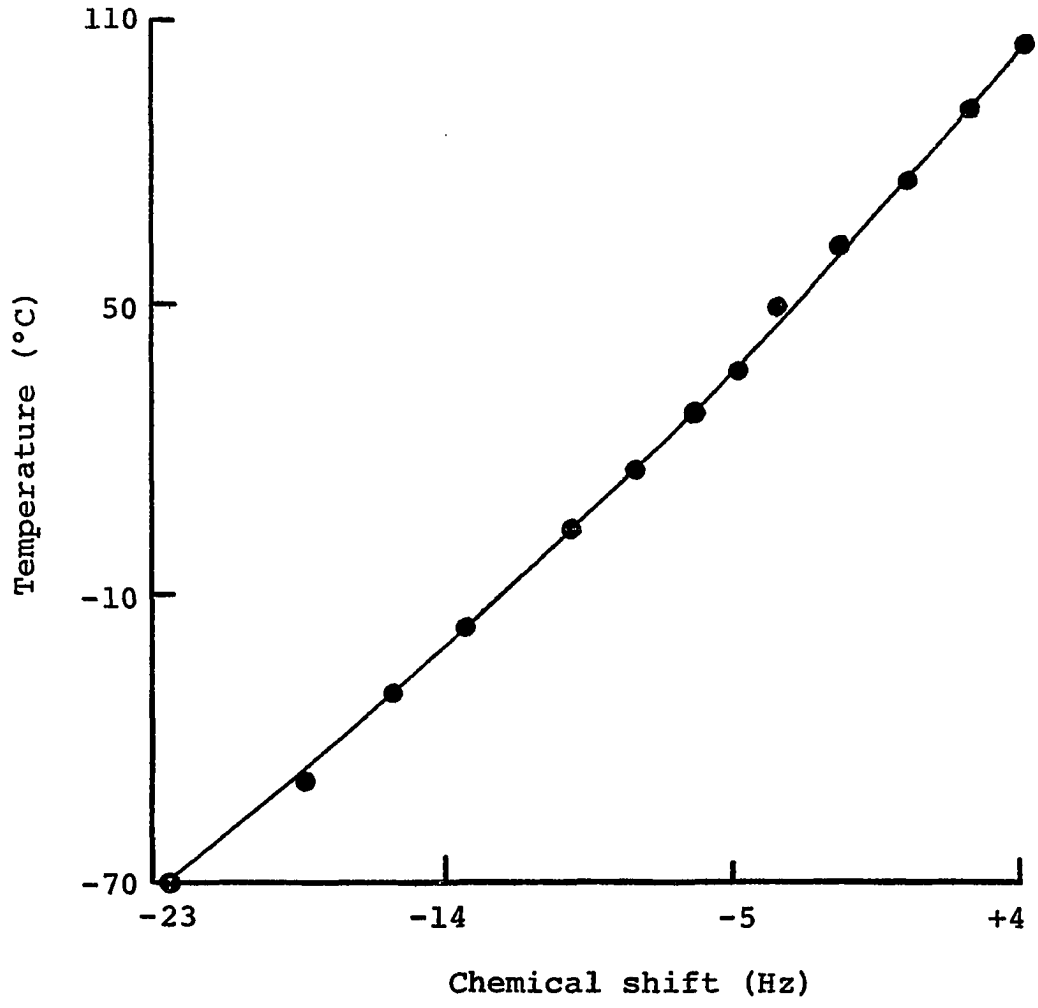


Figure 12. Plot of temperature versus chemical shift for the methyl protons of $P(\overline{OCH_2})_3CCH_3$ in toluene

The chemical shift is in Hz from internal TMS on the δ scale and the concentration of the solute was less than 3% wt/v

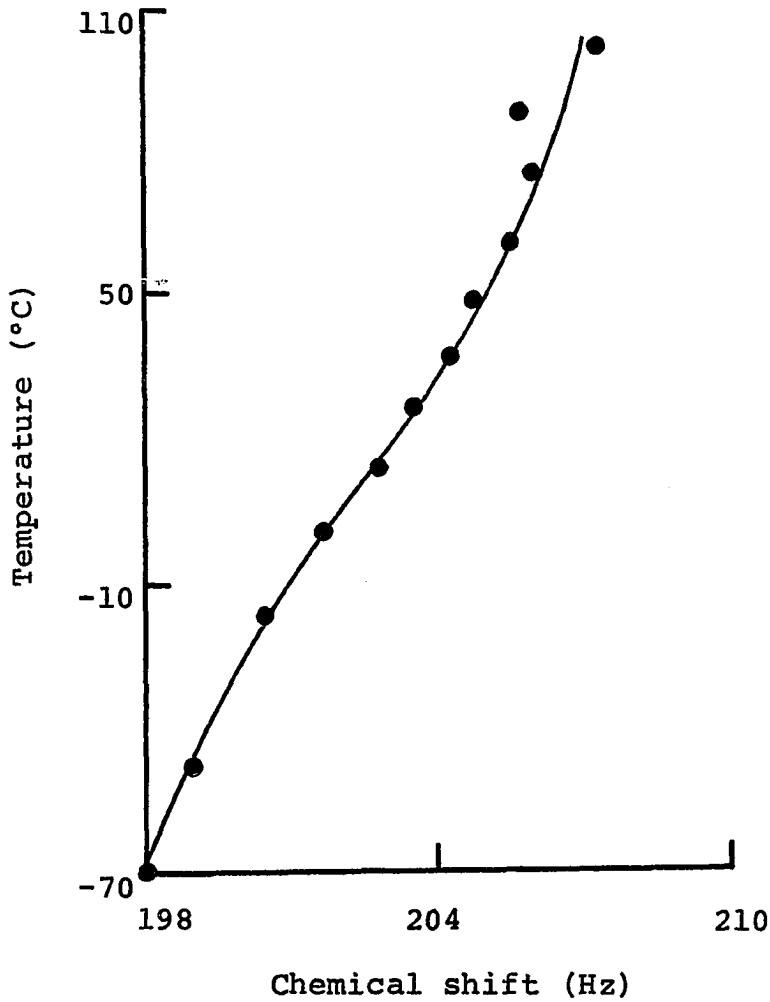


Figure 13. Plot of temperature versus chemical shift for the methylene protons of $P(OCH_2)_3CCH_3$ in toluene

The chemical shift is in Hz from internal TMS on the δ scale and the concentration of the solute is less than 3% wt/v

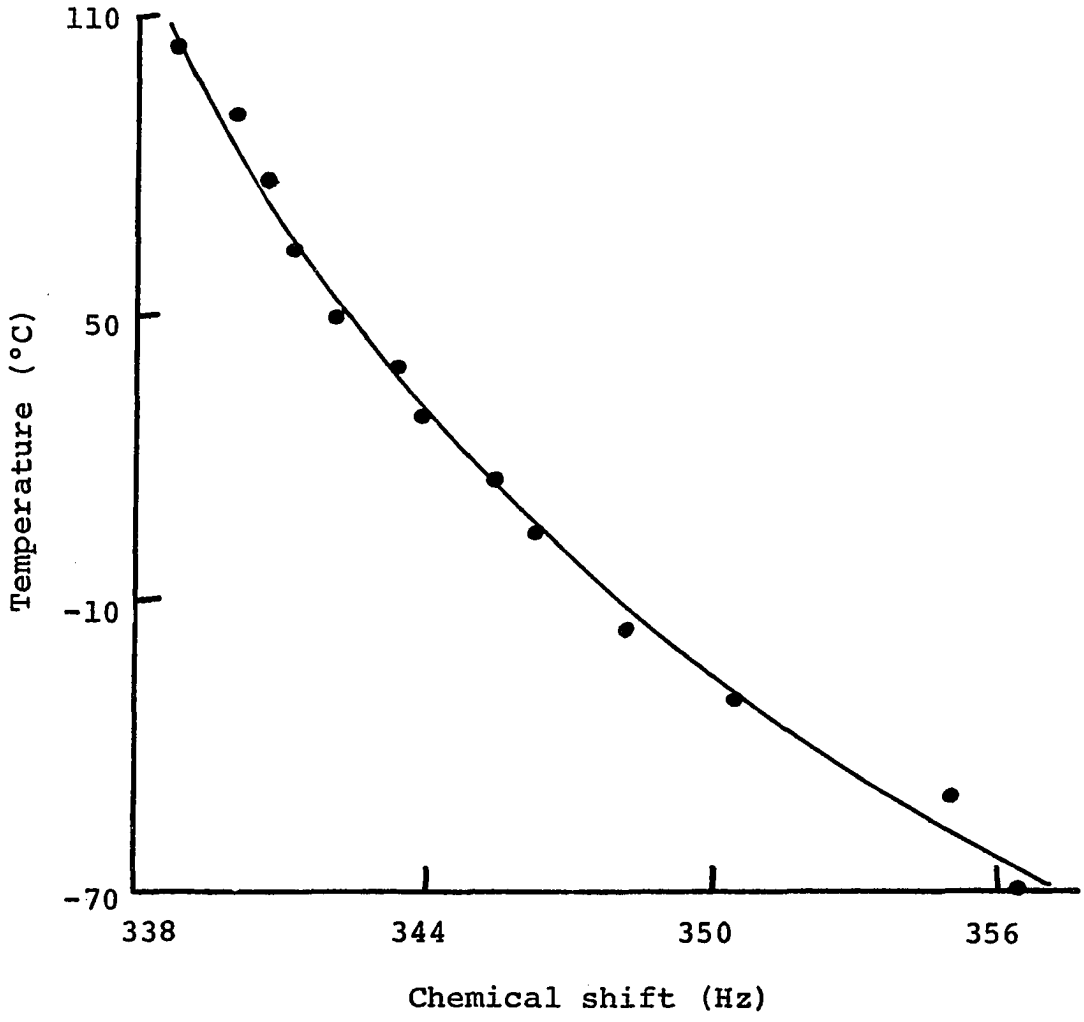


Figure 14. Plot of temperature versus chemical shift for the formyl proton of $HC(\overline{OCH})_3(CH_2)_3$ in toluene

The chemical shift is in Hz from internal TMS on the δ scale and the concentration of the solute is less than 3% wt/v

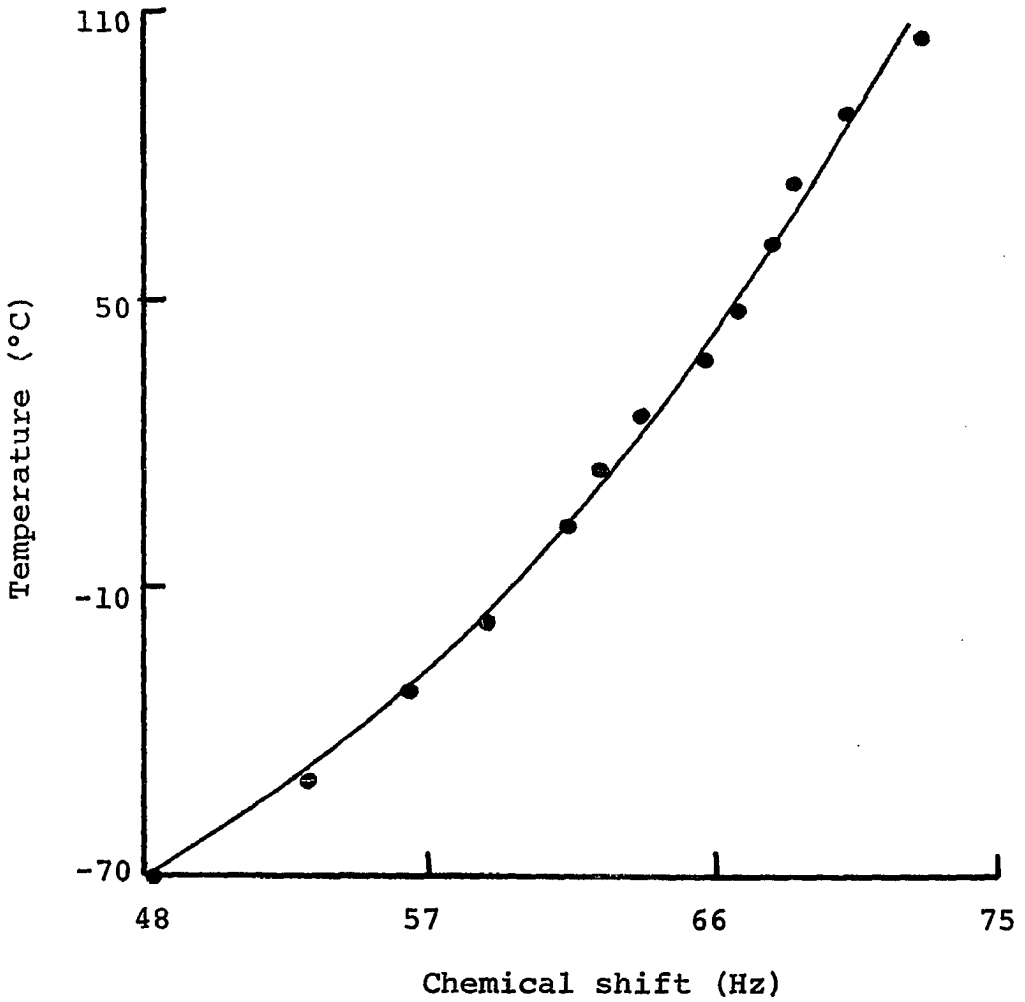


Figure 15. Plot of temperature versus chemical shift for the axial protons of $HC(\overline{OCH})_3(CH_2)_3$ in toluene

The chemical shift is in Hz from internal TMS on the δ scale and the concentration of the solute is less than 3% wt/v

given in Table 11. In all cases, except for the axial proton of $HC(OCH)_3(CH_2)_3$, n-hexane was used as the reference solvent. In this latter case, d_{12}-cyclohexane was used as reference solvent since the resonances of n-hexane obscured the resonance of the proton in question.

Table 11. Calculated parameters for solute·solvent complex in toluene

	$P(OCH_2)CCH_3$	$HC(OCH_2)_3CCH_3$		$HC(OCH)_3(CH_2)_3$	
	$C\underline{H}_3$	$\underline{H}C$	$C\underline{H}_3$	$\underline{H}C(O-)_3$	$C\underline{H}_{ax}$
ΔH (kcals/mole)	-1.76±0.07	-2.44±0.09	-1.70±0.06	-1.85±0.15	-1.41±0.13
ΔS (e.u.)	-4.75±0.14	-6.9±0.2	-4.9±0.1	-5.9±0.2	-4.6±0.1
δ_c [a]	-66.6±1.4	27.9±0.5	-60.2±0.7	37.8±1.6	-61.1±4.8
K at 27.5°C	1.78	2.04	1.51	1.14	1.00
% complex formation	65	67	60	53	50

[a] δ_c is indicated with respect to the value measured in n-hexane, except for CH_{ax}, where it is with respect to the value measured in C_6D_{12}.

DISCUSSION

$P(OCH_2)_3P$ and Its Derivatives

Characterization of compounds

The symmetries of the metal atoms in the complexes of $P(OCH_2)_3P$ determined from the characteristic infrared absorptions in the carbonyl region are reported elsewhere (53). The composition and molecular weights for these systems were confirmed by observation of the parent ion peaks in their mass spectra (61). The characterization of the symmetries of the two axial linkage isomers of the iron carbonyl complex and the unusual equatorial isomer are discussed by Allison and Verkade (61).

The possibility of linkage isomerism exists in these transition metal complexes as well as the phosphonium salts of $P(OCH_2)_3P$ since there are two chemically different phosphorus coordination sites in this ligand. Furthermore, $P(OCH_2)_3P$ is capable of coordinating to a metal atom on both donor sites as well as functioning as a positively charged ligand if one of the phosphorus atoms is quaternized. The disposition of $P(OCH_2)_3P$ as formulated in the compounds listed in Table 2 was determined from the nmr spectral parameters of these compounds.

The mode of attachment of $P(OCH_2)_3P$ to the metal cannot be unambiguously assigned on the basis of the positions of the CO bands. This was shown by the observation (53) that the bridged group VI carbonyl complexes showed only two unresolvable

carbonyl infrared bands when at least four were expected on the basis of two different $M(CO)_5$ moieties attached to the two different coordination sites of $P(OCH_2)_3P$. It is unlikely that exchange of metal carbonyl fragments on the ligand sites accounts for this result since for example, in a mixture of $(OC)_5WP(OCH_2)_3PW(CO)_5$ and free ligand, the ^1H spectrum showed the resonance of both species and those for the ligand occur at the normal chemical shift observed in the absence of the complex. The validity of the assignments of the ^{31}P chemical shifts (Table 2) and hence the structures for the two chemically non-equivalent phosphorus nuclei in $P(OCH_2)_3P$, $SP(OCH_2)_3P$, and $SP(OCH_2)_3PO$ was shown previously from a comparison of the ^{31}P chemical shifts of these compounds with the ^{31}P chemical shifts of the analogous compounds $P(OCH_2)_3CCH_3$, $OP(OCH_2)_3CCH_3$ and $SP(OCH_2)_3CCH_3$ (Table 4) (44). The ^{31}P chemical shift for this latter compound in conjunction with that now reported for $OP(CH_2O)_3CCH_3$ (Table 4) supports the present assignments made from the INDOR determination of the ^{31}P chemical shifts in $SP(OCH_2)_3PO$ which was not sufficiently soluble for measurement of its ^{31}P spectrum directly. It should also be noted that assignment of the ^{31}P chemical shift values for the "phosphine" $(P(C)_3)$ phosphorus in $P(OCH_2)_3P$ and $SP(OCH_2)_3P$ and the "phosphine oxide" phosphorus in $SP(OCH_2)_3PO$ and $OP(OCH_2)_3PO$ are now established more firmly by comparison of these values with those for $P(CH_2O)_3CCH_3$ and $OP(CH_2O)_3CCH_3$ which are now reported in Table 4.

The site of coordination in $P(OCH_2)_3P$ for the complexes was determined from a comparison of the ^{31}P chemical shifts of the complexes (Table 2) with those values observed in the free ligand and the analogous complexes of $P(OCH_2)_3CCH_3$ (Table 4) (44). For example, only a small change in ^{31}P chemical shift occurs for the $^{31}P(C)_3$ from $P(OCH_2)_3P$ (+66.99 ppm) to $(OC)_5Cr$-$P(OCH_2)_3P$ (+68.57 ppm) while the 65 ppm downfield shift in the $^{31}P(O)_3$ to -154.47 ppm in the complex is comparable to that observed for the shift from $P(OCH_2)_3CCH_3$ (-91.5 ppm) to $(OC)_5$-$CrP(OCH_2)_3$ (-162 ppm).

The linkage isomerism in the two axial $[(OC)_4Fe]P(OCH_2)_3P$ complexes is clearly supported by the ^{31}P chemical shift data. In axial - $(OC)_4FeP(OCH_2)_3P$ the ^{31}P chemical shift for $^{31}P(C)_3$ and $^{31}P(O)_3$ of +71.38 ppm and -157.44, respectively, are consistent with a coordinated phosphite and an uncoordinated phosphine moiety of $P(OCH_2)_3P$. The reverse situation obtains in axial - $(OC)_4FeP(CH_2O)_3P$ as the ^{31}P chemical shift for $^{31}P(O)_3$ and $^{31}P(C)_3$ of -87.37 ppm (uncoordinated phosphite) and -22.42 ppm (coordinated phosphine) suggest. The best evidence for these assignments comes from the values of the ^{31}P chemical shift of $^{31}P(O)_3$ (-160.40 ppm) and $^{31}P(C)_3$ (-22.06 ppm) in diaxial - $(OC)_4FeP(OCH_2)_3PFe(CO)_4$ in which both phosphorus nuclei must be coordinated. The geometrical isomer equatorial - $(OC)_4FeP(OCH_2)_3P$ contains $P(OCH_2)_3P$ coordinated through the phosphite end on the basis of the ^{31}P chemical shifts. In addition to the infrared evidence that this compound is isomeric

with the axial structure, the ^{31}P chemical shifts and $^{3}J_{PP}$ values also support this conclusion. Though the values for these parameters are similar in the two isomers, they are not equal since they are considerably outside experimental error.

The assignment of the linkage isomerism of $P(OCH_2)_3P$ in phosphonium salts was made by comparing the ^{31}P chemical shifts for $[CH_3P(OCH_2)_3P]BF_4$ ($\delta_{^{31}P_{(O)_3}}$ = -51.03 ppm, $\delta_{^{31}P_{(C)_3}}$ = +59.80 ppm), $[P(OCH_2)_3PCH_3]BF_4$ ($\delta_{^{31}P_{(O)_3}}$ = -89.58 ppm, $\delta_{^{31}P_{(C)_3}}$ = 2.56 ppm), $P(OCH_2)_3P$ ($\delta_{^{31}P_{(O)_3}}$ = -89.78 ppm, $\delta_{^{31}P_{(C)_3}}$ + 66.99 ppm) and $[CH_3P(OCH_2)_3CCH_3]BF_4$ ($\delta_{^{31}P}$ = -60.15 ppm).

The small effect on the chemical shift of one of the phosphorus nuclei caused by quaternizing the other in each case seems to indicate that a positive charge at one end of the molecule does not significantly affect the electronic properties of the phosphorus at the opposite end. This is particularly evident in the lack of any significant change in the frequencies of the carbonyl modes from $(OC)_5WP(OCH_2)_3P$ to $[(OC)_5WP(OCH_2)_3PCH_3]BF_4$ (61). There also appears to be little effect in the chemical shifts of one of the phosphorus nuclei by oxidizing the other end or coordinating it to a transition metal moiety. This is seen by comparing the appropriate ^{31}P chemical shifts in $P(OCH_2)_3P$ and $SP(OCH_2)_3P$; $SP(OCH_2)_3P$ and $SP(OCH_2)_3PO$;

$P(OCH_2)_3P$ and $(OC)_5MP(OCH_2)_3P$; $(OC)_5MP(OCH_2)_3P$ and $(OC)_5MP(OCH_2)_3PM(CO)_5$. These results suggest that electronic changes due to quaternization are rather localized near the phosphorus atom coordinated to the atom or ion. With regard to the positive ligand case, similar conclusions were drawn by Berglund and Meek (62) for several cationic metal complexes of the cationic ligand $(C_6H_5)_2\overset{+}{P}(CH_2)_2C(CH_3)CH_2P(C_6H_5)_2$ in which the donor phosphorus atom is one bond further removed from the quaternized phosphorus than in the $P(OCH_2)_3\overset{+}{P}CH_3$ cation.

A discussion of the trends in the various coupling constants is facilitated by the division of the compounds in Table 3 into the three classes shown below wherein the substituent group on the phosphorus in question can be an electron pair, a metal fragment, a methyl carbonium ion or a chalcogen atom. For each class,

Class A	$YP(OCH_2)_3P$
Class B	$P(OCH_2)_3PY$
Class C	$YP(OCH_2)_3PY$

plots have been constructed of $^3J_{PP}$ <u>versus</u> $^3J_{PH}$ (Figure 16) and $^3J_{PP}$ <u>versus</u> $^3J_{PH}$ (Figure 17) in order to reveal the various trends in these couplings which will be discussed in the following paragraphs. It should be noted that for each of the class C compounds, Y is the same Lewis acid except for $(OC)_5WP(OCH_2)_3PCH_3^+$ and $SP(OCH_2)_3PO$.

From Figure 16 it is seen that $^3J_{PH}$ increases substantially ($\sim$5 Hz) in positive magnitude for classes A and C but only

Figure 16. Plot of $^{3}J_{PP}$ versus $^{3}J_{PH}$ for $YP(OCH_2)_3P$(————) $P(OCH_2)_3PY$(– – – –) and $YP(OCH_2)_3PY$(—— – ——), where the Y groups are those indicated adjacent to each point

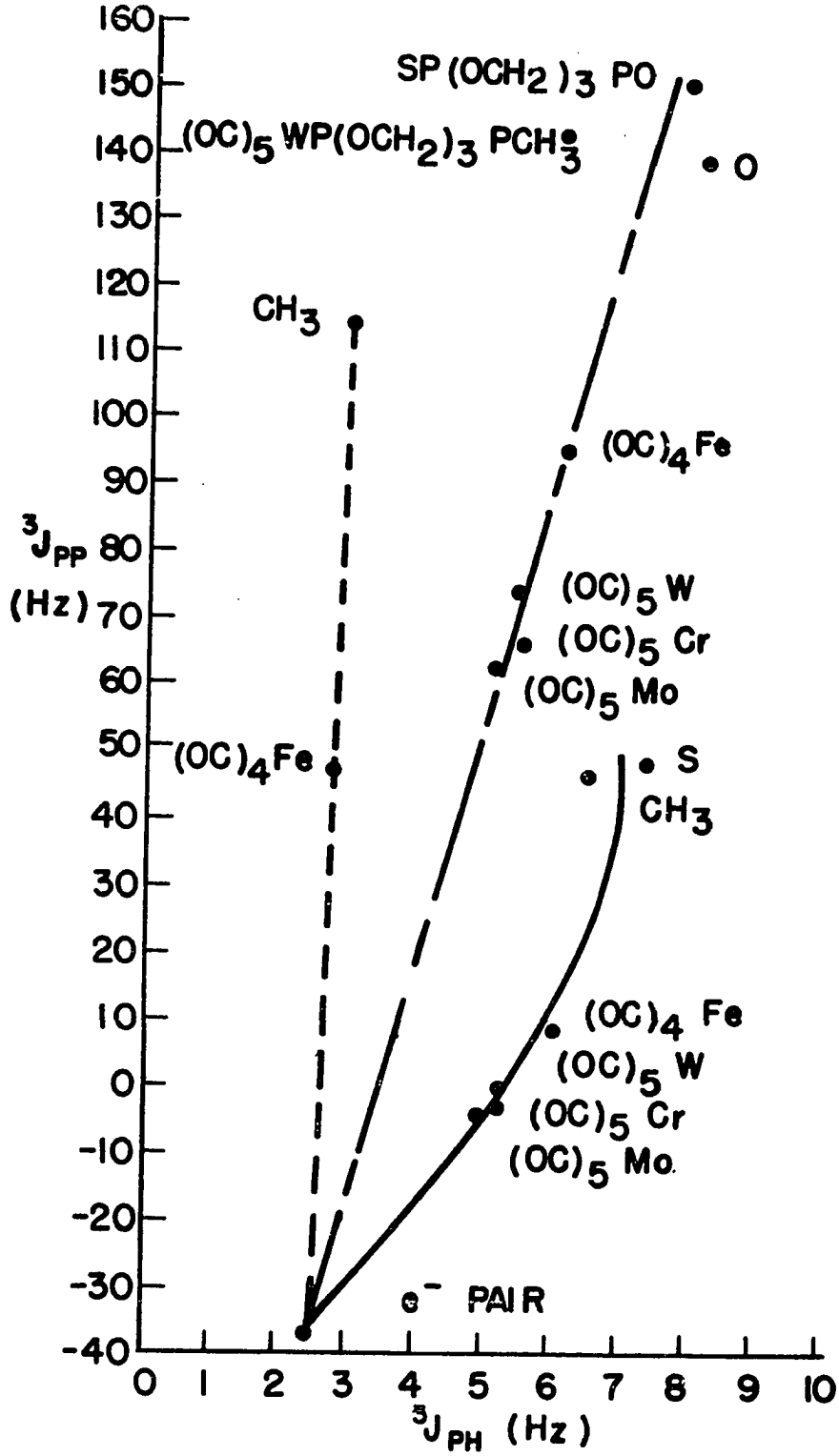
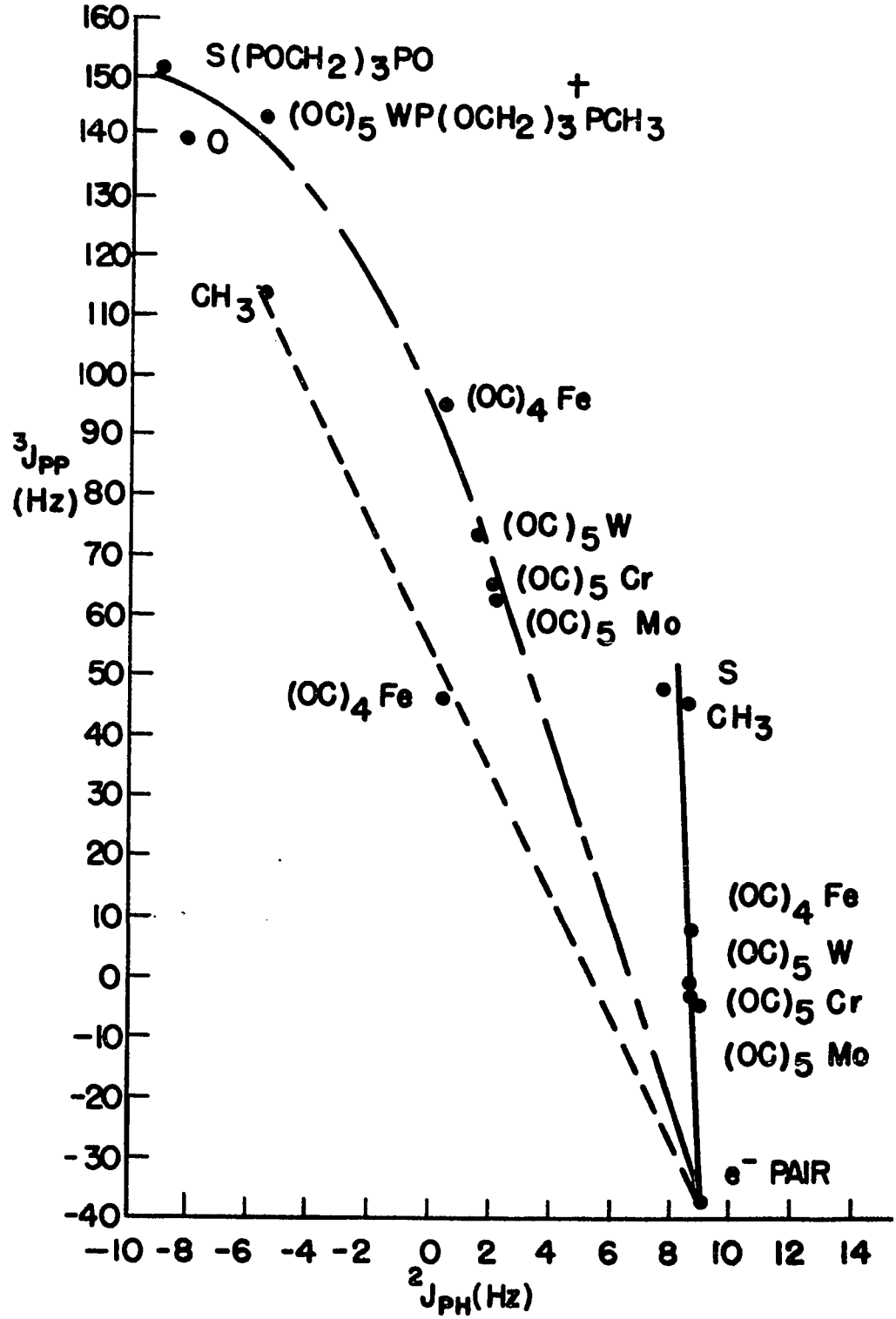

160
150
140
130
120
110
100
90
80
70
60
50
40
30
20
10
0
-10
-20
-30
-40
$^3J_{PP}$ (Hz)
0 1 2 3 4 5 6 7 8 9 10
$^3J_{PH}$ (Hz)
SP(OCH2)3PO
(OC)5WP(OCH2)3PCH3
O
CH3
(OC)4Fe
(OC)5W
(OC)5Cr
(OC)5Mo
S
CH3
(OC)4Fe
(OC)5W
(OC)5Cr
(OC)5Mo
e⁻ PAIR

Figure 17. Plot of $^{3}J_{PP}$ versus $^{2}J_{PH}$ for $YP(OCH_2)_3P$(————), $P(OCH_2)_3PY$(– – – –) and $YP(OCH_2)_3PY$(—— – ——), where the Y groups are those indicated adjacent to each point


160
150
140
130
120
110
100
90
80
70
60
50
40
30
20
10
0
-10
-20
-30
-40
$^3J_{PP}$ (Hz)
$S(POCH_2)_3PO$
$(OC)_5WP(OCH_2)_3\overset{+}{P}CH_3$
O
CH_3
$(OC)_4Fe$
$(OC)_5W$
$(OC)_5Cr$
$(OC)_5Mo$
$(OC)_4Fe$
S
CH_3
$(OC)_4Fe$
$(OC)_5W$
$(OC)_5Cr$
$(OC)_5Mo$
e^- PAIR
−10 -8 -6 -4 -2 0 2 4 6 8 10 12 14
$^2J_{PH}$(Hz)

slightly (∿0.5 Hz) for class B as the Lewis acidity of the Y group increases in the order electron pair < methyl < chalcogen. This is not unexpected in view of the increase in s character in the internal P-O bonds of the ligand and the rise in effective positive charge on the nuclei of the cage (particularly the coordinated $P(O)_3$ phosphorus) which would accompany an increase in Lewis acidity of Y. The very much smaller rise in $^3J_{PH}$ in the class B compounds might stem from the fact that the $P(C)_3$ phosphorus is coordinated to Y and this donor site is more remote from the POCH bond system through which $^3J_{PH}$ is transmitted. Extension of the argument given for the rise in $^3J_{PH}$ in the class A and C compounds to the very small rise in this parameter for the class B compounds must be viewed with some caution because of the small range of this parameter in the latter compounds (∿0.5 Hz) and the error in the measurements (0.1-0.2 Hz).

Figure 17 reveals that $^2J_{PH}$ becomes negative upon increasing the Lewis acidity of Y over a range of ca. 15 Hz for classes B and C whereas a range of less than ca. 1Hz is noted for the compounds in class A. It was recently suggested that $^2J_{PH}$ changes sign in a similar series of compounds from $P(CH_2O)_3CCH_3$ to $(OC)_4FeP(CH_2O)_3CCH_3$ to $OP(CH_2O)_3CCH_3$, but the absolute signs were not reported (45). The present data firmly support this postulate. Manatt and coworkers (63) discussed sign data obtained on other phosphine derivatives which indicated that as the s character in the P-C bonds increases due to increasing

electronegativity of the Y group on phosphorus $^2J_{PH}$ should become less positive or more negative. The data depicted in Figure 17 is in good agreement with this postulate.

Values of $^2J_{PH}$ for all the members of class A fall between +7.6 and +8.9 Hz. Albrand and coworkers (64) have found that there is a correlation which can be made in a large variety of phosphines between $^2J_{PH}$ and the dihedral angle made by a plane containing the P, C and H atoms and the plane containing the C-P bond and the three-fold axis of the $P(C)_3$ bond system. The expected value of $^2J_{PH}$ for class A compounds and $P(CH_2O)_3CCH_3$ according to their plot is +5 Hz which is somewhat below the +7.6 to +8.9 Hz observed for the former and the +8.0 Hz (45) for the latter. The small discrepancy can be explained in terms of the results of studies carried out by Pople and Bothner-By (8) and Manatt (63). From a molecular orbital treatment of the HCH system in hydrocarbon derivatives and a consideration of the available nmr data in these systems, Pople and Bothner-By have concluded that increasing the electronegativity of a substituent on carbon should increase the s character in the H-C bonds and thus increase $^2J_{HH}$ toward more positive values. The same conclusion was reached by Manatt and coworkers on carbon PCH systems from a study of the signs of $^2J_{PH}$ in phosphines. The apparently anomolous $^2J_{PH}$ values in our system compared with those of the phosphines examined by Albrand et al. (which contained only hydrocarbon substituents) could be due to the fact that the $P(C)_3$ carbons in our compounds are bound to electro-

negative oxygen groups such as $YP(O)_3$ in class A, and $CH_3C(O)_3$ in $P(CH_2O)_3CCH_3$. Such groups would tend to raise a positive $^2J_{PH}$ above the 5 Hz predicted for say $P(CH_2CH_2)_3CCH_3$ or $P(CH_2CH_2)_3P$. The former compound is as yet unknown whereas the nmr parameters for the latter have not been reported. A second contributing factor to the somewhat large $^2J_{PH}$ values in the compounds under discussion might be the slightly less-than-normal CPC bond angles (i.e., less s character in the PC links) due to constraint. The reason for the small rise in $^2J_{PH}$ with rising electron withdrawing power of the Y group in the class A compounds is not apparent at this time.

The values and signs of the vicinal ^{31}P-^{31}P couplings for the 18 compounds reported in Table 3 represent the first systematic study of this coupling constant. Figure 16 (or 17) shows that this coupling constant increases markedly from negative to positive values as the Lewis acidity of the Y group increases in the order electron pair<metal carbonyl fragment< methyl<chalcogen for each class of compounds. This trend parallels those discussed above for the changes in $^2J_{PH}$ and $^3J_{PH}$ and similar arguments based on effective nuclear charge and hybridization changes in the bicyclic portion of these systems may be applied here. It is interesting that $^3J_{PP}$ is more sensitive to coordination of the $P(C)_3$ phosphorus than the $P(O)_3$ phosphorus of $P(OCH_2)_3P$. This may arise from the greater polarizability of the "phosphine" phosphorus lone pair by the

Lewis acid moiety. Polarizing both phosphorus pairs (class C) augments the $^{3}J_{PP}$ coupling over that in analogous compounds in classes A and B as expected.

The parallel trends among the various coupling constants in all three classes of compounds are made more significant by the fact that the structural rigidity of the systems discussed here eliminates rotational averaging of coupling which could vary among the compounds studied and so these effects need not be considered in the coupling mechanism. It remains, however, to consider the possibility of a "through space" ^{31}P-^{31}P spin-spin coupling involving the phosphorus non-bonding orbital lobes which lie inside the bicyclic structure along the three-fold axis of the molecule. The distance between the phosphorus atoms is probably at least 2Å which would seem to mitigate against such a mechanism. Moreover it would be difficult to see how this coupling could rise positively with the increasing Lewis acidity of Y as observed, inasmuch as the phosphorus non-bonding lobe(s) would be expected to lose s character. It is tentatively concluded that a "through-space" for ^{31}P-^{31}P coupling need not be invoked presently.

The signs of the respective couplings of phosphorus to ^{13}C in I and its dioxide derivative agree with those reported by McFarlane (19) for $P(OCH_3)$, $OP(OCH_3)_3$, $P(CH_3)_3$, $SP(CH_3)_3$ and $SeP(CH_3)_3$. The $^{1}J_{PC}$ value of -15 ± 1 Hz for $P(OCH_2)_3P$ is only about 1 Hz larger in magnitude than the -13.6 Hz value reported

for the same coupling in $P(CH_3)_3$. The value of this coupling in $OP(OCH_2)_3PO$ is 67.1 ± 0.7 Hz which is 11 Hz larger than the value of 56.1 Hz reported for $SP(CH_3)_3$ and 18.6 Hz larger than the value reported for $SeP(CH_3)_3$. The value -8.5 ± 0.7 Hz for $^3J_{PC}$ in $OP(OCH_2)_3PO$ is close to the value of -5.8 reported for this coupling in $OP(OCH_3)_3$.

McFarlane also reported the chemical shifts of the ^{13}C nuclei in $P(OCH_3)_3$ and $OP(OCH_3)_3$ (19). He determined that the ^{13}C carbon in $P(OCH_3)_3$ is shielded by 6.0 ppm compared to the carbon in $OP(OCH_3)_3$. This same difference in chemical shift was observed between $P(CH_3)_3$ and $SP(CH_3)_3$ or $SeP(CH_3)_3$, the ^{13}C in the trivalent phosphorus compound being more shielded. The ^{13}C chemical shift of $P(OCH_2)_3P$ (-37.88 ± 0.1 ppm) was observed to be 0.6 ppm to lower field than its dioxide (-37.28 ± 0.02 ppm) which contrasts with the results for the aforementioned compounds.

A naive molecular orbital approach was considered in attempting to discuss these results in terms of the Pople-Santry theory. By considering the planar PCOP fragment, it can be seen that this has C_s symmetry. All σ mo's will be symmetric with respect to inversion through the plane of symmetry, hence, it is not possible to obtain a positive contribution to the contact term. However, it is observed that the entire molecule considered as a whole is not planar. This should result in mixing between the orbitals in the plane of a PCOP fragment and those

outside this plane. This mixing could give rise to molecular orbitals having some contribution due to the 3s orbital on each phosphorus that would give a nagative product for the coefficients (C) in Equation 9 and hence a positive contact term.

NMR Studies of Distributed Complexes

The determination of the magnitudes and signs of the geminal ^{31}P-^{31}P spin-spin coupling constants in transition metal complexes involving metal-phosphorus bonds is a prerequisite for any discussion of the mechanism of this coupling. The determination of the signs of such coupling constants is also necessary in order to discern trends in these couplings with changes in the chemical nature of the ligands. Such results would hopefully be interpretable in terms of the nature of the metal-phosphorus bond. The requirement that the signs of these couplings be determined in addition to their magnitudes arises because in numerous cases a given coupling constant involving phosphorus is known to change sign, depending on the nature of the molecule. For instance, $^{2}J_{PC}$ changes sign from $P(OCH_3)_3$ to $OP(OCH_2)_3$ and $^{2}J_{PH}$ changes sign from $P(CH_3)_3$ to $P(CH_3)_4^+$ (19). Indeed, by examining the results presented in Table 6, it can be seen that $^{2}J_{PP}$ has a different sign depending upon the geometry of the metal complex for a particular metal and ligand (compare cis-$(OC)_4MoL_2$ with its trans-analogue) as well as for the metal in a given geometry (compare trans-$(OC)_4MoL'_2$ with trans-$(OC)_4CrL'_2$). Evidence will be presented which suggests

that $^2J_{PP}$ changes sign for the trans-Cr complexes as the phosphorus ligand changes. Before discussing the results of the study of geminal ^{31}P-^{31}P couplings, the other nmr parameters will be examined for each ligand.

As indicated earlier, the value of N for the trimethyl phosphite complexes is expected to be equal to $^3J_{PH}$. The values reported for N and $^3J_{PH}$ in Tables 6 and 7 for the complexes of $P(OCH_3)_3$ compare with the value of +10.0 ± 0.1 Hz for $P(OMe)_3$ and +10.5 ± 0.1 Hz reported for $OP(OCH_3)_3$ by McFarlane (19) and the value of +11.4 Hz now reported for $[CH_3P(OCH_3)_3]^+$. Although the s character is the $P(O)_3$ bonds might be expected to change from $P(OMe)_3$ to $OP(OCH_3)_3$ to $[CHP(OCH_3)_3]^+$, the observation of a nearly constant $^3J_{PH}$ may indicate that a compensating effect operates in the OC or CH bond, thus lowering $^3J_{PH}$ for $OP(OCH_3)_3$ to 10.5 Hz. It is very likely that the stereochemistry of the POCH bond system plays a major role in the $^3J_{PH}$ coupling constant, since in the constrained phosphite molecules discussed previously, $^3J_{PH}$ in $P(OCH_2)_3CCH_3$ and $P(OCH_2)_3P$ is 1.8 Hz and 2.5 Hz, respectively, and for $OP(OCH_2)_3CCH_3$ and $OP(OCH_2)_3PO$, $^3J_{PH}$ is 7 Hz (54) and 8.3 Hz, respectively while in the transition metal complexes of these ligands, $^3J_{PH}$ possesses intermediate values. The free rotation of the $-OCH_3$ groups in the open-chain compounds probably allows $^3J_{PH}$ to average to a value which is larger than in the analogous bicyclic compounds.

Considering the values and signs of N_C and $^2J_{PC}$ for the trimethyl phosphite complexes, it would also appear that there

is a negligible contribution to N_C in the disubstituted complexes of this ligand from $^4J_{PC}$. Thus, N_C for these compounds is nearly equal to $^2J_{PC}$. The values of N_C reported in Table 6 are between the +10.0 ± 0.2 Hz reported for $P(OCH_3)_3$ and -5.8 ± 0.2 Hz for $OP(OCH_3)_3$ (19) which is slightly higher than the -6.8 ± 0.4 Hz observed for $^3J_{PH}$ in $[CH_3P(OCH_3)_3]^+$ (Table 5). It is concluded from this observation that as the electron withdrawing power of the group attached to phosphorus is increased, the two bond P-O-C coupling becomes more negative. This trend is the same as that observed for the change in the two bond P-C-H coupling as more electronegative groups are attached to phosphorus. The latter trend was discussed earlier for $P(OCH_2)_3P$ and its derivatives. The explanation for the former trend is believed by the author to be the same as that for the latter trend.

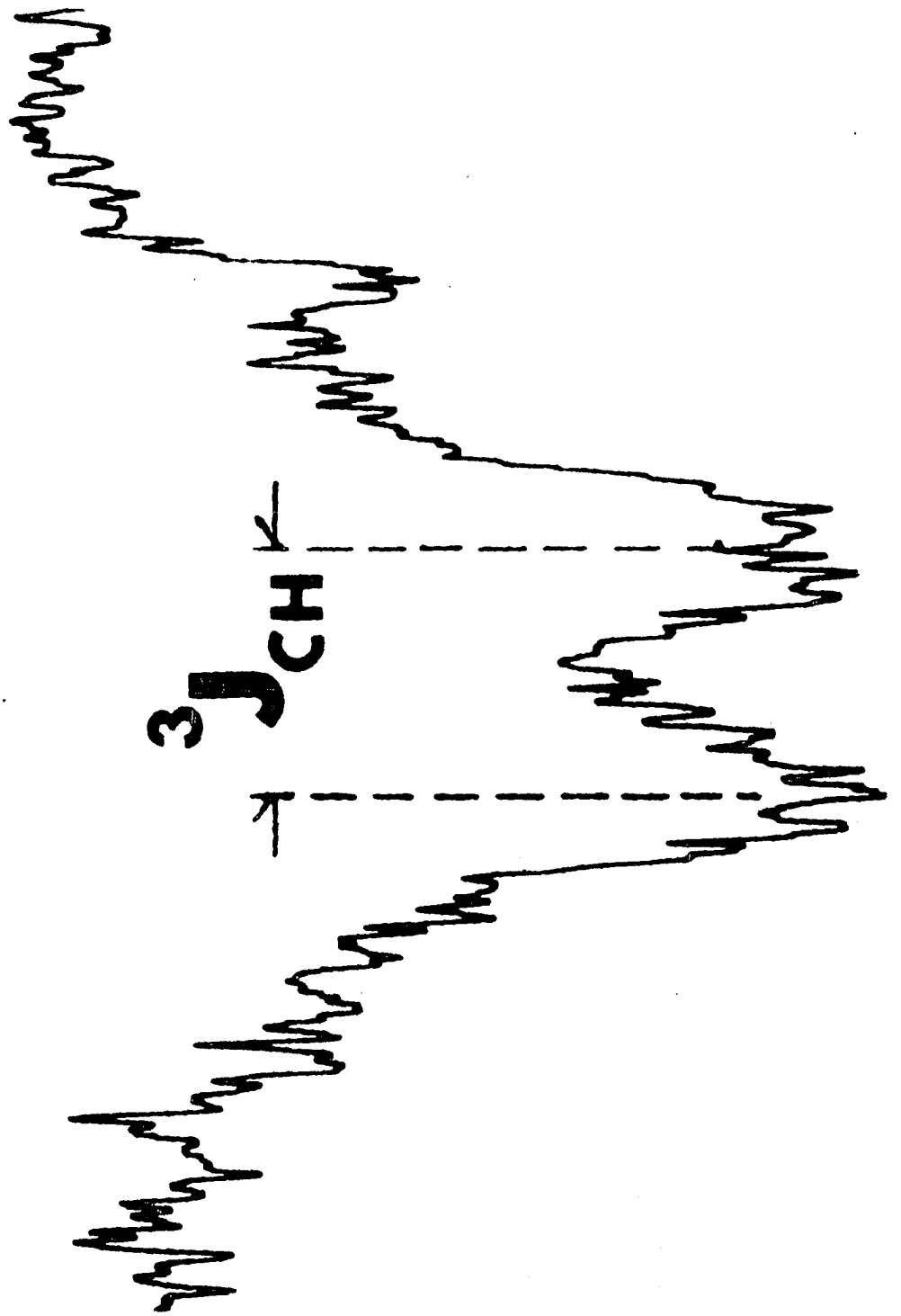
It is felt that the N values reported for the complexes of $P[N(CH_3)_2]_3$ are essentially $^3J_{PH}$ as was the case for the complexes of $P(OCH_3)_3$ since no splitting of the N doublet due to $^5J_{PH}$ was observed in the ^1H spectrum of mixed ligand complexes in which $P[N(CH_3)_2]_3$ was one of the ligands (59). The sign determinations for $^3J_{PH}$ reported in this dissertation represent the first such investigations involving a three-bond coupling through a nitrogen bound to phosphorus. The positive signs for these three-bond couplings are not unexpected in view of the same sign observed for this coupling in phosphites and their derivatives. As with the phosphite complexes, the transition

metal complexes of $P[N(CH_3)_2]_3$ have $^3J_{PH}$ values slightly larger than in the corresponding oxide. McFarlane has determined the $^3J_{PH}$ coupling in $P(C_2H_5)_3$ to be +13.8 ± 0.1 Hz (19). The values of 10.0 Hz and 8.8 Hz for $^3J_{PH}$ in $P(OCH_3)_3$ and $P[N(CH_3)_2]_3$, respectively, indicate that there is little correlation between this coupling and the electronegativity of the intervening atom attached to phosphorus.

It cannot be readily said that N_C for the complexes of $P[N(CH_3)_2]_3$ does not contain a significant contribution due to $^4J_{PC}$. The two values which are reported for this parameter differ by 5 Hz, and no monosubstituted complex of this ligand was studied. However, it is felt that $^4J_{PC}$ is not significant since it was found to be negligible for the trimethyl phosphite complexes. As in the case of trimethyl phosphite and its complexes, the values of N_C are intermediate between the $^2J_{PC}$ values observed the free ligand (+19.4 Hz) and its oxide (2.2 Hz). The trend towards less positive or more negative two-bond couplings with increasing electron withdrawing power of the group attached to phosphorus is again observed.

It was also found for $P[N(CH_3)_2]_3$ and its oxide that the ^{13}C INDOR spectrum of these compounds for one spin state of ^{31}P and ^{13}C was a quartet. An example of this is shown in Figure 18. The extra splitting is interpreted as being due to the long-range coupling between the ^{13}C and the three protons attached to the other methyl group on the nitrogen atom. The value of this coupling is reported in Table 7, but the sign of

Figure 18. ^{13}C INDOR spectrum of $OP[N(CH_3)_2]_3$ for one spin state of phosphorus and one spin state of the protons attached to the ^{13}C nucleus


$^3J_{CH}$

$^3J_{HC}$ was not determined.

It was shown by Ogilvie (58) from curve fitting techniques that N in the group VI complexes of $P(CH_3)_3$ reported in Table 6 has at most a contribution of +0.3 Hz due to $^4J_{PH}$. The values he reported are +0.2 ± 0.2 Hz for cis-$(OC)_4CrL"_2$, +0.3 ± 0.2 Hz for trans-$(OC)_4CrL"_2$, +0.3 ± 0.2 Hz for cis-$(OC)_4MoL"_2$ and +0.25 ± .05 Hz for cis-$(OC)_4WL"_2$. It was reported by Goodfellow that $|^2J_{PH}|$ is 10.1 Hz and that $|^4J_{PH}|$ is 2.7 Hz (for the $P(CH_3)_3$ moiety) in trans-$PdI_2P(CH_3)_3P(C_2H_5)_3$ (65). Thus, if $^4J_{PH}$ were opposite in sign to $^2J_{PH}$, they would sum to give 7.4 Hz. The value of -7.0 Hz for N in trans-$PdL"_2I_2$ suggests a $^2J_{PH}$ of ∿-10 Hz and $^4J_{PH}$ = ∿+3 Hz. Indeed, using the value for $^2J_{PP}$ obtained by this author, Ogilvie has found values of -10.0 ± 0.2 Hz and +3.0 ± 0.2 Hz, respectively, for these couplings by a band shape analysis.

It is noted again that by increasing the electron withdrawing power of the groups attached to phosphorus in the order metal<chalcogen, the $^2J_{PH}$ coupling constant decreases from +2.7 Hz in $P(CH_3)_3$ (19) to ∿-7 Hz in the neutral group VI complexes, to 10.0 Hz in the positively charged trans-$PdI_2L"_2$ and finally to -13.0 Hz in $SP(CH_3)_3$ or $SeP(CH_3)_3$. In this regard, it should be pointed out that when phosphorus is quarternized to $(CH_3)_4P^+$ or $(CH_3O)_3PCH_3^+$ the $^2J_{PH}$ becomes -15.4 Hz (19) and -17.8 Hz, respectively. This trend has been discussed previously with regard to the derivatives of $P(OCH_2)_3P$, and the arguments presented there are intended to apply here.

It is noted that even though the two-bond couplings in the neutral trimethyl phosphite derivatives and the trimethyl phosphine derivatives change sign whereas this is not the case for the $P[N(CH_3)_2]_3$ derivatives, the range of values is nearly the same in these three cases (15.8 Hz, 15.7 Hz and 17.2 Hz, respectively). This is surprising considering the fact that the magnetogyric ratio of ^{13}C is about one-fourth that of ^{1}H, and all else being equal, the P-C couplings might have been expected to be about one fourth that of the P-H couplings. This phenomenon does not seem to be dependent upon the fact that carbon intervenes between the proton instead of oxygen or nitrogen, for it has been reported that $^{2}J_{PC}$ in $(C_2H_5)_4P^+$ is -4.3 compared to the $^{2}J_{PC}$ value of +14.1 in $P(C_2H_5)_3$ (19) giving a range of 18.4 Hz (which corresponds to the 16.8 Hz difference between $^{2}J_{PC}$ for $P(OCH_3)$ and $[CH_3P(OCH_3)_3]^+$). It is therefore expected that $^{2}J_{PC}$ in $OP(C_2H_5)_3$ is somewhat higher than -4.3 Hz. This unexpected sensitivity of $^{2}J_{PC}$ to substitution at phosphorus requires further study.

No assessment of the contribution of $^{3}J_{PC}$ to N_C can be made at this time. However, it is not unreasonable to expect a considerable contribution although the values reported in Table 6 for N_C are intermediate between the $^{1}J_{PC}$ of -13.6 Hz for $P(CH_3)_3$ and the $^{1}J_{PC}$ of +56 Hz for $(CH_3)_3PS$ (19). It is noted that the value of $^{3}J_{PC}$ in $P(OCH_2CH_3)_3$ is +4.9 compared to +6.8 for $OP(OCH_2CH_3)_3$.

It is interesting that $^1J_{PC}$ in $[CH_3P(OCH_3)_3]^+$ is 132.4 Hz compared to $^1J_{PC}$ of +55.5 Hz in $P(CH_3)_4^+$. It might be argued that this is a result of an increase in the s character of the P-C link for two reasons. First, the replacement of the three methyl groups with three methoxy groups would, according to Bent (66), increase the s character in the phosphorus orbital involved in bonding to carbon. Bent's rule says that electropositive substituents form bonds having a greater degree of s character than electronegative substituents. This represents an increase in the C values of Equation 9 for the contribution due to a $\sigma \rightarrow \sigma^*$ transition, which means an increase in the contribution of a positive term in the contact interaction (8).

Furthermore, it might be expected that the one phosphine carbon and phosphorus in $[CH_3P(OCH_3)_3]^+$ support more positive charge than do any one of the methyl groups or the phosphorus in $[(CH_3)_4P]^+$. This would in general lead to a greater value for $(S_{3sP}|\delta\hat{r}_o|S_{3sP})(S_{2sC}|\delta\hat{r}_o|S_{2sC})$ in Equation 9, thus leading to an increase in the positive PC coupling in $[CH_3P(OCH_3)_3]^+$ compared to $[(CH_3)_4P]^+$. This reasoning is supported by considering the values of $^1J_{CH}$ in these compounds which are 142.9 Hz for the phosphine methyl carbon in $[CH_3P(OCH_3)_3]^+$ and 132.5 Hz in $[(CH_3)_4P^+]$. Although it might be argued that this change is due to the increased effective electronegativity of the phosphorus, it is felt that this change is almost wholly due to the increase in the positive charge which the phosphine methyl group in $[CH_3P(OCH_3)_3]^+$ must support, thus increasing

$(S_{2sC}|\delta\hat{r}_o|S_{2sC})$. It is found experimentally, for example, that increasing the electronegativity of groups attached to the atom bound to a methyl carbon has a very much smaller effect on the CH coupling constant than is observed here (1) (compare $^1J_{CH}$ for CH_3COOH of 130 Hz with CH_3CHO of 127 Hz, or, CH_3CN of 136 Hz with CH_3CCl_3 of 134 Hz. The changes in the energy levels of the σ molecular orbitals which would be brought about by this redistribution of positive charge is difficult to assess. It might be expected that both the phosphorus 3s and carbon 2s orbitals would be lowered in energy as these atoms support more positive charge, hence the change in the $\sigma\rightarrow\sigma^*$ excitation energy may or may not be changed.

The $^1J_{CH}$ values for the various ligands and their complexes seem to follow the expected trend. As a result of Bent's rule, $^1J_{CH}$ should increase as the substituent attached to carbon increases its electronegativity in the order P<N<O since increasing the electronegativity of the carbon substituent is expected to result in increased s character for the CH bonds. This observation has a theoretical basis in valence bond theory (67, 68) and numerous empirical correlations are in agreement with this observation (69-72). The idea that hybridization is solely responsible for the observed trends has been criticized, however (73). Grant and Litchman (73) have included the effective nuclear charge on carbon in considering coupling between directly bonded carbon and hydrogen. Since the coupling is proportional to the third power of this parameter, small changes in the

effective nuclear charge will greatly affect $^{1}J_{CH}$. Increasing the electronegativity of atoms attached to carbon should increase the effective nuclear charge, hence the coupling constant $^{1}J_{CH}$ should also increase. In the Pople-Santry molecular orbital treatment, increasing the charge on the carbon should tend to increase in $^{1}J_{CH}$. Furthermore, as the s character in the CH bond increases, as reflected by increasing the coefficients (C) in Equation 9, the positive $^{1}J_{CH}$ should become more positive.

The ^{31}P chemical shifts are as expected. It is observed for the transition metal complexes that the phosphorus becomes more deshielded upon complexation, and the size of this shift for a particular metal is the same as that observed by other workers (58, 59). Some of the changes in the ^{13}C chemical shifts are reasonable. For the complexes of $P(OCH_3)_3$ (Tables 6 and 7), a deshielding of 3.61 ppm is observed in going from the neutral molybdenum complexes to the dipositive palladium complex. The same trend was observed when comparing the ^{13}C chemical shift of $P(OCH_3)_3$ with $OP(OCH_3)_3$, where the electronegative phosphoryl oxygen causes a deshielding of 6.0 ppm in the ^{13}C of $OP(OCH_3)_3$ (19). An even greater deshielding is observed for the methoxy carbon $[CH_3P(OCH_3)_3]^+$. This same trend is observed in the chemical shift values of the derivatives of $P(CH_3)_3$ reported here and elsewhere (19). The fact that the ^{13}C in $OP[N(CH_3)_2]_3$ is more shielded than in

$P[N(CH_3)_2]_3$ is out of line with the observations involving the former compounds.

The trends in the geminal ^{31}P-^{31}P coupling constants can be discussed in terms of three factors: the sterochemistry of the metal complexes, the nature of the phosphorus ligand and the metal itself. Figures 19 and 20 represent the values of $^2J_{PP}$ as a function of the metal and ligand for the cis- and trans- complexes of the group VI carbonyls respectively. Included in these figures in addition to the values of the couplings reported by this author are the values obtained for the complexes of $P(OCH_2)_3CR$ (R = alkyl) and PF_3 (58). Although the signs of $^2J_{PP}$ for the $P(OCH_2)_3R$ (R = n-alkyl) and PF_3 complexes have not been determined, it is highly probable that they are as indicated. It is believed that the cis-PF_3 complexes have negative $^2J_{PP}$ values since it has been determined by Nixon that $^2J_{PP}$ for cis-$(OC)_4Mo[PCCl_3F_2]_2$ is -48.0 ± 0.5 Hz.[1] The positive $^2J_{PP}$ in the trans-PF_3 complexes is consistent with the change in $^2J_{PP}$ with the change in electronegativity of the atoms bound to phosphorus. The signs of the $^2J_{PP}$ values assumed for the complexes of $P(OCH_2)_3R$ are consistent with the fact that for complexes of a particular geometry containing one molecule of $P(OCH_2)_3CR$ and one of $P(OCH_3)_3$, the magnitude of $^2J_{PP}$ is between that observed for the complexes coordinated to two molecules of

---

[1]Nixon, J. F., Brighton, England. Magnitude and sign of $^2J_{PP}$ for cis-$Mo[(OC)_4PCCl_3F_2]_2$. Private communication. 1969.

Figure 19. Variation of $^{2}J_{pp}$ with the electronegativity of substituents on phosphorus for <u>cis</u>- complexes of group VI

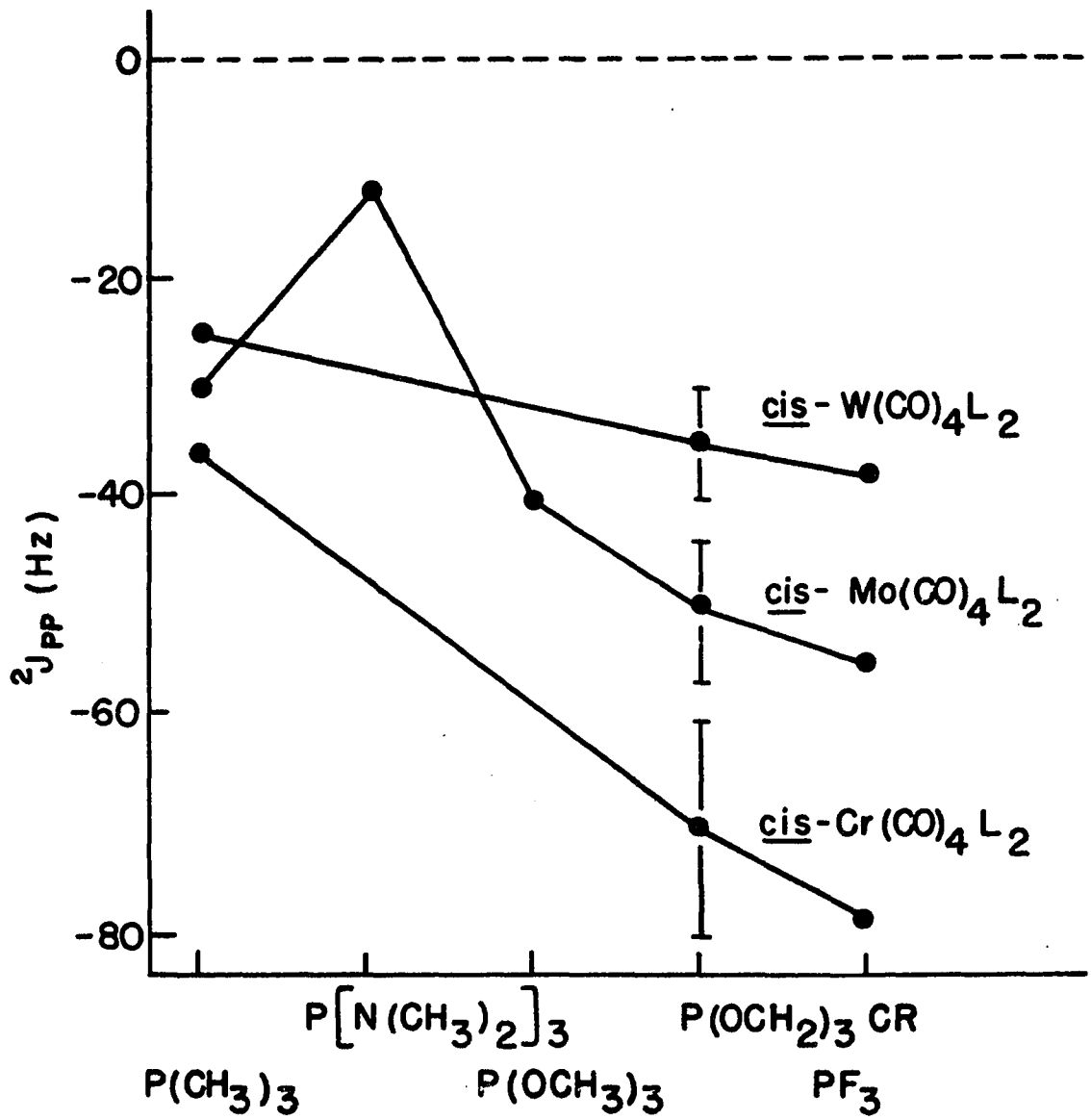
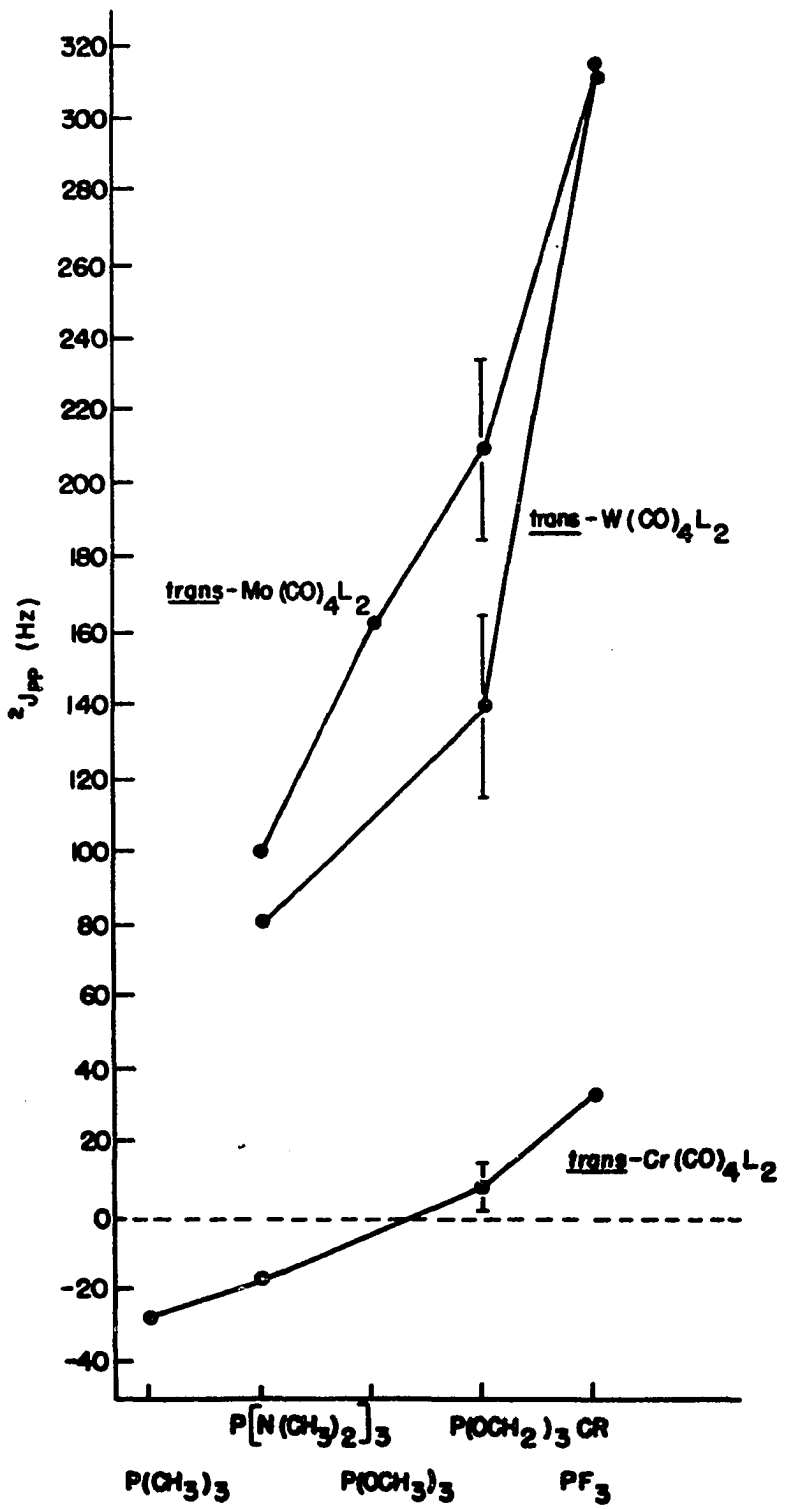

0
-20
-40
-60
-80
$^2J_{PP}$ (Hz)
cis - W(CO)$_4$L$_2$
cis - Mo(CO)$_4$L$_2$
cis - Cr(CO)$_4$L$_2$
P[N(CH$_3$)$_2$]$_3$
P(OCH$_2$)$_3$CR
P(CH$_3$)$_3$
P(OCH$_3$)$_3$
PF$_3$

Figure 20. Variation of $^{2}J_{pp}$ with the electronegativity of substituents on phosphorus for <u>trans</u>- complexes of group VI


320
300
280
260
240
220
200
180
160
140
120
100
80
60
40
20
0
-20
-40
$^2J_{PP}$ (Hz)
trans-Mo(CO)$_4$L$_2$
trans-W(CO)$_4$L$_2$
trans-Cr(CO)$_4$L$_2$
P[N(CH$_3$)$_2$]$_3$
P(OCH$_2$)$_3$CR
P(CH$_3$)$_3$
P(OCH$_3$)$_3$
PF$_3$

$P(OCH_3)_3$ or $P(OCH_2)_3CR$ (59). Had the sign of $^2J_{PP}$ for the complexes of $P(OCH_2)_3CR$ been different from that determined for the $P(OCH_3)_3$ complexes, it is expected that the magnitude of $^2J_{PP}$ for the mixed ligand complex would have been smaller than that observed for the $P(OCH_3)_3$ complexes (59). The value of $^2J_{PP}$ for <u>trans</u>-$(OC)_4Cr[P(OCH_2)_3CR]_2$ is 9 Hz (58) and could be either positive or negative in view of the present lack of a magnitude of $^2J_{PP}$ for the analogous $P(OCH_3)_3$ complex. In either case, none of the trends to be discussed are affected.

The value of $^2J_{PP}$ for <u>cis</u>-$(OC)_4Mo[P(N(CH_3)_2)_3]_2$ is 12.4 $\pm$ 0.2 Hz. Since this complex isomerizes very rapidly to the <u>trans</u>-isomer, it was not possible to determine the sign of this coupling. Its sign is assumed to be negative, and the point in the graph of Figure 19 for this complex is discussed later.

Consider first the effect of stereochemistry of a particular metal upon $^2J_{PP}$. It has been recognized for some time that $^2J_{PP}$ is a function of the stereochemistry of the metal and it has been proposed that this parameter is a useful tool in characterizing transition metal complexes containing two molecules of a phosphorus ligand (74-76). In general it is found that for a particular metal and ligand $^2J_{PP}$ is larger in magnitude in <u>trans</u>- complexes than in <u>cis</u>- complexes. However, in the case of the chromium complexes, this is not observed to be the case for the ligands considered in Figures 19 and 20. However, a consideration of the signs of $^2J_{PP}$ for the chromium

complexes makes this apparent anomaly understandable for it can be seen that for any ligand, the values of the cis-complexes are indeed algebraically smaller than those for the trans-complexes. Indeed, all the cis-complexes of the group VI metal carbonyls for which sign determinations of $^2J_{PP}$ were carried out have negative $^2J_{PP}$ values. It should be noted that cis-Pd $[P(OCH_3)_3]_2Cl_2$ has a positive $^2J_{PP}$, which indicates that not all cis-complexes should be expected to have a negative $^2J_{PP}$ value.

It should also be pointed out that the range of values observed for a particular metal is larger for the trans-complexes than it is for the cis-complexes for the ligands which have been studied. This seems to indicate that $^2J_{PP}$ in the trans- complexes is much more sensitive to changes in the nature of the phosphorus donor than is $^2J_{PP}$ for the cis-complexes.

The order in $^2J_{PP}$ with metal for a particular stereochemistry and ligand appears to be somewhat variable. For the trans-complexes, it appears that the order is Cr<W<Mo except for the PF_3 complexes of W and Mo wherein the $^2J_{PP}$ values are separated by only 3 Hz. For the cis-complexes. The order appears to be Cr<Mo<W. Values for the cis-complexes of $P[N(CH_3)_2]_3$ for chromium and tungsten are not available for comparison with the point indicated for cis-$(OC)_4Mo[P(N(CH_3)_2)_3]_2$. The same holds true for the cis-$P(OCH_3)_3$ complexes of chromium and tungsten.

A more meaningful trend appears in $^2J_{PP}$ as the nature of the atoms attached to phosphorus changes. For the cis-complexes it appears that the magnitudes of the couplings become larger as the atoms bound to phosphorus become more electronegative. There is one exception to this, namely the cis-molybdenum complex of $P[N(CH_3)_2]_3$. This complex is quite unstable to rearrangement to its trans-isomer. This may indicate that the two phosphorus ligands in the cis-configuration sterically hinder one another. Therefore, the P-Mo-P angle may be somewhat larger than that for the $P(CH_3)_3$ complexes. Such a distortion could account for anomalously high $^2J_{PP}$ value. Without exception, the trans-complexes of a particular metal follow the trend of increasing $^2J_{PP}$ with increasing electronegativity of the atoms attached to phosphorus.

It should be mentioned that it was observed by Ogilvie, et al., (59) and Grim et al. (77) that for mixed ligand complexes (i.e., disubstituted carbonyl complexes containing two different phosphorus ligands) the above trends are generally observed. For the trans-complexes, however, the order of $^2J_{PP}$ for any pair of ligands with group VI metals is Cr<Mo<W. It was also observed by Ogilvie et al. (59) that the values of $^2J_{PP}$ for a mixed ligand complex were intermediate between the values observed for the two analogous complexes in which the two ligands in question were identical.

The molecular orbital treatment of Pople and Santry (4) represents a basis for discussion of the trends in $^2J_{PP}$.

However, a complete explanation of the trends which have been observed must await a complete molecular orbital treatment of these complexes, with a good wave function and energy level description. Since the contact term is considered dominant, the problem as outlined previously is to determine the relative energies of the transitions between the molecular orbitals that have some contribution due to the 3s orbital on both phosphorus atoms as well as the symmetry of the orbitals involved. Since the contribution to the coupling constant of a particular transition is inversely proportional to its energy, those transitions of lowest energy contribute greatest, if the coefficients of the ao's forming the mo's remain constant.

A possible molecular orbital diagram for the cis and trans group VI complexes is shown in Figure 21.[1]

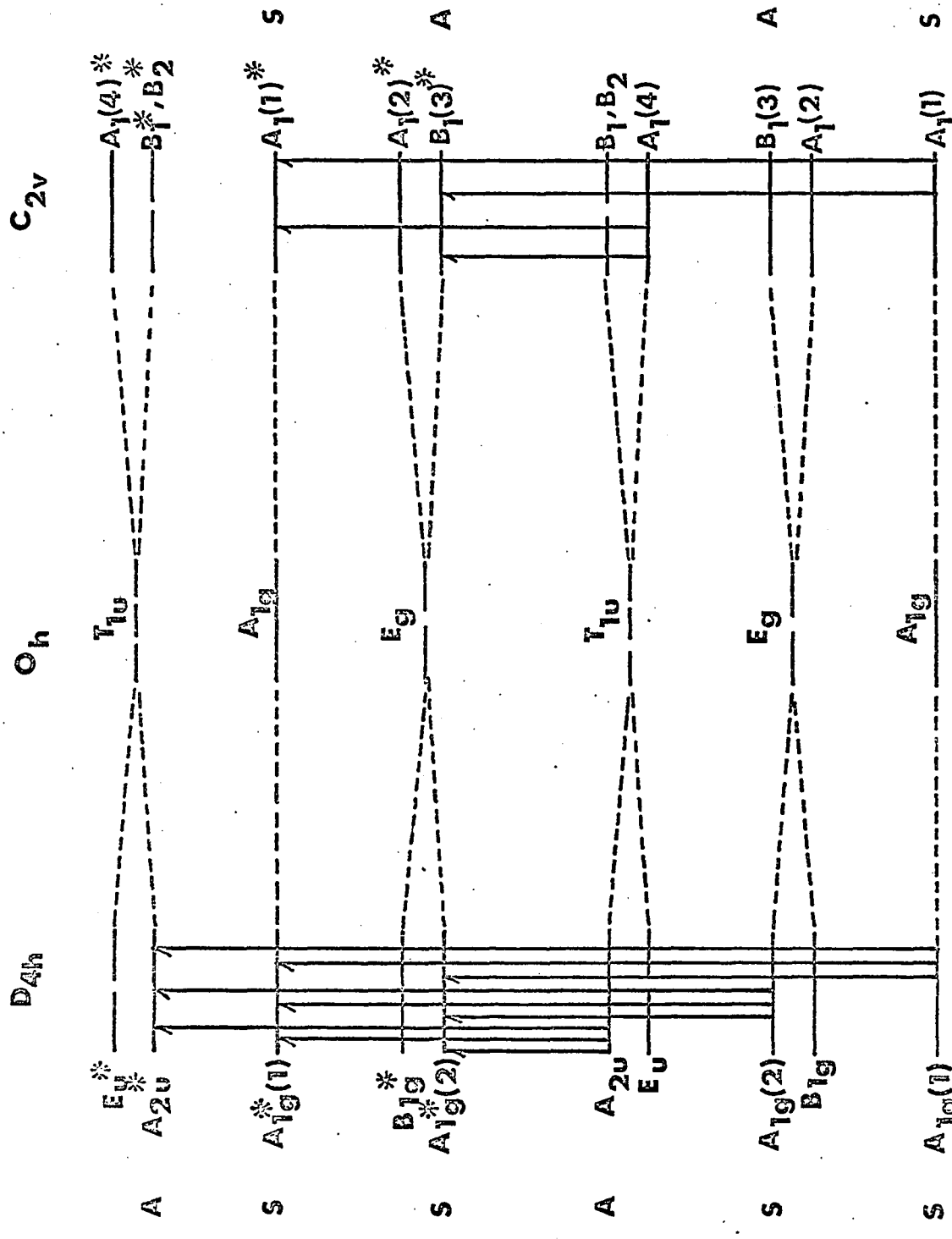
The vertical arrows indicate transitions between filled molecular orbitals that involve overlap between an atomic orbital on the metal and orbitals on both phosphorus atoms which contain some contribution due to the 3s of each phosphorus. This diagram was constructed employing the coordinate systems shown below, and is simplified by ignoring configuration interaction. Furthermore, only σ interactions are shown, as it is expected that π interactions involving d orbitals, on phosphorus will provide only a negligible contact interaction.

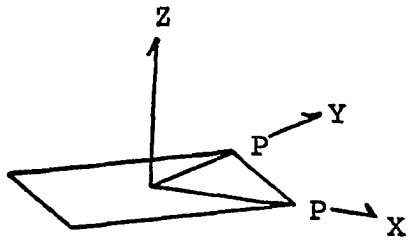
---

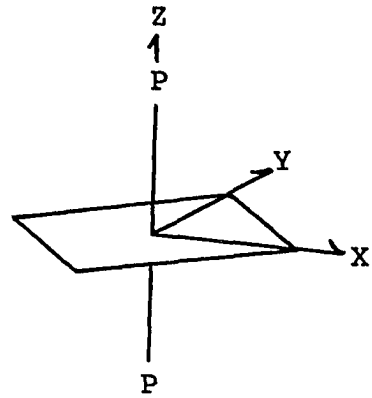
[1]Ogilvie, F. B., Ames, Iowa. Information on molecular orbital diagram for cis- and trans-distributed group VI carbonyls. Private communication. 1969.

Figure 21. Simplified mo diagram for cis- and trans-octahedral complexes showing qualitatively the possible ordering of energy levels

The z coordinate was taken to be through the four-fold axis in the trans-case and perpendicular to the two-fold axis in the cis-case.


D_{4h}
O_h
C_{2v}
E_u^*
A_{2u}^*
T_{1u}
$A_1(4)^*$
B_1^*, B_2
A
S
$A_{1g}(1)^*$
A_{1g}
$A_1(1)^*$
S
B_{1g}^*
$A_{1g}(2)^*$
E_g
$A_1(2)^*$
$B_1(3)^*$
A
A_{2u}
E_u
T_{1u}
B_1, B_2
$A_1(4)$
A
$A_{1g}(2)$
B_{1g}
E_g
$B_1(3)$
$A_1(2)$
S
$A_{1g}(1)$
A_{1g}
$A_1(1)$
S





cis-C_{2v} trans-D_{4h}

It can be seen that the lowest energy transition for C_{2v} symmetry involves a transition from a molecular orbital that is antisymmetrical with respect to reflection in its mirror plane (A) to another such A orbital. This transition gives rise to a negative contribution to the coupling constant. The remaining three transitions shown, $A_1(1) \rightarrow A_1(3)^*$, $A_1(3) \rightarrow A_1(1)^*$ and $A_1(1) \rightarrow A_1(1)^*$ make a positive, a positive and a negative contribution, respectively. However, these transitions are of higher energy and apparently cannot outweigh the contribution due to the lowest energy transition. This postulate agrees well with experiment, since the cis- group VI complexes have negative $^2J_{PP}$ values. Phosphorus substituent electronegativity influences $^2J_{PP}$ values in several ways. First, it will tend to increase the positive charge on the phosphorus and should increase the electron density at the phosphorus nucleus. According to Equation 9, this should increase the magnitude of the coupling,

hence, the negative couplings will become more negative. Secondly, according to Bent's rules, the increase in electronegativity should tend to increase the contribution of the 3s orbital to the hybrid on phosphorus which binds the phosphorus to the metal. This should increase the value of the coupling constant. The C values in Equation 9 are also expected to be affected by the increase in the electronegativity of the phosphorus substituents. Since the symmetry of the molecular orbitals determines the sign of the contribution of a particular transition to $^2J_{PP}$, this cannot change with increased electronegativity. However, the values of these C's will tend to weight certain transitions more than others, as does the energy term involved. The trends in these two factors with increasing electronegativity at phosphorus are difficult to assess at this time. The fact is that increasing the electronegativity of the phosphorus substituents causes an algebraic decrease in $^2J_{PP}$ and may indicate that the weighting of the negative contributions may be increased by either the C values for the atomic orbitals comprising the molecular orbitals and/or the energy terms.

The same sort of arguments about the effects of electronegativity of the phosphorus substituents upon $^2J_{PP}$ for the trans-complexes can be made. As indicated, there are apparently many more transitions which must be considered. The same problem of determining the relative weight of each transition and its contribution to the total $^2J_{PP}$ is encountered. The

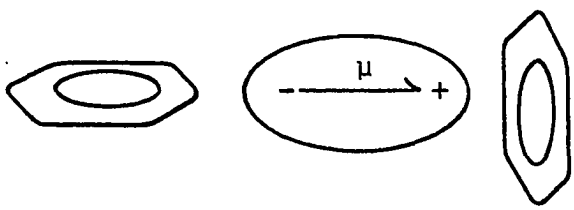
arguments with regard to the effect of electronegativity upon the s electron density at the phosphorus nucleus presented above are relevant. The $^2J_{PP}$ values are expected to increase with increasing electronegativity of the substituents attached to phosphorus. However, there is a sign change for the chromium complexes, which indicates that the relative contributions of the various transitions to $^2J_{PP}$ must change such that the positive contributions increase their importance with increasing electronegativity of the phosphorus substituents. Further discussion of these trends must await the determination of the eigenfunctions and eigenvalues for these systems before assignment of the trends in $^2J_{PP}$ values to the changes in these terms can be made.

Aromatic Solvent Induced Shifts

It was not possible to perform dilution experiments such as those described in the introduction, since the solubility of the compounds studied was not great enough. The following discussion and conclusions rests on the data presented earlier.

The model which is proposed to explain the observation of the ASIS phenomenon for the bicyclic compounds studied in this dissertation is similar to the specific-geometry collision complex model discussed in the introduction. It is noted from the results presented in Tables 8 and 9 and Figures 9-15 that protons residing near the positive end of the molecular dipole are shielded by hydrocarbon aromatic solvents and that those protons

near the negative end of the molecular dipole are deshielded by hydrocarbon aromatic solvents. The methylene protons of $P(OCH_2)_3CCH_3$ and $HC(OCH_2)_3CCH_3$ or the methine and equatorial methylene protons of $HC(OCH)_3(CH_2)_3$ are very much less if at all affected by such solvents. These observations lead to the postulate that the ASIS phenomenon is a result of a complex such as that shown below. It is postulated that the solvent preferentially collides with the positive end of the molecule to

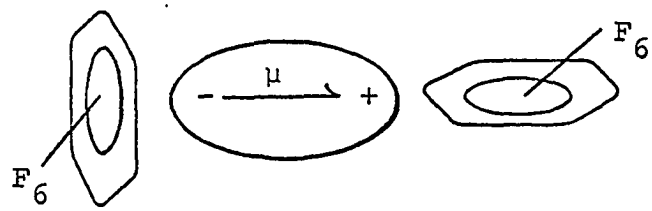


form an axially symmetric complex as shown. The model indicated may also be considered as an effective complex resulting from specifically oriented collisions of more than one solvent molecule with the solvent. The complex could result from a dipole induced-dipole interaction between the dipole of the solute and the polarizable π electron system of the solvent. The protons at the positive end of the dipole would then be subjected to a shielding effect due to the diamagnetic anisotropy of the complexed solvent molecule. In a similar manner, the relatively positive periphery of the aromatic solvent molecule is postulated to independently interact with the negative end of the dipole as shown above. The protons attached at this end of the molecule will then be deshielded by the complexed solvent molecule.

The results of the temperature studies are in accord with this postulate. It is expected that as the temperature is lowered, the formation of the complex will be favored, since the random distribution of solvent molecules around the solute breaks down. Hence, those protons that are observed to be shielded by an aromatic solvent should show a trend towards increased shielding as the temperature is lowered. Likewise, those protons that are deshielded by aromatic solvents are expected to show a trend towards increased deshielding as the temperature is lowered. Indeed, this is what is observed as demonstrated by the data in Table 8 and the plots in Figures 10-15.

The thermodynamic data presented in Table 11 indicate that the ΔH of formation of the complexes are quite low and negative. The negative ΔH indicates that the formation of the complex is favored as the temperature is lowered as is expected. The calculated equilibrium constants at 27.5° indicate that between 50 and 67% of the solute molecules are specifically complexed to a solvent molecule at one of the complexing sites of the molecules considered. These parameters are comparable in magnitude and sign to those obtained by Abraham (25) for a similar study of iodoform and methyl iodide in toluene. He observed $\Delta H = 1.6 \pm 0.2$ kcals/mole and $\Delta S = -6.4 \pm 0.2$ e.u. for the iodoform complex with toluene and $\Delta H = -1.3 \pm 0.5$ kcals/mole and $\Delta S = -4.9 \pm 0.4$ e.u. for the methyl iodide complex with toluene.

The opposite effects were observed when hexafluorobenzene was used as solvent. That is, those protons that were shielded by hydrocarbon aromatic solvents were observed to be deshielded by hexafluorobenzene and those protons that were observed to be deshielded by hydrocarbon aromatic solvents are shielded by hexafluorobenzene. If it is assumed that the fluorocarbon aromatic has a diamagnetic anisotropy in the same sense as does the hydrocarbon aromatics, then the geometry of the collision complex that would explain the observed results is as shown below. The positive end of the solute dipole interacts with



the relatively more negative periphery of the hexafluorobenzene molecule, and causes it to solvate specifically as shown. The negative end of the dipole interacts preferentially with the relatively more positive central region of the ring, causing the solvent to orient itself with respect to the solute as shown.

The origin of the shielding or deshielding effect is again assumed to be due to the same sort of diamagnetic anisotropy known for hydrocarbon aromatics. However, it was suggested[1] that the effect of the electric field of the CF bond might play

---

[1]Musher, J. I. Rehovoth, Israel. Suggestion that the electric field effect of the CF bond dipole may be important in determining the shielding or deshielding effects observed with hexafluorobenzene. Private communication. 1967.

an important role in determining the shielding of a proton near the fluorine atom. Calculations employing the Buckingham equation (27) were carried out. Three geometric cases were considered and are represented in Figure 22.

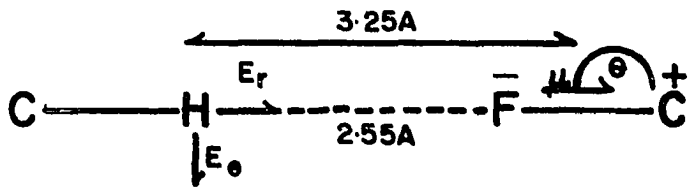
Buckingham states that the effect of a dipolar electric field on the chemical shift of a proton attached to carbon is given by Equation 28, where E_z is the component of the electric field along the CH

$$|\Delta\sigma| = 2 \times 10^{-12} Ez + 10^{-18} E^2 \qquad 28$$

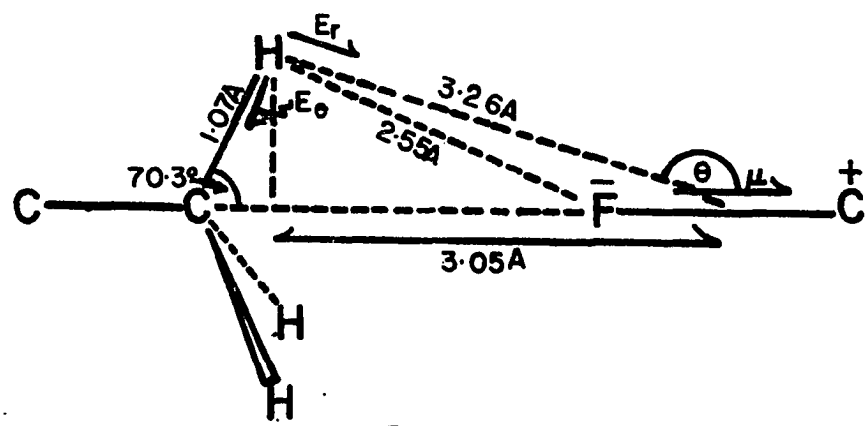
bond, and E is the magnitude of the electric field perpendicular to the bond. The second term is neglibible and can be ignored. The problem involves determining the component of the electric field along the CH bond (Ez) due to a point dipole half way along the CF bond. The radial component of the dipole electric field is given by $E_r = 2\mu \cos\theta/r^3$ and the tangential component is given by $\mu \sin\theta/r^3$, where θ is the angle between the point dipole and the radius vector from the point dipole to the ^1H atom (78). If the component of the dipole electric field is in the C→H direction then the ^1H nucleus will be deshielded while if the component is in the H→C direction, the proton will be shielded.

The distances employed throughout are considered to be the distance of closest approach - the sum of the Van der Waals radii for the interacting atoms (79). Bond distances are the sums of covalent radii (79). Furthermore, the bond dipole for

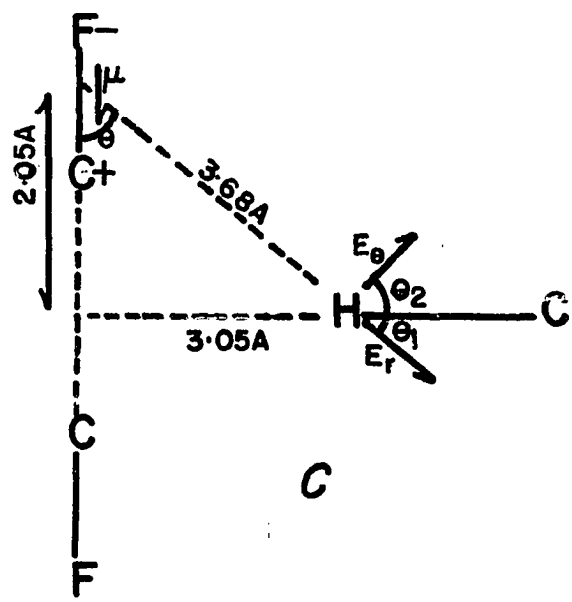
Figure 22. Three geometries for the interaction of the point dipolar electric field of a CF bond with a proton attached to carbon


3·25A
Er
C
H
F
C
2·55A
Eθ
θ
μ

A


Er
H
1·07A
Eθ
3·26A
2·55A
70·3°
C
C
F
C
θ
μ
3·05A
H
H

B


F
μ
θ
C
2·05A
3·68A
Eθ
θ2
H
C
3·05A
θ1
Er
C
F

C

the CF bond (2.0 D) is calculated from the dipole moment of fluorobenzene (1.6 D) (80) wherein the negative end is assumed towards F, and the 0.4 dipole of a CH bond (81) in which the negative end is assumed towards H.

Case A represents a geometry in which the CF bond is co-linear with the CH bond. Such a situation might obtain for the interaction of hexafluorobenzene with one of the methyl protons at the positive end of the molecules under consideration. The association may be due to either a hydrogen bonding mechanism or a dipole-induced dipole interaction. In any event, $E_\theta = 0$, since sin 180° = 0, and Ez = 1.17×10^5 esu/cm^3 = E_r. Therefore, $\Delta\sigma = 0.23 \times 10^{-6}$ or 0.23 ppm which is 14 Hz at 60 MHz. Since the component of the dipolar electric field points towards the hydrogen atom, the effect will be to deshield the hydrogen.

Case B is an attempt to determine the effect of the CF bond dipole upon the chemical shift of the protons of a methyl group, assuming the CF bond is colinear with the three-fold axis of the methyl group. The angles at carbon were assumed tetrahedral. It can be shown that E_θ makes an angle of only 1°26' with the CH bond axis, hence the radial component of the dipolar electric field has a negligible component along the CH bond axis and the component of E_θ along the CH bond axis is essentially E_θ. Since θ is 160°30', E_θ is 1.72×10^4 esu/cm^3 towards carbon. This gives a $\Delta\sigma$ of 0.03×10^{-6} that is shielding, and represents 1.8 Hz at 60 MHz.

Model C represents the case of a proton at the negative end of the dipole interacting with the π cloud of the hexafluorobenzene ring such that the CH bond is perpendicular to the plane of the carbon atoms. The half-thickness of the electron cloud is taken to be that for benzene which is given by Gould (81) to be 1.85 Å. θ is 56° and E_r = 4.45 x 10^4 esu/cm^3 and E_θ is 3.31 x 10^4 esu/cm^3. Employing angles θ_1 and θ_2 which are 34° and 56°, respectively, the component of E_r along the CH bond is 3.78 x 10^4 esu/cm^3 and the component of E_θ along the CH bond is 1.85 x 10^4 esu/cm^3. These are both towards carbon, and sum to give 5.63 x 10^4 esu/cm^3. This gives a $\Delta\sigma$ of 0.11 x 10^{-6}. Since there are six such CF bonds symmetrically distributed about the CH bond, the contributions of all six should add to give the total effect. This would result in a shielding of 0.66 ppm which is 39.5 Hz at 60 MHz.

By performing these calculations employing the bond dipole of 0.4 with the negative end at the hydrogen in benzene and a proton-proton interaction distance in cases A and C of 2.4 Å (the sum of the Van der Waals radii), it can be shown that for the three cases of Figure 22 the $\Delta\sigma$'s are one fifth that stated above. This result is a consequence of the geometries employed. The sense of these effects is the same as quoted for hexafluorobenzene.

Further light is shed upon the possible mechanism of these effects from the results of the shifts of the methyl groups of

$CH_3C(OCH_2)_3CCH_3$ in fluorobenzene and fluorotrichloromethane. It was found that fluorobenzene behaves like benzene in that the methyl protons at the positive end of the dipole were shielded by 22.8 Hz compared to their value in carbon tetrachloride and the methyl protons at the negative end were deshielded by 17.1 Hz, the same magnitude as observed for the shielding by benzene. The shifts of these protons were +0.3 Hz for the $CH_3C(O)_3$ methyl and -1.7 Hz for the $CH_3C(C)_3$ methyl protons in $CFCl_3$. These results tend to suggest that apparently model A is not important, for even with dipolar monofluorobenzene shielding was observed for the methyl protons at the positive sites of the solute. Furthermore, the negligible effect produced by fluorotrichloromethane tends to indicate that the CF bond does not align colinearly with the CH bond. Model B then seems reasonable, the origin of the effect being largely the diamagnetic anisotropy of the hexafluorobenzene rather than the electric field effect.

The origins of the shielding observed for the protons at the negative end of the dipole in hexafluorobenzene is somwhat less clear. Model C gives a value for the shielding comparable with the observed effect. However, the electric field model of Buckingham has been observed to give results inconsistent with observation. For instance, Huttemann (82) found that the electric field of a molecular dipole could not explain the relative chemical shifts of the equatorial and axial methylene protons in $P(OCH)_3(CH_2)_3$. In our case, the electric field effect gives

a good agreement with experiment if anisotropy effects are absent. In the presence of the apparent anisotropy, however, the observed shielding effect should be twice that observed.

The electric field of the CH bond in benzene is apparently too small to reasonably account for the observed trends, and the magnetic anisotropy of this molecule must be invoked to explain the results.

Incidentally, the model proposed herein differs somewhat in concept with those proposed previously (26). The model herein presented involves the interaction of the molecular dipole with the solvent. The models which have previously been proposed have involved the interaction of the solvent with the dipole moment of a specific substituent in the molecule. This is particularly significant, for it is observed that the protons of the open chain analogues of the caged species studied have little or no chemical shift change in going from carbon tetrachloride to benzene. This may indicate that the rigid structure and the particular geometry of the cage species is important in allowing the specific solvation described to take place.

The postulate that the complex is a result of a dipole induced-dipole interaction is supported by the observation that the shielding of the methyl protons of the three compounds $CH_3C(OCH_2)_3CCH_3$, $HC(OCH_2)_3CCH_3$ and $P(OCH_2)_3CCH_3$ by benzene increases as their dipole moments increase. The dipole moments (83) and $\delta_{C_6H_6} - \delta_{CCl_4}$ values for the analogous methyl groups

of these compounds are 2.71 D, 3.19 D and 4.13 D and 40.0 Hz, 47.0 Hz and 55.2 Hz, respectively.

SUGGESTIONS FOR FURTHER WORK

The investigations presented in this dissertation suggest several areas of further research. With regard to the studies of $P(OCH_2)_3P$ and its derivatives, further studies should include complexes of other Lewis acids, such as the boron Lewis acids and cationic transition metals. Such studies would not only extend the ranges of such complexes, but also would help elucidate the effect of positive charge on the nmr parameters. In order to determine the effects of dihedral angle and free rotation upon $^3J_{PP}$, systems such as $(RO)_2P\text{-}O\text{-}CH_2\text{-}P(R)_2$, $ROP(OCH_2)_2PR$ and their derivatives should be investigated for trends in $^3J_{PP}$. Indeed, there are numerous other compounds of varying structure that have been prepared which should give rise to $^{31}P\text{-}^{31}P$ coupling over three bonds. Reinvestigation of these compounds for this parameter should be done so as to accumulate data that might aid in the determination of the mechanism of such couplings and in the hope that such data will correlate with molecular structure.

In order to more completely understand the origins in the trends in the couplings for $P(OCH_2)_3P$ and its derivatives, a complete CNDO calculation should be performed on these systems. A computer program is available to do this calculation for the derivatives studied, except those involving transition metals.[1]

---

[1]Gordon, M. Ames, Iowa. Information on CNDO calculations for $P(OCH_2)_3P$ and its derivatives. Private communication. 1969.

For such a calculation to be more than semi-quantitative, accurate bond angles and distances are required, which suggests that these parameters should be obtained from single crystal x-ray diffraction studies.

Numerous studies are suggested as a result of the nmr studies reported on the disubstituted complexes. The postulate that the sign of $^2J_{PP}$ for the trans- group VI PF_3 complexes is positive should be verified, if possible, by determining the sign of $^2J_{PP}$ for a trans-complex of PF_2CCl_3. It is noted that the resonance lines in Figure 6 for cis-$(OC)_4W[P(CH_3)_3]_2$ due to the mixing of the αβ and βα spin states of the two phosphorus nuclei are broader than those due to the αα or ββ spin state. This observation suggests that the mixed spin states of phosphorus have a different relaxation time than the αα or ββ spin states. The cause of this phenomenon should be investigated, not only from the theoretical point of view, but also by employing experimental methods, such as variable temperature nmr experiments. If the differential relaxation is due to some presently unrecognized exchange process, such studies might verify this point.

The fact that $^1J_{PC}$ for $[CH_3P(OCH_3)_3]^+$ is much larger than for $[(CH_3)_4P]^+$ leads this author to suggest that an investigation of this parameter for the "intermediate" compounds $[(CH_3)_2P(OCH_3)_2]^+$ and $[(CH_3)_3P(OCH_3)]^+$ be done. This would reveal whether or not that there is a smooth trend in $^1J_{PC}$ with

the increase in the number of electronegative oxygens attached to phosphorus.

There seems to be a paucity of data involving geminal ^{31}P-^{31}P coupling through atoms such as oxygen and carbon. It would seem reasonable that studies of such couplings might be fruitful, since the results would be much more amenable to interpretation, as the central atom attached to phosphorus would not have d orbitals. Thus full CNDO-SCF and INDO-SCF calculations could be performed.

With regard to the observations on the effects of hexafluorobenzene on the ^{1}H chemical shift, it is suggested strongly that the diamagnetic anisotropy of this molecule be determined so that this factor can be assessed in explaining the observed shifts. It might also be appropriate to study the solvent effects for solvents of the type $C_6F_{6-x}H_x$ where x is increased from 1 to 5. At some value of x between 1 and 5 a reversal of chemical shift should occur for a particular solute proton. Such a study would aid in determining the mechanism by which the protons that are shielded by benzene become deshielded by hexafluorobenzene and vice versa.

LITERATURE CITED

1. J. W. Emseley, J. Feeney and L. H. Sutcliffe, High Resolution Nuclear Magnetic Resonance Spectroscopy, Pergamon Press, New York, N.Y., 1965.

2. J. A. Pople, W. G. Schneider and H. J. Bernstein, High-resolution Nuclear Magnetic Resonance, McGraw-Hill Book Co., Inc., New York, N.Y., 1959.

3. J. D. Memory, Quantum Theory of Magnetic Resonance Parameters, McGraw-Hill Book Co., Inc., New York, N.Y., 1968.

4. J. A. Pople and D. P. Santry, Mol. Phys. 8, 1(1964).

5. N. F. Ramsey, Phys. Rev., 91, 303(1953).

6. L. Pauling and E. B. Wilson, Introduction to Quantum Mechanics, McGraw-Hill Book Co., Inc., New York, N.Y., 1935.

7. H. M. McConnell, J. Chem. Phys., 24, 460(1956).

8. J. A. Pople and A. A. Bothner-By, J. Chem. Phys., 42, 1339 (1965).

9. J. A. Pople, J. W. McIver and N. S. Ostlund, J. Chem. Phys., 49, 2965(1968).

10. A. H. Cowley, W. D. White and S. L. Manatt, J. Am. Chem. Soc., 89, 6433(1967).

11. A. H. Cowley and W. D. White, J. Am. Chem. Soc., 91, 1913 (1969).

12. A. H. Cowley and W. D. White, J. Am. Chem. Soc., 91, 1917 (1969).

13. V. M. S. Gill and J. J. C. Teixeria-Das, Mol. Phys., 15, 47(1968).

14. V. M. S. Gill and S. J. S. Formosinko-Simões, Mol. Phys., 15, 639(1968).

15. V. M. S. Gill, Mol. Phys., 15, 645(1968).

16. V. Mark, C. H. Dungan, M. M. Crutchfield and J. R. Van Wazer in Topics in Phosphorus Chemistry, Vol. 5, M. Greyson and E. J. Griffith, Eds., John Wiley and Sons, Inc., New York, N.Y., 1967, p. 227.

17. I. Ionin, V. B. Lebedev and A. A. Petrov, J. Gen. Chem. U.S.S.R., 37, 1117(1967).

18. W. McFarlane and J. A. Nash, Chem. Commun., 1969, 127.

19. W. McFarlane, Proc. Roy. Soc., A, 306, 185(1968).

20. K. A. McLauchlan, D. H. Whiffen and L. W. Reeves, Mol. Phys., 10, 13(1966).

21. E. G. Finer and R. K. Harris, Mol. Phys., 13, 65(1967).

22. E. F. Friedman and H. S. Gutowsky, J. Chem. Phys., 45, 3158(1966).

23. D. H. Whiffen, J. Chem. Phys., 47, 1565(1967).

24. R. Freeman and W. A. Anderson, J. Chem. Phys., 37, 2053 (1962).

25. R. J. Abraham, Mol. Phys., 4, 369(1961).

26. P. Laszlo in Progress in N.M.R. Spectroscopy, Vol. 3, J. W. Emsley, J. Feeney and L. H. Sutcliffe, Eds., Pergamon Press, New York, N.Y., 1967, p. 231.

27. A. D. Buckingham, Can. J. Chem., 38, 300(1960).

28. L. Pauling, J. Chem. Phys., 4, 673(1936).

29. J. S. Waugh and R. W. Fessenden, J. Am. Chem. Soc., 79, 846(1957).

30. C. E. Johnson and F. A. Bovey, J. Chem. Phys., 29, 1012 (1958).

31. J. I. Musher, J. Chem. Phys., 43, 4081(1965).

32. J. I. Musher in Advances in Magnetic Resonance, Vol. 2, J. S. Waugh, Ed., Academic Press, New York, N.Y., 1966, p. 177.

33. J. M. Gaidis and R. West, J. Chem. Phys., 46, 1218(1967).

34. J. I. Musher, J. Chem. Phys., 46, 1219(1967).

35. M. W. Hanna and A. L. Ashbough, J. Phys. Chem., 68, 811 (1964).

36. R. C. Fort, Abstracts, 152nd ACS National Meeting, New York, N.Y., September, 1966.

37. I. D. Kuntz, Jr. and Milton D. Johnston, Jr., J. Am. Chem. Soc., 89, 6008(1967).

38. A. D. Buckingham, T. Schaefer and W. G. Schneider, J. Chem. Phys., 32, 1227(1967).

39. L. M. Jackman, Applications of Nuclear Magnetic Resonance Spectroscopy in Organic Chemistry, Pergamon Press, New York, N.Y., 1959.

40. J. Ronayne and D. H. Williams, J. Chem. Soc., B, 1967, 540.

41. J. Ronayne and D. A. Williams, Chem. Commun., 1966, 712.

42. C. W. Hertsch and J. G. Verkade, Inorg. Chem., 1, 392 (1962).

43. W. Doering and A. K. Levy, J. Am. Chem. Soc., 77, 509 (1955).

44. K. J. Coskran and J. G. Verkade, Inorg. Chem., 4, 1655 (1965).

45. E. J. Boros, R. D. Compton and J. G. Verkade, Inorg. Chem., 7, 165(1968).

46. J. Guyer, J. Rathke and J. G. Verkade, to be published.

47. H. Meerwein in Organic Synthesis, Vol. 46, E. J. Corey, Ed., John Wiley and Sons, Inc., New York, N.Y., 1966, p. 120.

48. E. B. Baker, L. W. Burd and G. N. Root, Rev. Sci. Instr., 34, 243(1963).

49. A. D. Buckingham and K. A. McLauchlan in Progress in Nuclear Magnetic Resonance Spectroscopy, Vol. 2, J. N. Emsley, J. Feeney and L. H. Sutcliffe, Eds., Pergamon Press, Oxford, 1967, p. 63.

50. D. W. White, R. D. Bertrand and J. G. Verkade, to be published.

51. E. B. Baker, J. Chem. Phys., 45, 609(1966).

52. W. McFarlane, J. Chem. Soc., A, 1967, 1922.

53. R. D. Bertrand, D. Allison and J. G. Verkade, to be published.

54. J. G. Verkade and R. W. King, Inorg. Chem., 1, 948(1962).

55. D. G. Hendricker. Metal Carbonyl Complexes of Polycylic Phosphite Esters. Unpublished Ph.D. thesis. Library, Iowa State University of Science and Technology, Ames, Iowa. 1965.

56. P. L. Corio, Chem. Rev., 60, 363(1960).

57. R. H. Harris, Can. J. Chem., 42, 2275(1964).

58. F. B. Ogilvie. ^{31}P-^{31}P Spin-Spin Coupling in Metal Complexes of Phosphorus Ligands. Unpublished Ph.D. thesis. Library, Iowa State University of Science and Technology, Ames, Iowa. 1969.

59. F. B. Ogilvie, R. L. Keiter, G. W. Wulfsberg and J. G. Verkade, to be published.

60. R. H. Moore and R. K. Zeigler, The Solution of the General Least Squares Problem With Special Reference to High-speed Computers, AEC Report LA-2367, Los Alamos, New Mexico, Los Alamos Scientific Laboratory, 1960.

61. D. A. Allison and J. G. Verkade, to be published.

62. D. Berglund and D. W. Meek, J. Am. Chem. Soc., 90, 518 (1968).

63. S. L. Manatt, G. L. Juvinall, R. I. Wagner and G. D. Elleman, J. Am. Chem. Soc., 88, 2689(1966).

64. J. P. Albrand, D. Gagnaire and J. B. Robert, Chem. Commun., 1968, 1469.

65. R. Goodfellow, Chem. Commun., 1968, 114.

66. H. A. Bent, Chem. Rev., 61, 275(1961).

67. M. Karplus and D. M. Grant, Proc. Natl. Acad. Sci. U.S., 45, 1269(1959).

68. C. Juan and H. S. Gutowsky, J. Chem. Phys., 37, 2189(1962).

69. J. N. Shoolery, J. Chem. Phys., 37, 1427(1962).

70. N. Muller and D. E. Pritchard, J. Chem. Phys., 31, 768 (1959).

71. N. Muller and D. E. Pritchard, J. Chem. Phys., 31, 1471 (1959).

72. N. Muller, J. Chem. Phys., 36, 359(1962).

73. D. M. Grant and W. M. Litchman, J. Am. Chem. Soc., 87, 3994(1965).

74. M. S. Lupen and B. L. Shaw, J. Chem. Soc., A, 1968, 741.

75. J. Powell and B. L. Shaw, J. Chem. Soc., A, 1968, 211.

76. P. R. Brooks and B. L. Shaw, J. Chem. Soc., A, 1967, 1079.

77. S. O. Grim, D. A. Wheatland and P. R. McAllister, Inorg. Chem., 7, 161(1968).

78. E. R. Peck, Electricity and Magnetism, McGraw-Hill Book Co., Inc., New York, N.Y., 1953.

79. L. Pauling, The Nature of the Chemical Bond and the Structure of Molecules and Crystals, 3rd ed., Cornell University Press, Ithaca, N.Y., 1960.

80. A. L. McClellan, Tables of Experimental Dipole Moments, W. H. Freeman and Co., San Francisco, Calif., 1963

81. E. S. Gould, Mechanism and Structure in Organic Chemistry, Holt, Rinehart and Winston, Inc., New York, N.Y., 1959.

82. T. J. Huttemann, Jr. The Chemistry and Transition Metal Complexes of 2,8,9-Trioxa-1-phospha-adamantane. Unpublished Ph.D. thesis. Library, Iowa State University of Science and Technology, Ames, Iowa. 1965.

83. A. C. Vandenbroucke. Synthesis, Characterization and Metal Carbonyl Complex Formation of Polycyclic Phosphorus Ligands. Unpublished Ph.D. thesis. Library, Iowa State University of Science and Technology, Ames, Iowa, 1967.

ACKNOWLEDGMENTS

First, I would like to thank Dr. Roy King for building and maintaining much of the electronic gear that went into the "HR-60+" spectrometer used in the double irradiation work and in teaching me the operation of this instrument. Without his help, this work could not have been done. I would also like to acknowledge David Allison for the preparation of most of the derivatives of $P(OCH_2)_3P$ and Fred Ogilvie for the preparation of the disubstituted complexes for which the prime interest was the determination of the magnitudes and signs of $^2J_{PP}$. I would also like to thank Fred for many helpful discussions concerning the theory of spin-spin coupling. A thank-you also goes to Dr. Ross Compton for gifts of some of the compounds used in the ASIS studies, as well as helpful discussions. Dr. James Espenson is thanked for providing a copy of the non-linear least squares computer program used in the ASIS studies.

I would also like to thank the other members of the Verkade group, both past and present, for the exchange of ideas and equipment during my years at Iowa State.

A great deal of thanks goes to my major professor, Dr. Verkade, for his helpful suggestions during the course of this research and during the writing of this dissertation. His patience during the course of my studies is greatly appreciated.

A special thank-you goes to my wife Charla for her patience and understanding during the term of this research and the period during which this dissertation was written. She helped a great deal by reading and recopying the manuscript for final typing.

I would also like to thank Iowa State University and the Chemistry Department for financial aid in the form of teaching and research assistantships during my graduate studies. The Petroleum Research Fund is thanked for a fellowship for my last year of graduate school.